ABSTRACT

Title of Document:	EFFECTS OF CHANNEL MORPHOLOGY ON FLOODPLAIN INUNDATION AND SURFACE-GROUNDWATER INTERACTIONS IN AN URBAN WATERSHED
	Dorothea Lundberg, Master of Science, 2011
Directed By:	Dr. Karen L. Prestegaard, Department of Geology

The purpose of this study is to evaluate groundwater-surfacewater interactions between a stream and the adjacent floodplain. The study site includes two reaches on Paint Branch Creek: an incised reach with inset gravel bars and a non-incised reach with active accretion of gravels bars onto the floodplain and off channel features. Topography, sediment grain size and hydraulic conductivity, groundwater head, and floodplain/channel characteristics were measured. Groundwater head data in gravel bars and adjacent floodplains were monitored for one year to determine seasonal variations in groundwater flow directions, rates, and to develop groundwater probability curves. Identification of groundwater-surfacewater interactions and off channel features roles was determined. In the reach with attached gravel bars, water flows from the creek into the adjacent gravel bars for the most of the year. Evapotranspiration and tropical storms influence seasonal reversals in flow directions between the gravel bar and the floodplain.

EFFECTS OF CHANNEL MORPHOLOGY ON FLOODPLAIN INUNDATION AND SURFACE-GROUNDWATER INTERACTIONS IN AN URBAN WATERSHED

By

Dorothea June Lundberg

Thesis submitted to the Faculty of the Graduate School of the
University of Maryland, College Park, in partial fulfillment
of the requirements for the degree of
Master of Science
2011

Advisory Committee:
Professor Karen L. Prestegaard, Chair
Professor Naijun Zhou
Professor Kaye Brubaker

Acknowledgements

I would like to thank my advisor, Dr. Karen Prestegaard and committee members, Dr. Naijun Zhou, and Dr. Kaye Brubaker for their continual academic encouragement in writing and conducting the research for this thesis. I am very thankful for the time and efforts Dr. Karen Prestegaard has provided in seeing this project through start to finish and giving me a chance to grow as a hydrologic researcher. Much gratitude goes to Alan Leslie and Marcie Occhi for their assistance in installing and surveying some of the piezometers needed for this research. I would also like to thank my mom and dad for their love, support and daily encouragement. Without my parents, I would not be who or where I am today, and I am truly thankful to have such great parents that I can make proud. You are the best parents a daughter could ask for. I love you.

Table of Contents

List of Tables

List of Figures

List of Illustrations

List of Symbols

K	Horizontal hydraulic conductivity
A_H	Dimension coefficient (= 1.0 for m/d)
C	Empirical constant
T	Temperature
D_{10}	Effective grain size
I_0	Intercept of grain size distribution curve between D_{10} and D_{50}
D_{50}	Median grain size
V	Darcy velocity
dh/dl	Horizontal groundwater gradient
Q	Groundwater discharge
A	Area of groundwater flow

1. Introduction

1.1. Introduction and Definitions

Stream valleys commonly contain floodplains, active stream channels, and sometimes abandoned floodplains or terraces. Leopold et al., 1964, defined floodplains as valley flats built and maintained by an active channel. Junk et al., 1989, added a hydrologic component to the definition: floodplains are periodically inundated by lateral overflow, direct precipitation, or groundwater inputs (Figure 1). Stream channels build floodplains by either (or both) lateral migration or vertical accretion of sediment carried onto the floodplain. Models of floodplain development are based on these sediment depositional styles. Common floodplain evolution models include meander migration as a driving force (through bank erosion and point bar formation or overbank deposition as an accretion mechanism (e.g. Howard, 1992). Although models of floodplain formation have mainly addressed meandering rivers, floodplains, form along most rivers, with a variety of plan-view morphologies and accretion mechanisms. In more recent years, rivers and their floodplains have been studied as integrated channel-floodplain systems that influence sediment, water, and organic budgets (Junk et al., 1989).

Most definitions of active alluvial channels emphasize that they are self-formed and that they tend towards equilibrium or quasi-equilibrium morphology (Lane, 1955; Leopold et al., 1964). Given a naturally-varying range of discharge and sediment characteristics, fluvial geomorphic systems appear to maintain equilibrium channel geometry through time, although the channel form may migrate through space (Hack, 1960; Leopold et al., 1964; Osterkamp and Hedman, 1977; Knighton, 1998). This quasi-equilibrium condition is defined as an equilibrium channel form (although not position), that is maintained while neither aggrading nor degrading the bed (Strahler, 1957; Hack, 1960; Leopold et al., 1964). No explicit equilibrium conditions have been defined for the hydrologic processes in the channel-floodplain system.

Recent research on hydrologic interactions between floodplains and stream channels has focused on documentation of various hydrological processes (e.g. evapotranspiration, groundwater response to precipitation, etc.) or on evaluation of the hydrological connectivity between floodplains and stream channels (e.g., Poole, 2006; Lautz, 2008; Park 2008). Groundwater systems, in particular, can provide continuous exchanges between stream water and adjacent groundwater flow systems. Groundwater and stream water can interact in several ways (Figure 2). First, groundwater can flow through the floodplain and discharge into the stream. In this case, stream baseflow discharge increases downstream between tributary inputs, creating a "gaining" stream segment. Alternatively, stream water can flow into the adjacent floodplain or hyporheic zone under the stream. This creates a "losing" stream that recharges the local groundwater system. A third condition is a floodplain aquifer that transports groundwater largely parallel to the stream. Stream-floodplain flow directions can be spatially and/or temporally heterogeneous. Both gaining and losing stream segments can exist within the same stream system or at various times within the same stream reach (Winter et al., 1998; Woessner, 2000; Sophocleous, 2002). Flow directions of floodplain groundwater depend on the distribution of hydraulic heads relative to the stream surface elevation. In a gaining stream, the elevation of the groundwater is higher than the elevation of the stream water surface. The opposite is true for losing streams. Seasonal variations in precipitation patterns and/or evapotranspiration can alter the stream levels relative to groundwater elevations, and thus groundwater flow directions.

The timing, magnitude, duration and frequency, and source of water to floodplains reflect both local floodplain processes and the overall watershed processes (Poff et al., 1997; Wroblicky et al., 1998; Malard et al., 1999; Wondzell and Swanson, 1999). Floodplain characteristics, (Poff et al., 1997), climate, hydrologic processes, erosion and aggradation, land use channel morphology, and hydrological events affect streamflow, sediment transport, and exchanges of water and sediment between the stream and floodplain (Johnson et al., 1976; Tyus, 1990; Hill et al., 1991; Sparks, 1995; Castleberry et al., 1996; Stanford et al., 1996; Richter et al., 1997). Floodplains can regulate surface runoff rates and amounts (Woessner, 2000; Butturini et al., 2002), and can provide sources or storage of water during hydrological extremes (Wondzell and Swanson, 1999; Sophocleous, 2002; Krause and Bronstert, 2004, 2007).

A limited number of studies have identified the hydrological pathways, particularly groundwater flow patterns, within floodplains (Nortcliff and Thornes, 1984; Hill, 1990; Haycock and Burt, 1993; Waddington et al., 1993; Squillace, 1996; Burt, 1997; Mertes, 1997; Burt et al., 1999). Due to their topographic location and geomorphology, most floodplains are characterized by shallow water table levels. Gillham, (1984), Burt and Haycock (1996) and Burt (1997) have described the water balance of a floodplain in significant detail. Floodplain water tables are maintained by a variety of hydrologic processes including: tributary inflow, groundwater discharge from local or regional flow system, inflow from the channel (overbank bank inundation, etc), and direct precipitation, which is especially important in large floodplains. Low hydraulic gradients and often complicated hydraulic gradients within floodplains help to sustain saturated conditions, especially in wide, complex floodplains. Flow directions between floodplain groundwater and surface streams can change seasonally or during storms as the elevation of the groundwater changes with respect to the stream-surface elevation (Rosenberry and Winter, 1997; Zhang and Schilling, 2006). With continued evapotranspiration and lower contributions of groundwater from hill slopes, hydraulic gradients may reverse from flowing towards the stream during winter conditions to a summer condition, with discharge from the river to the floodplain (Haycock and Burt, 1993; Bates et al., 2000; Burt et al., 2002. In the lower reaches of some watersheds, including coastal streams such as Little Paint Branch, floodplains can remain inundated for long periods such as weeks to month (e.g., Benke, 2000). Therefore, floodplains often support seasonal wetlands with saturated conditions that persist throughout the year (Burt, 1997).

1.1.1. Influence of floodplain hydrology on ecological processes

The importance of hydrology in controlling riparian zone functions has been reviewed by Haycock et al. (1997), Hill (1997), and Cirmo and McDonnell (1997).Floodplains are also important sites for biogeochemical alteration of solutes and particulates, such as nutrients and pollutants (Lowrance et al., 1984; Triska et al., 1989, 1993; Duff and Triska, 1990; Haycock and Burt, 1993; Gilliam, 1994;

Lowrance et al., 1995; Hill, 1996; Brunke and Gonser, 1997; Komor and Magner, 1996). Exchanges between surface and groundwater sources have significant influence on structural and functional quality of stream ecosystems (Brunke and Gonser, 1997) and are produced by physical and biological processes.

Hydrological processes (e.g. surface water dynamics, groundwater flux, etc.) affect local soil moisture characteristics that can affect biological heterogeneity and diversity of flora and fauna in floodplain systems (Bencala, 2000). Channel bars, channel steps, flow obstacles (i.e., debris), and meander bends are all features that generate local hyporheic flow (Hendricks & White, 1988; White, 1990; Harvey & Bencala, 1993; Wroblicky et al., 1998). These geomorphological units are often sites with high rates of hydrological exchange with the surface stream. Due to grain size heterogeneities and permeability variation, different sediment bars can provide a range of hydrological exchange rates within the stream system (Rouch, 1992). Thus, variations in channel geomorphology and sediment permeability can result in a variety of hydrological processes and hydrological exchange rates. Inter-relationships among the hydrological and biological systems can be complex. Therefore, disruption in individual system components can have short and long term effects on ecological processes.

1.1.2. Effects of urbanization on floodplain processes

Urbanization, particularly in unmitigated watersheds, often causes an increase in storm runoff, which can affect channel morphology, sediment mobility, and the relationship between the channel and the floodplain (Leopold et al., 1964; Hammer, 1972). Common stream responses to urban runoff include channel widening

(Hammer, 1972) and channel incision (Rosgen, 1994). Incised stream channels can contain floods larger than the bankfull (~1.5 years recurrence interval) within the channel, resulting in high shear stress during flood flows, which can lead to further channel incision (Darby and Thornes, 1992; Hupp, 1992). The bed erosion that creates incised channels may facilitate drainage of the groundwater from the floodplain. These hydrological changes, particularly the lowering of groundwater tables and changes in the frequency of floodplain inundation result in only one direction of groundwater flow: from the floodplain to the channel (disconnection of the floodplain). These hydrological changes may cause decreases in nutrient and sediment retention along channelized reaches (Noe and Hupp, 2005) which may translate into accelerated storage of sediment and nutrients in channels and floodplains downstream of incised reaches (Darby and Thornes, 1992; Shankman and Smith, 2004; Noe and Hupp, 2005).

Modification of channel morphology therefore can influence exchanges of water, sediment, and nutrients between surface and groundwater systems (Harvey and Bencala, 1993; Wondzell and Swanson, 1996; Hill et al., 1991, Wroblicky et al., 1998, Wondzell and Swanson, 1999). Recently, restoration scientists have begun to consider the role of floodplain hydrology in restoration designs (e.g. Kaplan et al., 2010). For example, “cutting down the floodplain” is a procedure used to facilitate water, nutrient, and sediment exchanges between the floodplain and channel (Palmer et al. 2005). Restoration of exchanges between floodplain and channel can also occur due to natural deposition of sediment bars on the stream beds and banks. These attached sediment bars (of gravel, sand, etc.) can build up the channel bed and accomplish these re-connections without causing disturbances of the natural floodplain. Although the effects of urbanization on channel morphology have been examined for several decades, the long-term effects of urbanization on floodplain hydrology and hydroecology have only recently gained attention.

1.2. Scope of study

The purpose of this study is to examine floodplain hydrological processes in an urban stream channel that has undergone a series of morphological changes. The study is conducted on a channel-floodplain remnant of a once extensive floodplain along the Northeast Branch of the Anacostia River and its tributaries. The stream channel in the Little Paint Branch watershed has experienced widening, channel incision, and recently local aggradation and formation of sediment bars in and along the channel (Blanchet, 2009). Stream channel incision and sediment characteristics of the floodplain and stream channel provide major local controls on fluxes between the stream and the adjacent floodplain (Figure 3).

1.3. Objectives

In this study, the processes that influence exchanges of water between a stream and floodplain are examined in Little Paint Branch creek, which is a tributary to the Anacostia River, MD. Although two sites are examined, most of the study will focus on the upstream site where recent channel aggradation has caused bar formation to build up the level of the floodplain and re-attach the channel to the floodplain. I hypothesize that these attached gravel bars facilitate exchanges of water between the channel and the floodplain. The other site contains an incised channel with a low width to depth ratio and high banks that restrict overbank flooding deposition. A gravel bar is also present at this site, but I hypothesize that it does not facilitate exchanges with the floodplain. The objectives of the study are:

1. To evaluate water exchanges between the stream channel and adjacent floodplain by examining stream water surface elevation and groundwater heads for sites with incised and non-incised channel morphology.
2. To examine seasonal variations in groundwater flow directions in the floodplain and stream channel sediment bars.
3. To evaluate the effects of storm events on groundwater flow directions and rates.

1.4. Review of previous studies

1.4.1. Importance of floodplains in urbanized systems

Floodplains can provide temporary and long term storage for water, sediment, and contaminants (Hupp et al., 2008). Vegetation and soils within a floodplain can store, transform or filter pollutants; shade and cool the stream; and reduce flood by storing or reducing the velocity of flood waters. Within a river-floodplain system, stream banks, chute channels, and other features are created and maintained through the wide range of stream discharges. Stream channels and floodplains and gravel bars are formed and maintained by both bankfull and overbank discharges (Poff et al.,, 1997) that carry sediment, and thus modify the channel and floodplain (Wolman and Miller, 1960). Streams with a low range of bankfull flows intensities, have active floodplains that often migrate laterally and thus maintain the morphology of the floodplain (Leopold et al. 1964). Streams with a wide range of flood flows produce floodplains that contain major bar deposits formed during large flood events (Miller, 1990). Urbanized streams (e.g. Little Paint Branch), in particular, show signs of increased magnitude and frequency of high flows (Hammer, 1972), downward incision and floodplain disconnection (Prestegaard, 1988), reduced baseflows, bank erosion and channel widening (Hammer, 1972) and reduction in the infiltration ability of the soils within the floodplain (Dunne and Leopold, 1978).

Floodplains are natural buffer zones alongside stream channels (Hill 1996; Lowrance et al., 1995), creating hotspots of ecological function within an area of urbanization. There is tremendous variability of the conditions of urban streams and floodplains, depending on historic development, redistribution of sediments, and the overall hydrogeologic conditions of the watershed (Booth, 1990; Trimble, 1997; Pizzuto et al., 2000). However, the conversion of floodplains to urban land use and the subsequent increase in impervious surfaces within the watershed cause stream incision. Incised streams in urban watersheds are typically disconnected from their floodplains (Riley, 1998; Booth et al., 2001), and possess low riparian groundwater levels. Reduction in groundwater levels then drastically affects soils, plants, and the microbial processes found in floodplains (Groffman and Crawford, 2003) by increasing the area of unsaturated soil levels below the surface. The watertable within a floodplain is critical for control of the ecosystem structure and function.

1.4.2. Effects of urbanization on watershed hydrology

Urbanization is one of the most dramatic alterations of ecosystems (Grimm et al. 2000; Pickett et al., 2001). Streams and groundwater are particularly vulnerable to altered hydrology in urban landscapes. The increase in impervious surfaces can alter the rates and flow of water moving into, through, and out of stream and groundwater systems (Arnold and Gibbons, 1996; Dale et al., 2000; Paul and Meyer, 2001). These impervious surfaces decrease interception, infiltration, percolation and storage of water in watershed, which leads to increased runoff during storm events (Dunne and Leopold, 1978). Watersheds with large amounts of impervious cover typically experience decreases in groundwater recharge, stream base flow, and surfacewater groundwater connectivity than undeveloped watersheds (Lazaro, 1990, Bohlen and Friday, 1994; Braune and Wood, 1999; Paul and Meyer, 2001).

Stream and floodplain systems are responsible for the transfer of energy and materials (Gleick, 1998; Palmer, 2000; Naiman et al., 1995). Urbanization of watersheds can decrease baseflow and increase the magnitude of floods (Groffman et al., 2003; Walsh et al., 2005). Geomorphic alterations, and nutrient pulses are two of the specific effects on the floodplains ecosystem attributes due to flooding events (Tockner et al., 2000). Geomorphic alterations specifically, may impact the interactions of the channels with the floodplains and the depth to the groundwater table in floodplains. Changes to groundwater table and interactions between surfacewater and groundwater have effects on floodplain functions and ecological processes (Groffman et al., 2003).

Overbank flooding and floodplain features such as riparian vegetation, chute channels, soils characteristics are closely mutually dependent and these physical characteristics shape the amount of overbank flooding, flows and patterns. The amount of overbank flooding also depends on direct rainfall, tributary water, runoff from the nearby upland areas, and height of groundwater tables (Tockner et al., 2000). The patterns of overbank flooding can affect topography and soil stratification. Flood discharges that spill onto floodplains can recharge local groundwater, therefore, gravel bar formation and floodplain accretion, are important channel processes that mediate the connectivity of channels to the floodplain.

1.4.3. Effect of channel morphology on floodplain hydrology

Channel morphology is influenced by sediment input of upstream sources and ability of the channel to transport sediment loads to downstream reaches. Potential channel adjustments in response to altered discharge and sediment load include changes in width, depth, velocity, slope, roughness, and sediment size (Leopold and Maddock, 1953). Wide, shallow channels have more contact with the bed, which creates an increase in friction. Incised channels have less friction due to low contact with channel bed. Natural channels increase in width when sediment supply exceeds transport capacity. Smooth stream bottoms allows for higher velocities while gravel slows the flow. The size of particles on the streambed is a function of the gradient and confinement.

Channel morphologies have been comprehensively studied and classified (Shumm, 1963; Church, 1992; Rosgen, 1994). Change in stream channel morphology caused by watershed land-use change and channelization, is the basis of river and riparian ecosystem degradation (Naiman et al., 2005; Steiger et al., 2005). Channel morphology is the principal determinant of streamflow and sediment transport rate, where sediment transport rate equals sediment supply (e.g., Lane, 1955; Blench, 1957; Schumm, 1971). Changes in channel morphology that alter groundwater-surfacewater interactions between the stream and floodplain can change soil and groundwater flow regimes across the floodplains (Loheide and Booth, 2010).

1.4.4. Groundwater-surfacewater interactions within floodplains

Patterns of surfacewater and groundwater interactions across floodplains are shaped by local and regional watershed and stream channel geomorphology and hydrology. The degree of interaction is determined by the sediment characteristics and hydraulic conductivity of the streambed and associated floodplain soils (Valett et al., 1996, Dahm et al., 1998, Boulton et al., 1998). Understanding surfacewater-groundwater interactions require the identification of groundwater flow paths and their connectivity to streams, rates of exchange between stream and groundwater systems, and seasonal variations (Wroblicky et al., 1998).

Geomorphic characteristics, such as off-channel features (chute channels) and topographic structures of the streambed and floodplains, can influence groundwater and surface-subsurface rates and patterns within the associated floodplain's hyporheic zone (Harvey and Bencala, 1993; Wondzell and Swanson, 1999; Woessner, 2000; Kasahara and Wondzell, 2003; Anderson et al., 2005; Gooseff et al., 2006a,b; Poole et al., 2006). In addition, timing, duration, magnitude, and source of water input and delivery across the floodplain influences the groundwater fluctuation (Wroblicky et al., 1998; Malard et al., 1999; Wondzell and Swanson, 1999).

Hydrologic studies done at small scales focus on near stream interactions with a particular focus on stream geomorphic characteristics, such as bed form and its influence on the hydrologic exchange between streams and their associated floodplain groundwater systems. Studies have documented hydrologic relationships focused on either variation in groundwater flow pathways with changing river stage (Wondzell and Swanson, 1996, Wroblicky et al., 1998; Malard et al. 1999) or on the variation in geomorphic structure and patterns (Harvey and Bencala, 1993; Wroblicky et al., 1994; Wondzell and Swanson, 1999; Kasahara and Wondzell, 2003). Harvey and Bencala, (1993) established that topographic variations in stream mountain catchments are hydrologically isolated at the head of riffles pools from floodplain groundwater under baseflow conditions. Another study showed that meander bends in streams are expected to generate floodplain flowpaths depending on their orientation relative to the local groundwater flow system (Larkin and Sharp, 1992). Another study showed that hyporheic flow in coarse-grained rivers have been conducted, mainly through field experiments and modelling (Harvey and Bencala, 1993; Wondzell and Swanson, 1996; Worman et al., 2002; Storey et al., 2003; Gooseff et al., 2006a,b). Although multiple studies strengthen the view of the hyporheic zone as a dynamic system (Gibert et al. 1994, Jones and Mulholland 2000), studies that consider geomorphology and groundwater flow regime concurrently (Henry et al. 1994, Storey et al. 2003) are scarce and analyses on larger gravel dominated floodplains excluding Poole et al. (2006).

2. Study Site and Methods

2.1 Floodplain study site

The purpose of this study is to examine the effects on channel morphology and sediment bar accretion on the interactions between stream flow and groundwater flow in a floodplain-channel system. Therefore, requirements for the study site include: a) presence of an intact floodplain, b) variations in stream channel morphology within the floodplain site, and c) lack of rip-rap or channelization features that could influence channel-floodplain interactions. With these criteria in mind, a study site was chosen along the lower reaches of Little Paint Branch, a tributary of the Northeast Branch of the Anacostia River (Figure 4). The relationship between the channel and floodplain changes along the length of the study reach. The upstream portion of the site is not incised and the stream flows overbank during bankfull and higher flood events. The downstream reaches of the river are incised and overbank flooding is less frequent. Both sites have been gauged, thus partial hydrographs are available for storm events at the upstream and downstream locations.

Two sites were chosen within the floodplain-channel system in which to monitor groundwater flow and its relationship to the stream (Figure 4). The upstream site is at the location of active gravel bar formation. Blanchet (2009) found that bar formation has caused shoaling of the channel bed and that the river overtops the banks 3-4 times per year. At the downstream site, gravel bars are inset into a channel with higher banks than those at the upstream reach. Site 1 at the upstream reach has banks ranging from 0.01 to 1 meter above streambed whereas at Site 2 the bank height ranges from 0.6 to 1.56 meters above streambed. During the study period, overbank flooding occurred only during very large flood events, while the upstream site exhibits overbank flooding during bankfull and higher events that have occurred several times a year during the study period.

Gravel bars have recently formed and accreted onto the floodplain at the upstream site; this creates a veneer of gravel and sand over the floodplain sediments (Blanchet, 2009). At depth, both the stream bed and adjacent floodplain are underlain by compacted fine-grained (clay) sediment. Along the stream, this clay layer is overlain by sand and gravel. The recently accreted gravel bars have created a bar and chute topography. The small chute channels carry flow from Little Paint Branch onto the floodplain during flow events, including events that are below bankfull stage. The largest of the adjacent chute channels runs parallel to the channel in the northwest corner of the study site (Figure 5A). There are also two active gravel bars present at this site (Figure 5A.-a, c). Figure 5B shows the downstream study site and gravel bars.

2.2. Methods

2.2.1. Channel cross sectional surveys

Channel and floodplain topography was surveyed to determine channel elevations and the relationship of the channel morphology to the adjacent floodplain. This survey included a total of 11 channel-floodplain transects. A tripod was setup at a central location and multiple transects were surveyed using a surveying level. Horizontal distances along each transect were measured with a taut measuring tape that extended from along the entire transect of the floodplain-channel system. A stadia rod was used to obtain the elevations measurements and was held along the bottom of the stream bed or floodplain topography. Topography was measured at 1 m interval across both the floodplain and stream channel.

2.2.2. Groundwater monitoring

2.2.2.1. Piezometer installation:

At both sites, piezometers were installed in a series of transects that extended from the stream edge into the adjacent floodplain. The locations of the piezometer transects were chosen to provide groundwater elevations and flow directions in the floodplain. Groundwater piezometers were installed on both vegetated and non-vegetated gravel bars. The upstream site, Site 1, includes eight transects, labeled A-H and the downstream site, Site 2, contains five transects labeled V-Z. Transects varied from one piezometer to eight piezometers. The length of the sites and the width of the monitored sites were determined by the length and width of the gravel bars. Distances between piezometers in each transect ranged from 4 to 6 meters. Distances between transects varied from 12 to 20 meters. A total of fifty-one piezometers were installed at Site 1. A total of nine piezometers were installed at Site 2. The differences in size of the piezometer networks are based on the observed stream water excursions onto the floodplain at the two sites as well as floodplain size. A simplified version of the topographic map of Site 1 is shown in Figure 6 along with the location of the piezometers. Piezometers are distributed along transects between the stream and the higher level floodplain. The map also shows the position of the chute channel that enters the stream above the study site and reenters the stream slightly downstream of the study site. This chute channel conveys a secondary channel during flood events and is active at least four times a year. Cross section equipotential diagrams will show the relationship between flow in the chute channel and the adjacent groundwater during high flow periods. Piezometers were installed in holes bored with a 2.54cm auger to a depth of approximately 1.3 meters. All the piezometers were installed above the basal clay layer and were installed to depths at or greater than the mid summer water table, which is the expected minima for the period of study. Each piezometer was ventilated to allow for proper pressure equalization with the insertion of a hole near the top of each piezometer in the above ground section.

2.2.2.2. Surveys of ground surface and piezometer elevations:

After the piezometers were installed, the ground surface and piezometer elevations were surveyed starting at the stream bank. Elevations of the ground surface was measured at one meter intervals along transect locations using a stadia rod. At each piezometer, the elevations of each piezometer top and base were surveyed in order to depict piezometer locations along transects. Once again a measuring tape was stretched from the stream bed to approximately 2 meters passed the last piezometer in each transects. The tripod was minimally relocated in order to avoid error in calculating back sites and foresights.

2.2.2.3. Monitoring of Piezometric head:

Measurements were taken from July 15th, 2009 through August 19th, 2010 in the morning hours between 9am and 11am to minimize diel influences. Total head in the piezometers was determined using a steel measuring tape that was used to measure the depth of water in the piezometers relative to the top of the piezometer.

Measurements were made at least once a week to determine seasonal variations. Measurements were also made before, during, and following a storm event in late September to October to determine piezometric response to a tropical storm. Total head is calculated from the water depth measurements:

Total Head = Piezometer Bottom Elevation + Depth of water in piezometer

2.2.2.4. Determination of hydraulic conductivity:

Hydraulic conductivity is a property of both the fluid and the porous media. Hydraulic conductivity can be measured in the lab, measured in the field, or estimated from grain size. In shallow groundwater systems, the presence of macropores increases the hydraulic conductivity of silt, clay, and mixtures of sand, silt and clay. Thus, the hydraulic conductivity is not a simple function of grain size and hydraulic conductivity should be measured *in-situ*. Macropores, however, collapse in coarse sediment (sand and gravel) and thus hydraulic conductivity is more closely related to grain size for study site such as this one. Due to the high hydraulic conductivity, slug tests are often difficult to conduct for sand and gravel mixtures as found at Little Paint Branch field site. Therefore, hydraulic conductivity was estimated from grain size.

Samples of gravel bar sediments and floodplain soils were collected along each transect. Samples were collected for each geomorphic surface along each transect. In all, 14 samples were collected and analyzed to determine grain size distribution, which was used to estimate hydraulic conductivity. Once collected, samples were taken to the lab and spread out within individual trays and allowed to air dry for two weeks. Sediments were sieved to determine particle size distributions. Nested sieves at half phi intervals (16mm through 0.063 mm) were used to determine the weight percentage in each size class. Grain size distributions were plotted as semi-logarithmic graphs to determine grain-size distribution curves and grain size statistics for each sample. Empirical relationships were then used to estimate hydraulic conductivity from standard grain size parameters. The grain size diameter at which 10% of the sediment is finer (D_{10}) could be applied using empirical formula, initially developed by Hazen (1892): $K=A_HCT(D_{10})^2$ (Equation 1) where A_H is a dimension coefficient (= 1.0 for m/d), C is an empirical constant (=860) and T is a temperature correction factor (=1 at 10° C). A second empirical relationship that utilizes the grain size distribution was also used. This empirical relationship, developed by Alayamani & Sen (1993), uses the slope and intercept (I_0) of the grain size distribution curve between D_{10} and the median grain size (D_{50}): $K= 1300(I_0 + 0.025(D_{50}-D_{10}))^2$ (Equation 2). Where K is the hydraulic conductivity (m/day), I_o is the intercept (in mm) of the line formed by D_{50} and D_{10} with the grain-size axis, D_{10} is the effective grain diameter (mm), and D_{50} is the median grain diameter (mm).

2.2.2.5. Analysis of groundwater head data

Groundwater head was analyzed by a) plotting time series graphs of total head data to determine seasonal changes in groundwater heads, b) by constructing groundwater probability graphs that depict the amount of time that the groundwater table is at various depths below the ground surface, and c) by constructing flow nets of equipotential and flow lines of groundwater flow in the floodplains.

Time series graphs of total head

During the course of study period between July 15th, 2009 and August 19th, 2010, each measurement of total head for each piezometer was graphed as a function of time to obtain time series graphs of water table elevations for each piezometer.

Over the period of the study, these time series measurements were used to determine seasonal variations in the elevation of the groundwater table. Seasons were broken down as follows: June, July, August for the summer season; September, October, November for the fall season; December, January, February for winter season; March, April, May for the spring season. In addition, the data was used to evaluate steady state conditions in addition to identify storm influences indicated by peaks in the time series graphs during the year. Piezometer total head data from steady state periods can be used to determine equipotential maps of the water surface.

2.2.2.6. Construction of flow nets:

Flow nets were constructed from equipotential maps of groundwater head that are used to determine groundwater flow directions. These maps were constructed using the topographic base map and head data for individual dates and piezometers using ArcGis version 10.0 (ESRI, Redlands, California, USA). Maps were made for steady state conditions determined from time series data over the past year to depict groundwater flow. High groundwater conditions during winter and summer months, and low groundwater conditions of late summer, have also been constructed.

The groundwater flow nets and hydraulic conductivity data were used to determine groundwater flow in the flood plain. For each steady state condition, groundwater flow rates were determined using Darcy's law: $v = K(dh/dl)$. Where K is the horizontal hydraulic conductivity, dh/dl is the difference in height over the change in length, and v is the Darcy velocity. Groundwater discharge carried by the floodplain is calculated as: $Q = vA = A*K(dh/dl)$. Where A is the cross sectional area perpendicular to flow, this analysis can be simplified through the use of flow nets.

2.2.2.7. Use of GIS to determine flow patterns and elevations

ArcMap was used to determine the flow patterns and elevation gradients along Little Paint Branch floodplain. Using the results from the time series graph created above, steady state conditions for each season was obtained as well as the year's high and low conditions. These six conditions and corresponding dates were then formatted in a excel spreadsheet. In addition to adding a shapefile of a satellite map of Little Paint Branch, I added tabular data that contained geographic locations in the form of x,y coordinates to the map. Latitude and longitudinal values were determined using Google Earth and then the values were converted to decimal degrees. In order to have spatial reference, the longitude and latitudes were projected from GCS North American 1983 coordinate system, state plane of Maryland, creating a shapefile.

In order to minimize ArcMap response and estimation, the study site was fitted with a mask that encompasses the piezometers. Two masks were created, a full mask with all the piezometers, and a partial piezometer mask to accommodate the partial data set of piezometers from July to December. Some steady state conditions had data for all piezometers for the full year, where as some piezometers were installed later in the study consisting of half of a year worth of data for each piezometer. These masks were fitted based off the area surrounding the piezometers and minimized empty space. Setting an analysis mask allowed processing of only the selected locations. All other locations were assigned values of NoData and cells with values were only considered in the interpolation.

The water level elevations were then interpolated using kriging spatial analysis. Kriging interpolation uses geostatistical models including autocorrelation.

Kriging allowed for the surface prediction while providing some measure of certainty or accuracy of the predictions. Kriging assumes the direction between piezometer points reflects a spatial correlation that can be used to explain variation. The Kriging tool was set to the specified points located with the determined mask and given an output value for each location. Using a Gaussian influenced semivariogram depicting the spatial autocorrelation of the sampled piezometers, the nugget (intercept of y-axis), range (where model flattens), sill (value on y-axis at range) and lag size (size of a distance class) were calculated and added into the interpolation. Each of the six conditions were fitted to a kriging interpolation output and displayed with use of four classification groups determined by natural breaks. Natural classes are based on natural cluster present in the data. ArcMap identifies break points by picking the class breaks that best group similar values and maximize the differences between classes. The features were then divided into classes whose limits are set where there are values relatively different.

Using the contour lines function and the created kriging interpolation output raster, equipotential lines were created based off of the piezometers hydraulic head elevational values with intervals of 0.05 and 0.1 meters. This was completed for every condition for both sites. Next 3D maps were created using ArcScene using the kriging interpolation from the previous step. Here the layers were stacked on top of each other based on the kriging output to show the water levels and topography over the course of time in a 3D view.

3. Results

The results section is organized as follows: 1) Hydrological framework (precipitation and streamflow), 2) Hydrostratigraphic units, 3) Seasonal distributions of groundwater head depicted as both time series diagrams and seasonal groundwater equipotential maps, 4) Probability distributions of groundwater head at various distances the channel, and 5) Response to fall storm event.

3.1. 2009-2010 Precipitation and stream discharge

3.1.1. Precipitation

Precipitation data were obtained from the NWS Beltsville gauge. A total of 111.6 cm of precipitation occurred throughout the monitoring period from July 15th, 2009 to August 19th, 2010 with a mean of 0.24±0.76 cm (Figure 7), which corresponds to an annual precipitation of 80.2 cm. Precipitation in Maryland does not usually exhibit pronounced seasonality, and this was observed during the study period, note the nearly constant slope of the cumulative precipitation diagram (Figure 8).

Major storm events generated overbank flooding onto the floodplain and activation of the chute channel, which also brought water into the floodplain. Although baseflow showed some seasonal variation (Figure 9), overbank flooding was generated only by storm events. A minimum of 2.2 cm of precipitation per day appeared to be required to initiate overbank flooding events. Daily precipitation exceeded 2.2 cm seven times during the study period. These major storms occurred in both summer and winter periods. In late summer, tropical storms occurred on: 9/26/09, 8/12/2010, 8/18/10, and 9/30/10. Several major winter storms occurred on 12/9/09, February 5-6 and February 9-10. The February storms were snowfall events, and snowmelt was distributed over a period of time, which attenuated the flood events. The largest daily rainfall total of 7.04 cm of precipitation occurred on August 18, 2010. The largest snow event occurred on February 6, 2010, with a total of 8 cm of water equivalents of snowfall. Storm flow hydrographs were generated by storm events throughout the year, with the largest events occurring in late summer and winter periods (Figure 9).

3.1.2. Topography and grain size distribution at Site 1

The movement of water between the floodplain and the stream channel is facilitated by both topography and the permeability of the sediment. Therefore, maps of a) gravel-bar and floodplain topography and b) of the spatial distributions of surface grain size were constructed for Site 1. This upstream study site contains two gravel bars that have been accreted into the floodplain. A simplified version of Site 1 topography is shown in Figure 6. This map of the topographic surface shows the distribution of topography relative to the stream channel as well as the locations of piezometers and chute channels. Piezometers are distributed along eight transects that extend from the stream channel, across the accreted gravel bars and into the higher level floodplain are also shown on this map (Figure 6; Illustration 1). Surface topography controls stream flow advection onto the floodplain. Streamflow could be transported onto the floodplain in two distinct ways: overbank flooding directly onto the floodplain and via a chute channel that occupies the space between the two accreted gravel bars (Figure 6). The main chute channel flows from the stream onto the floodplain and then reenters the stream slightly downstream of the study site. This chute channel (Illustration 1) conveys flow into two secondary channels during flood events (Illustration 3). The chute channel actively conveyed water onto the floodplain at least four times during the period of study.

Illustration 1: Photo showing floodplain characteristics of Site 1. (A) Little Paint Branch stream channel; (B) immediate floodplain/gravel bar; (C) Primary chute channel; (D) Uplands. Photo shows view looking downstream.

Illustration 2: Photo looking down chute channel for Site 1. (A) Little Paint Branch stream channel; (B) immediate floodplain/gravel bar; (C) Primary chute channel; (D) Uplands. Photo shows view looking downstream.

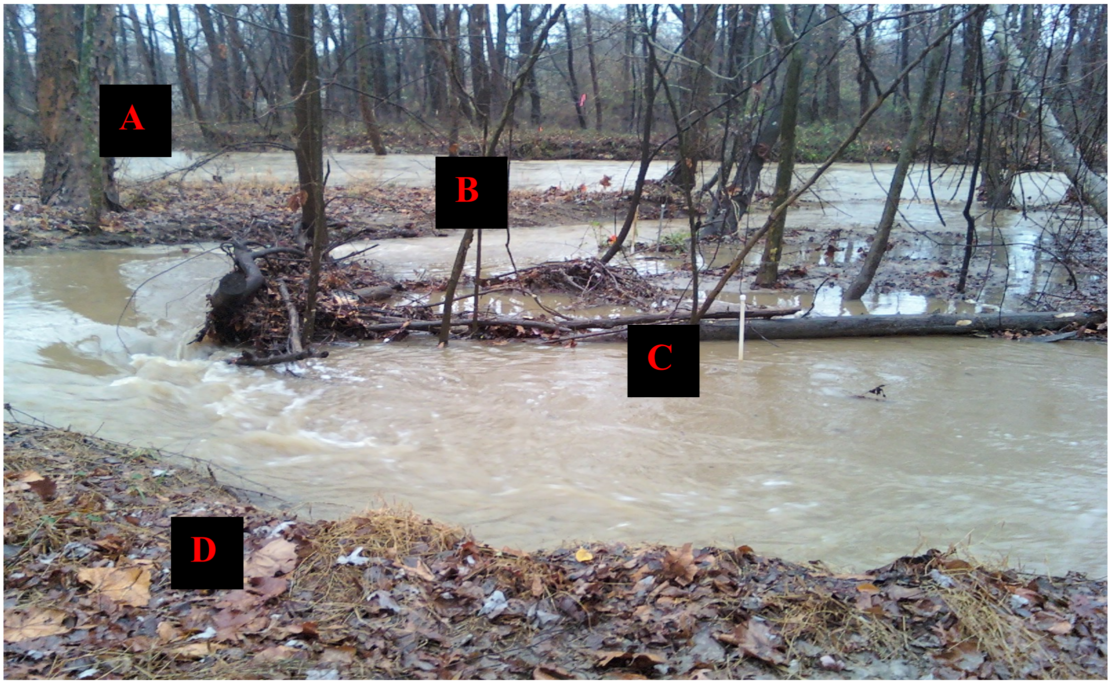

Illustration 3: Photo showing various channels during storm event on Site 1. (A) Little Paint Branch stream channel; (B) secondary chute channel; (C) Primary chute channel (D) uplands. Photo taken during a major storm event. Photo shows cross sectional view from uplands towards stream.

3.2. Identification of hydrological units

Hydrostratigraphic units are defined as a stratigraphic formation or groups of formations that have similar hydraulic characteristics (Fetter, 2001). Hydrostratigraphic units are usually defined by hydraulic conductivity or grain size similarities for heterogeneous alluvial floodplain sediments. In this section, grain size distributions of floodplain and gravel bar materials are presented. These data are used to estimate hydraulic conductivity values and to define hydrostratigraphic units.

3.2.1. Determination of hydraulic conductivity values

The hydraulic conductivity of floodplain and gravel bar systems often reflects underlying stratigraphic characteristics (Rovey, 1990; Rovey and Cherkauer, 1994a, b; Rovey and Cherkauer, 1995). Floodplain hydraulic conductivity is often measured in the field or estimated from grain size data for representative samples of identified hydrostratigraphic units. A variety of methods have been used to estimate hydraulic conductivity from grain size data. These methods use mean grain size or a smaller size fraction (D_{10}) that is thought to represent equivalent pore sizes (e.g. Hazen, 1892; Fetter, 2001). An alternative method uses the entire grain size distribution rather than a single "representative" grain size (e.g. Alyamani and Sen, 1993). Both the representative method (D_{10}) and the grain size distribution method were used to estimate hydraulic conductivity for the sediment in the gravel bars and floodplains at the study sites. These methods were compared and were considered to give different results when K values estimated by the two methods placed the soil sample in different classes (Table 1). These differences occurred for 42 percent of the time of the samples tested. Reference size and hydraulic conductivity classes were based from studies presented by Lappala, 1978 and Schwartz et al. 2003 using ranges of hydraulic conductivities for unconsolidated sediments (Table 1). Sediment and soil samples were sieved and D_{10} and D_{50} values were obtained from grain size distribution curves (Figure 10). Hydraulic conductivity values for the various sediments vary over orders of magnitude (Table 2), as would be expected for sediment sizes that range from silt to gravel. Hydraulic conductivity values that were estimated by the two grain-sized based methods varied by less than one order of magnitude, indicating a relatively homogeneous hydrostratigraphic unit. The greatest difficulty was with the estimate of hydraulic conductivity for gravel samples, which are difficult to measure by *in-situ* field tests, and are not well-defined by most grain-size dependent methods. The value of C for the Hazen method was estimated to be 120 for the gravel samples. A value of C for most of the other samples was estimated to be 60, because they were fine sands. Comparison of the two methods suggests that the methods diverge significantly for the coarser samples suggesting grain-size based estimates of hydraulic conductivity for this site may be improved by calibration with *in-stiu* field tests.

Table 1: Ranges of hydraulic conductivities of sediment types

Sediment Class	Hydraulic Conductivity K (m/d)
Sandy silt	1-2
Fine to medium sand	2-10
Course sand	10-20
Fine to medium gravel	20-50
Course gravel	50-100
Gravel and cobbles	100-1000

Table 2: Hydraulic conductivities calculated from grain-size analysis

Gravel Bar Piezometer	D10, (mm)	D50, (mm)	A&S K, m/day		Hazen K, m/day		
A2 (0-53 cm)	0.11	0.25	8.01	Med. Sand	6.27	Med. Sand	*
A2 (53-92 cm)	0.12	0.50	1.55	Fine Sand	7.46	Med. Sand	
B3 (0-79 cm)	0.21	0.34	42.47	Course Sand	22.86	Course Sand	*
B3 (80-98 cm)	0.11	0.23	8.96	Med. Sand	6.27	Med. Sand	*
C1 (0-23 cm)	0.11	0.28	6.69	Med. Sand	6.27	Med. Sand	*
C1 (24-66 cm)	0.08	0.25	2.27	Fine Sand	3.32	Fine Sand	*
C2 (0-77 cm)	0.13	0.27	12.61	Med. Sand	8.76	Med. Sand	*
C2(78-100cm)	0.10	0.50	0.13	Silt	5.18	Med. Sand	

D1 (0-35 cm)	0.13	0.27	11.09	Med. Sand	8.10	Med. Sand	*
D2 (0-30 cm)	0.14	0.51	4.19	Fine Sand	10.16	Med. Sand	
D2 (30-60 cm)	0.20	1.40	6.37	Med. Sand	20.74	Course Sand	
E3 (0-33 cm)	0.13	0.25	12.20	Med. Sand	8.10	Med. Sand	*
E3 (33-53 cm)	0.14	1.70	57.88	Course Sand	**20.32**	Course Sand	*
Uplands Piezometer	**D10, (mm)**	**D50, (mm)**	**A&S K, m/day**		**Hazen K, m/day**		
A5 (0-40 cm)	0.19	3.00	254.2	Gravel	**37.41**	Course Sand	
A5 (40-52 cm)	0.20	2.00	54.6	Course Sand	**41.47**	Course Sand	*
A5 (52-72 cm)	0.08	0.50	0.27	Silt	3.32	Fine Sand	
A6 (0-34 cm)	0.06	0.18	1.42	Fine Sand	1.87	Fine Sand	*
B6 (0-38 cm)	0.19	6.00	1622.72	Gravel	**37.43**	Course Sand	
B6 (38-64 cm)	0.09	0.27	3.19	Fine Sand	4.20	Fine Sand	*
B7 (0-36 cm)	0.06	0.14	2.29	Fine Sand	1.87	Fine Sand	*
B7 (36-61 cm)	0.09	0.40	0.53	Silt	4.20	Fine Sand	
B7 (61-78 cm)	0.07	0.40	0.02	Silt	2.54	Fine Sand	
C5 (0-66 cm)	0.06	0.17	1.62	Fine Sand	1.87	Fine Sand	*
D4 (0-70 cm)	0.01	0.20	1.39	Fine Sand	0.05	Silt	
D4 (70-93 cm)	0.14	0.60	1.73	Fine Sand	10.16	Med. Sand	
F4 (0-70 cm)	0.06	0.18	1.42	Fine Sand	1.87	Fine Sand	*
* indicate same sediment class for both methods. Bold numbers indicate Hazen C coefficient was based off of course sand.							

3.2.2. Spatial distributions of grain size, and hydraulic conductivity values

The grain size distributions of the gravel bar, floodplain, and chute channel samples were heterogeneous with grain sizes that ranged from gravel to silt. The gravel bars near the stream channel contain coarse, well-sorted sediment. The floodplains further from the active stream are much finer grained sediment and also more poorly sorted. Hydraulic conductivity values estimated from grain size distribution data ranged from 0.02 to 1622.72 m/day (table 2). The Alyamani and Sen (1993) method indicated that the highest values of hydraulic conductivity, K, were found in and along the chute channel. Active sediment transport in the channel brings in coarse sediment and carries out fine sediment. Therefore, the chute channel had a much higher hydraulic conductivity value for the upper 0-40cm soil layer than the other sites. The gravel bars have a thin layer of gravel at the surface, but the subsurface material and the pore spaces are dominantly medium sand. Most locations indicated larger grain sizes at the surface, with the exception of piezometer location E3, which has a lower grain size near the surface. Table 3 summarizes these data and indicates that the uplands are dominated by fine sands whereas the gravel bar is dominated by medium sands.

3.2.3. Map of average hydraulic conductivity

Maps of grain size distribution and hydraulic conductivity were constructed using the surface D_{50} and the hydraulic conductivity values for each of the sampled locations based of the Alymani and Sen method, 1993 (Figure 11). The grain size distribution map indicates that the chute channel has the highest D_{50} values. Lower grain size values are found on both sides of the chute channel. Excluding the chute channel, however, the hydraulic conductivity values decrease from the stream towards the uplands. The upland floodplain exhibited homogeneous values of hydraulic conductivity ranging from 1 to 2 m/day, which is consistent with the sandy-silt material found in the floodplain. The highest values of hydraulic conductivity are found in the chute channel (> 100 m/day), which represent sandy gravel. The downstream end of the chute channel has K values of 2-50 m/day. The immediate gravel bar floodplain area showed fine to medium sand/gravel mixture.

3.2.4. Cross sectional view of grain size data

Sediment and soil samples were taken at various depths in the uplands and the gravel bar. These data are shown in Figure 12, which shows the soils to about 1 meter depths (similar to the elevation of the active channel). In the upland floodplain the grain size is fairly homogeneous with depth. The gravel bars are composed of layers of sand and gravel, which vary from site to site. Soil profiles indicate that grain size and hydraulic conductivity is highest near the surface at most locations, this is consistent with the observation that the gravel bars are recent additions to the floodplain system and have been accreted on top of and adjacent to pre-existing floodplain sediments. An exception is in transect E, which shows evidence of deposition of the sediments over a shallow gravel bar at depth.

3.3. Seasonal distributions of groundwater heads depicted as both time series diagrams and seasonal groundwater equipotential maps

3.3.1. Groundwater head data

Groundwater head data were monitored to determine the relationship between the stream channel and the floodplain groundwater system at both the accreted gravel bar site (1) and the incised channel gravel bar (2). At the floodplain site, an extensive groundwater monitoring network was installed to determine exchanges of flow between the channel and the floodplain. Piezometric head data were also used to evaluate the effects of the chute channel on local recharge and discharge from the adjacent groundwater system. Total heads in the piezometer networks were monitored weekly for the study period July 15th, 2009 to August 19th, 2010. The groundwater data from the two sites will be discussed separately; the most extensive analysis is for the upstream site, which is the site of aggradation and attachment of gravel bars to the floodplain.

The groundwater head data have been analyzed and presented three formats: a) time series analyses, b) map views, c) cross section views of total head. The time series data were used to identify steady-state time intervals for each season. Head data during these intervals were used to generate equipotential maps and cross sectional equipotential diagrams that illustrate steady state heads within the gravel bars and adjacent floodplain groundwater.

3.3.2. Time series data of total head

Time series of groundwater head data were measured at all transects within Site 1. Transects A, C, and E were selected to illustrate total head time series for piezometers installed in the floodplain (Figure 13). In these time series diagrams, selected piezometers are identified by their distance from the stream bank (meters) and categorized by location within the floodplain (inset gravel bar, chute channel, and uplands). Extreme high events (12/9/09 and 8/12/10) were removed to show seasonality. At Site 1, total head steadily increased from early fall through spring. This increase in total head is primarily associated with the decline in evapotranspiration demand. The spring increase in evapotranspiration demand is associated with the observed decline in groundwater levels that began in the spring

(March 13th, 2010) and reached a minimum in the late summer. In late summer in both 2009 and 2010, large-magnitude tropical storms ended the summer decline in groundwater levels. Storm-induced spikes in groundwater levels occur throughout the year, but are of varying duration and magnitude. Maximum groundwater head elevations were observed as consequences of large storm events. The largest storm events for which groundwater conditions were monitored were the two largest storm events in the period of record: the December 9th, 2009 and the August 12th, 2010 events. The groundwater minimum occurred on September 23rd, 2009, a result of cumulative evapotranspiration demand over the summer months.

Although seasonal variations in groundwater heads were observed at all sites, the timing and amount of seasonal variation in groundwater head varied with position on the transect. Piezometers located in floodplain materials (silts and clays) showed a slow increase in head in the fall as evapotranspiration decreased in the late fall into the winter months. These sites also drained slowly as evapotranspiration demand increased in the spring and continued into the summer months. This behavior is very different than the adjacent sand and gravel bar that maintained much more constant groundwater heads over the time period. The time series data of the gravel bar located at Site 2 (transects Z, W, V) responded similarly to the upstream gravel bar (Figure 14). The inset gravel bar at Site 2 showed minor changes in groundwater table elevations, which reflect baseflow conditions. The gravel bar piezometers at Site 2 also indicate perturbations associated with the major storms that were observed at Site 1 Minor storms were less observable at Site 2 compared with Site 1.

The time series data were used to identify steady state conditions to generate equipotential diagrams. Dates were selected to illustrate: fall (10/14/2009), winter (1/13/2010), spring (4/15/2010) and summer (7/21/2010) conditions. In addition to creating equipotential diagrams for each of these steady state conditions, equipotential diagrams for two high flow conditions were also generated and examined. The first high flow event was an above-bankfull flood event that occurred on 12/9/2009 and the second, a high flow event, that caused chute channel flow onto the floodplain, but did not cause overbank flooding. This event occurred during a tropical storm on 8/12/2010 (Figure 15).

3.3.3. Seasonal Equipotential Maps

Equipotential maps of the water surface were constructed for the fall, winter, spring, and summer steady state conditions, using groundwater head data (Figure 16). Total head values varied less than 0.7 m within the sediment bar-floodplain system (head values ranged from 9.14 to 8.45 m). In summer and fall periods (intervals of high evapotranspiration demand; Illustration 4), groundwater elevations were highest near the stream and adjacent gravel bar for transects A-C (Figure 17). During periods of low evapotranspirative demand (winter and spring), the highest total head values were associated with the higher elevations in the floodplain at all transect locations (A-D) (Figure 18). During winter and spring conditions, the lowest head values were located at sites within transects with low topographic elevations, similar to stream water surface values.

Illustration 4: Photo showing vegetation at Site 1. (A) gravel bar; (B) Primary chute channel (C) uplands. Photo taken during a storm event looking down the chute channel.

The maps of groundwater equipotential values and associated groundwater flow directions (Figure 17) indicate that groundwater flows from Little Paint Branch into the floodplain for both the fall and summer seasons. During this time of year, piezometric heads are low in the floodplain, therefore water flow directions are from the stream into the adjacent gravel bar and then into the finer-grained floodplain. The equipotential gradient is opposite of topographic gradient due to the continuous source of water from the stream and the continuous sink for groundwater caused by evapotranspiration in the floodplain. The equipotential maps showed that the stream water seeped into the floodplain in transects A-C, distributed throughout the floodplain, and drained into the chute channel and back into the stream near transects D and E.

The equipotential maps for winter and spring conditions indicate that the groundwater flowed from the floodplain towards the stream. The floodplain during the winter and spring (Figure 18) months is recharged by precipitation and local runoff, during periods when evapotranspiration is low. This results in groundwater equipotential maps that follow the topography, with some modification due to the variations in hydraulic conductivity in the floodplain, particularly along the chute channel. Groundwater at the north end of the floodplain flowed sub-parallel to the stream seeped into the stream at the topographic lows located near the stream at transects D and E.

During all four seasons (Figure 16), a significant component of the flow is sub-parallel to the stream. The source of flow, however, switched from the uplands in the winter and spring, to the stream in the summer and fall. This resulted in two groundwater flow reversals annually. One reversal occurred between the fall and winter seasons and the other occurred between spring and summer. These reversals are also observed on the time series diagrams. The source of flow was calculated and determined to show a greater quantity of flux for summer and fall with flow from the stream rather than flux from the uplands during winter and spring (Figure 19).

3.3.4. Cross section diagrams

Cross section views of groundwater potentials were constructed for the upstream transects at Site 1 where groundwater equipotential gradients are approximately perpendicular to the transects, sub-parallel to the stream. The steady state total head data that were used to construct the equipotential diagrams were also used to generate cross-sectional views of groundwater potential. These cross section views were used to examine the role of the chute channel as a groundwater recharge or discharge feature. Cross section diagrams were created for individual transects of the stream-floodplain system for seasonal steady-state conditions, low conditions in addition to the tropical storm and winter storm events. Each diagram shows surface topography along transects and the total head data for the four steady state conditions and groundwater potential maximum and minimum conditions. At Site 1, transects A, C, and E (Figure 20), were examined because they emphasize the role of the chute channel that enters upstream of the floodplain site. Spatially across the floodplain, all transect show similar patterns (Figure 21).

The cross section equipotential diagrams for Site 1 were summarized as three main scenarios. These scenarios are: 1) flow from stream to floodplain, 2) flow potential from floodplain into the stream, and 3) third bowl-shaped condition, which demonstrates the influence of the chute channel. Transects A, B, and E display declining slope of potential surface from the stream to floodplain for fall and summer seasons. The majority of transects (7 out of the 8) indicate that groundwater flows from the stream to the floodplain in the summer to early fall seasons (Table 3).

The second scenario flows from the floodplain into the stream, consistently occurred at transect F. This was due to the higher elevations at this transect and the absence of a gravel bar attached to the floodplain. At transects A, D, and E, groundwater flowed from the floodplain towards the stream during the winter and spring months. The third scenario is a bowl-shaped distribution of groundwater potentials, with higher values near both the stream and the upland floodplain. This scenario displays the role of the chute channel in distributing flow. This scenario is observed most prominently at transect C, which received flow from both the upland and the gravel bar. Flow was routed down the chute towards the stream channel or towards other sinks during fall, winter, and spring conditions. Transects B and G also showed this distribution of groundwater potential in winter and spring (Table 3).

Table 3: Three scenarios observed in Site 1 cross section equipotential diagrams

Seasons	**1: Stream to floodplain**	**2. Floodplain to stream**	**3: Bowl-shaped**
Fall	A, B, E	F	C, D
Winter	H	A, D, E, F	B, C, G
Spring		A ,D, E, F, H	B, C, G
Summer	A,B, C, D, E, G, H	F	

The potential surfaces illustrated in both the map and cross section views indicate seasonal reversals in flow due primarily to seasonal variations in groundwater levels in the upland floodplain. This is likely caused by two processes, seasonal variations in evapotranspiration rates and lag times in piezometric responses between the coarse grained gravel bar and the fine-grained floodplain. These grain size-based characteristics were examined in the previous section.

3.4. Probability distribution of groundwater heads

Groundwater head data also provide information on the depth to the groundwater table at the site. Many models of floodplain ecological functions are based on inundation times or the amount of time that the floodplain sediments are saturated (Junk et al. 1989). Groundwater probability diagrams were constructed for the groundwater data at each of the transect locations. These data are plotted as the percent of time that the groundwater table is at or above a given depth relative to the ground surface (Figure 22). For Transect A, the groundwater reached the ground surface 2% of the time at the gravel bar adjacent to the channel (piezometer A3) and 12% of the time in the chute channel (piezometer A5). Depth of flow in the chute channel was greater than 0.55 meters 2% of the time, consistent with overbank flooding on both the gravel bar and in the chute channel. At transect C, the groundwater reached the surface of the chute channel 14% of the time (piezometer C4). The groundwater table was always below the ground surface for the upland floodplain piezometers, but the water table approached the surface (0.4-0.2 m) 2% of the time for many of the upland floodplain sites within the study reach. For the upland floodplain, most of these high water tables occurred in the winter and early spring. Due to the lower topography at transect E, the gravel bar was flooded 3% of the time to depths of 0.1 m, however, the chute channel and upland piezometers for transect E indicated that the water table never reached the surface, although the chute channel was within 0.1 m of the surface 2% of the time. In summary, for this floodplain groundwater system the water table is closest to the surface in the coarse grained portions of the reach. Due to the high hydraulic conductivities, however, the water table maintains saturated conditions only for short periods. The finer-grained upland floodplain had lower groundwater elevations for most of the summer season. Groundwater tables were closest to the surface during the non-growing season, when evapotranspirative demand was lowest.

3.5. Piezometric and stream responses to storm events

Equipotential maps were also constructed for the maximum of the transient groundwater conditions associated with the two major storm events (December 9th, 2009 and August 12th, 2010; Figure 23). The December 9th, 2009 event occurred when groundwater tables were high and flow was from the floodplain towards the stream channel. This event caused overbank flooding and it generated the highest equipotential values. This storm activated the chute channel and the major flow direction was sub-parallel flow to the stream direction. Groundwater discharged into the stream near transects E and F.

The other major storm that was monitored was a late summer tropical storm on August 12th, 2010. This storm occurred near the groundwater and baseflow minimum. This tropical storm did not generate overbank flooding, but water flowed into the chute channel and seeped into the floodplain at the gravel bar. The highest groundwater heads were at the upstream end of the reach and localized at the stream bank. The highest single point groundwater elevation was in the chute channel. This high flow event occurred during low groundwater conditions, which caused recharge from the chute channel into the adjacent gravel bar and floodplain groundwater system. Equipotential diagrams generated for the summer groundwater minimum also produced groundwater flow patterns that ran parallel to the stream channel. Water flowed from the stream channel into the groundwater at the upstream end of the reach.

3.5.1. Precipitation from a major tropical storm

A significant tropical storm occurred on September 29th, 2010 around 10:00 pm and continued until 10:30 am October 1st, 2010 and produced 6.9 cm of precipitation (Figure 24). The cumulative distribution of precipitation is shown in (Figure 25), which was constructed with 15 minute interval data. There were four main distinct peaks in storm precipitation at 60, 270, 735, and 1,350 minutes into the storm. The center of mass of rainfall, centroid, occurred approximately at the 710th minute with a value of 3.5cm (Figure 26). The average rainfall intensity was 0.71±1.17 cm/min. The storm occurred in several bursts, as indicated in Figure 26.

3.5.2. Floodplain piezometric response to the tropical storm

The groundwater heads were monitored during and after the storm. As shown in the photograph (Illustration 3), the chute channel at peak flow had a similar peak gauge height as the main stream channel. Therefore, in the evaluation of piezometric response to the storm event, groundwater time series graphs were constructed for the recession limb of the hydrograph. The groundwater recession curves were compared with the recession curve for the chute channel shown in blue. Groundwater time series graphs were constructed for the recession limb of the hydrograph. These graphs are shown for transects A, C, and E in figure 27.

Illustration 3: Photo showing various channels during storm event on Site 1. (A) Little Paint Branch stream channel; (B) secondary chute channel; (C) Primary chute channel (D) uplands. Photo taken during a major storm event.

The response of the shallow groundwater to the storm event varied with sediment type and position along the floodplain. At the two upstream transects, the groundwater table in the gravel bar responded differently from the upland floodplain due to both position and hydraulic conductivity. At transects A and C, the gravel bar piezometers responded similarly. The gravel bar piezometers had lower heads than the adjacent chute channel, but had similar recession curves to the chute channel. At transects A and C, the chute channel level remains higher than the gravel bar piezometers throughout the recession limb of the hydrographs. The adjacent fine-grained floodplain responded more slowly to water inputs than the gravel bar, but floodplain total heads eventually were higher than both the chute channel and gravel bar (Figure 25). This increase in head in the fine-grained floodplain occurred as a response to flooding of the chute channel. The rapid rise of the upland floodplain piezometers may be due to the capillary fringe response, or due to the relatively low specific yields of these finer-grained sediments. The delayed response of upland piezometers confirms the lower hydraulic conductivity assigned to these sediments in the upland floodplains. The upland floodplain piezometers on all transects showed a peak at 210 minutes after the storm started, this is significantly later than the peak in the chute channel and adjacent gravel bar. At transect E, the chute channel and the gravel bar are both less distinct features, the gravel bar has significantly lower surface sediment sizes than the upstream gravel bar. The piezometric responses at this location could be due to dissipation of flow from the chute channel into the surrounding region, which recharges the groundwater.

One interesting aspect of these time series diagrams is that the flow reversal observed between the upland floodplain and the gravel bar occurs during the recession limb of a major storm. The seasonal reversal in flow between the upland floodplain and the stream channel gravel bar segments appear to be initiated by the large tropical storms described here.

4. Discussion

The major controls on exchanges of water between floodplains and stream channels include floodplain and channel topography, groundwater head values and gradients, and the distribution of hydraulic conductivity in both the floodplain an regionally if the site is not bounded by fine-grained sediment (Woessner, 2000). Little Paint Branch site is characterized by spatial variability in topography and grain size resulting in heterogeneous hydraulic properties (Miall, 1996; Kollet et al., 2002). The floodplain and stream are underlain by very compact fine clay that limits hyporheic exchange under the stream, but facilitates exchanges within the shallow surface sediment. Wroblicky et al. (1998), identified floodplain and riverbed heterogeneity as a major control on floodplain-channel exchange. The recently deposited gravel bars (Blanchet, 2009) are significant hydrologic features of the channel-floodplain sediment and provide heterogeneity of hydraulic conductivity with n the floodplain system.

4.1. Effects of channel morphology on floodplain-channel characteristics

In this study, the channel and floodplain morphology along with sediment characteristics influenced exchanges of water between the channel and the floodplain exchanges. The bar formation along the channel created low bank elevations that facilitated overbank flooding. Along the gravel bar, fine-grained floodplain boundary, fine-grained sediment transport maintains a chute channel that brings streamflow onto the floodplain. These chute channels are found at the gravel-fine sediment transition along all of the gravel bars in this portion of Little Paint Branch. Examination of the site during flood events, however, indicated that chute channels play a significant role in bringing water onto the floodplain. The chute channel carries streamflow onto the floodplain even when overbank flooding does not occur. In the incised reach, formation of a chute channel along the edge of the gravel bar only serves to further isolate the gravel bar from the floodplain. Within incised reaches, groundwater elevations in the floodplain constantly drain towards the stream flow, indicating a gaining stream with a loosing floodplain (Tucci and Hileman 1992). This drainage alters the normal connectivity between the floodplain and stream channel (Kroes and Hupp 2007). Isolation of the floodplain from stream floodplain interactions and water level fluctuation is detrimental (Kwak, 1988; King and Grant, 1996). In addition to vegetation complications, Groffman et al. (2002) observed that lower water tables within floodplains of incised streams result in the inability of saturated soils to offer potential for denitrification and biological uptake of nitrate (Burt et al., 1999; Hill, 1996; Gilliam, 1994).

The natural aggradation at Site 1 resulted in complex floodplain features such as attached gravel bars and chute channels that influenced groundwater levels and thus active floodplain vegetation and biota. This natural re-attachment processes occurred due to streambed aggradation and thus without disruption of floodplain vegetation. Complex, vegetated floodplain can serve multiple functions, including buffering streams against pollution (Burt et al., 1999; Schultz et al., 2000; Lee et al., 2000), facilitating exchanges between surface and groundwater, and reducing stream bank erosion (Micheli and Kirchner, 2002; Schultz et al., 2000; Palone and Todd, 1997). Site 2 shows a direct disconnection with its associated floodplain. This is common for incised streams that are hydrologically disconnected from their floodplains (Schilling, 2004).

4.2. Importance of chute channels

Chute channels along the boundary between the gravel bar and the floodplain and were observed throughout the larger study reach, including the incised reach. Where channels are not incised, the chute channels play a significant role in bringing water onto the floodplain and recharging local groundwater levels In this study, this role is demonstrated through use time series diagrams during storm vents, cross section diagrams of high flow conditions and equipotential maps of high flow conditions. The time series diagrams indicate the rapid response of the gravel bars to streamflow events, but they also show that the chute channel is influential in bringing water into the less conductive upland side of the chute channel. Groundwater heads indicate that flow moves from the chute channel into the floodplain during both summer and winter storm flow conditions. The chute channel also appears to function as a stable point for groundwater levels within the floodplain and maintains similar levels throughout the year. Lastly, the effect of the chute channel decreases downstream as grain size decreases and size of the chute channel decreases downstream. This allows more water to be distributed within the floodplain before exiting and returning to the stream channel. Previous studies have shown that chute channel features and bar topography can alter hyporheic flux rates and patterns (Harvey and Bencala, 1993; Wondzell and Swanson, 1999; Kasahara and Wondzell, 2003; Anderson et al., 2005; Gooseff et al., 2006a,b; Poole et al., 2006). In this study, the chute and bar topography facilitates horizontal exchanges between the channel and floodplain.

Results from this study also support other studies citing floodplain geomorphological characteristics as significant influence on flow dynamics (Wondzell and Swanson, 1999; Kasahara and Wondzell, 2003). In addition, similar results were found in hydrogeologic modelling experiments preformed by Kasahara and Wondzell (2003) and Poole et al. (2006), which suggests that the surface hydrology of floodplain channels can create temporally dynamic variations that deviate significantly from the steady state hydraulic gradients within alluvial aquifers (Woessner, 2000) altering groundwater elevations and flow directions among seasons.

4.3. Groundwater reversal-seasonal variations

Seasonal variations in groundwater tables are can be caused by seasonal variations in precipitation, precipitation intensity, and evapotranspiration. In the mid-Atlantic United States, precipitation is not seasonal, but variations in precipitation intensity do occur (Winter, 1994) and variations in evapotranspiration are very significant. Seasonal variations were observed in both time series graphs of groundwater potential and in sequential stead-state maps of the groundwater system. The reversal of groundwater flow occurred twice a year. Flow moved from the channel into the floodplain in the summer. This flow reversed in the fall, and the reversal occurred rapidly, induced by tropical storms that caused an increase in groundwater heads in the uplands. The second reversal occurred in the spring, (March-April, shortly after leaf-out occurred). These seasonal variations in water levels associated with evapotranspiration changes drives many of the exchanges between the floodplain and the stream channel.

Although the seasonal variations were observed at all transects, the timing and the amount of seasonal variation in groundwater head varied with position within transects. The piezometers installed in the floodplain filled up slowly as evapotranspiration decreased but also drained slowly as evapotranspiration demand increased in the spring and continued into the summer months. This difference in response of the piezometers is likely caused by both their position on the floodplain and hydraulic conductivity. Middle piezometers exhibited lower elevations for both winter and spring seasons, suggesting that the chute channel did not supply water to the floodplain for most of these channels. During high storm events, piezometers in the chute channel are more likely to have surface and over top flow compared to piezometers in the floodplain and uplands. Seasonal variation and spatial results are similar to that observed within other systems with strong seasonal variations in evapotranspiration or seasonal precipitation (Hill, 1990; Waddington et al., 1993; Squillace, 1996; Burt, 1997).

Field data indicate that focused recharge of the floodplain occurs along the upstream edge of the gravel bar for summer and fall months. Chute channels can initiate transient groundwater mounds and enhanced seepage rates. Although hydrological flow paths in near-stream floodplain zones can be intricate, owing to a variety of groundwater sources such as inflow from uplands, urban runoff, upwelling from deeper strata, bank storage, overbank inundation, etc. (Hill, 1990; Squillace, 1996; Cey et al., 1999; Clement et al., 2003), the net effect of converging groundwater flow paths in the floodplain results in seasonally or perennially saturated conditions.

4.4. Soil hydraulic conductivity estimates

Hydraulic conductivity was estimated from grain-size measurements. These techniques tend to give higher averages with lower variances than *in-situ* measurements that incorporate other hydraulic characteristics of the soils (Eggleston and Rojstacze, 2001). In this study, grain size was used to separate the coarse grained sediment of the gravel bar from the fine-grained sediments of the floodplain. Although previous studies indicate that grain size estimates of hydraulic conductivity often do not correspond well to field measured hydraulic conductivity for fine-grained sediments, they perform better for sand-sized and other coarse grained sediments, such as on the gravel bars. Both the grain size-based estimates of hydraulic conductivity and the observed piezometric responses indicate that the upland floodplain has significantly lower hydraulic conductivity and lower specific yields than the adjacent gravel bars. Studies have shown that field measures are generally greater than or similar to laboratory analysis in which laboratory analyses underestimated the hydraulic conductivity (Taylor et al., 1987; Herzog et al., 1989; Fetter, 2001).

4.5. Limitations

Studies of dynamic processes in heterogeneous materials are often limited by the available data. This study was motivated, in part, by a need to understand the major processes that influence water exchanges between floodplains and stream channels. Identification of these processes can then guide future field work.

Two types of limitations were present in this study: site limitations and modeling approach. Groundwater monitoring requires arrays of piezometers that increase in complexity with the size and both geomorphic and sediment heterogeneity of field sites. Mapped results are influenced by the lack of piezometers in floodplain locations at Site 2. Piezometers at further distances from the stream at Site 1 would be useful do determine flow from the upland towards the channel. In addition, continuous monitoring of piezometers (versus once a week) would have produced more accurate results for the unique events such as storm or drought events,.

In this study, equipotential diagrams were created in GIS rather than in MODFLOW or other modeling programs, which only recently have been adapted to shallow groundwater and wetland environments. Equipotential diagrams in all these models are commonly determined by Kriging. This option is available in GIS and was used to construct the equipotential maps. In some cases, (particularly with the chute channel data) over-smoothing can be identified as a limitation. Despite this limitation, kriging offered less restrictions of mapping the groundwater compared to other interpolation models such as inverse distance weighted interpolation.

In addition, model predictions are limited by the geohydrological data for the study site. It was assumed that horizontal flux would dominate because the sediment layers within the aquifer are horizontally continuous and a shallow confining layer is found throughout the study site. Groundwater equipotential flow maps were produced strictly with use of the hydraulic head values obtained from field data.

Although this project focused on defining surfacewater- groundwater interactions and identifying seasonal variations in groundwater floodplain patterns, these data could be used in future research as part of a floodplain mass balance model. This would include measurements of evapotranspiration, stream discharge, precipitation directly at the site, and urban runoff to complete a proper mass balance of the site to determine the groundwater input to and from the stream.

5. Conclusion

Measurement of hydrological processes in a small urban floodplain revealed a complex interaction between streams and groundwater systems. Exchanges of floodplain groundwater with streamflow were initiated by changes in streamflow and evapotranspiration. Three zones were established within the Site 1 floodplain, having common heads and sub-parallel flow. Local surfacewater circulation in the underlying sediments created areas of groundwater recharge and discharge characterized by gaining and losing stream sections. This emphasizes the importance of characterizing surfacewater-groundwater exchange at the floodplain and channel scale and determined the seasonal, location, and magnitude of the interactions within a small scale. Future studies should use these results to develop a monitoring network to examine exchange processes in large segments of the floodplain. This research suggests that these studies should be conducted over an annual cycle. Piezometers should be installed to document the effects of sediment heterogeneity, and to monitor the effects of chute channels on floodplain groundwater.

It is important to note that the reversal in groundwater flow directions from the channel into the floodplain is facilitated by the hydraulic conductivity of the sediment, but also the high evapotranspiration rates of the mature forest that is growing in the floodplain. This forest canopy would be significantly disturbed by “cutting down the floodplain”. This suggests that channel aggradation methods might provide an alternative restoration technique.

Appendices A-Figures

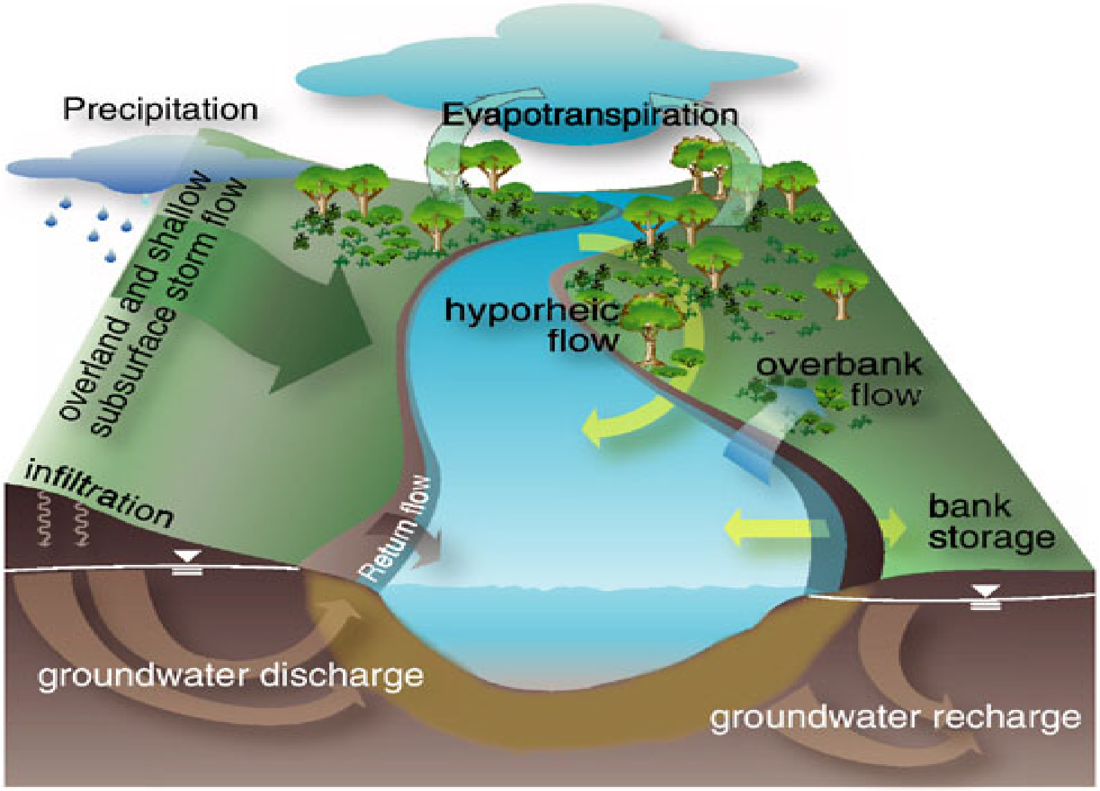

Figure 1: Conceptual diagram showing floodplain and channel of near channel surface and subsurface features and active exchange of groundwater-surfacewater (NRC, 2002)

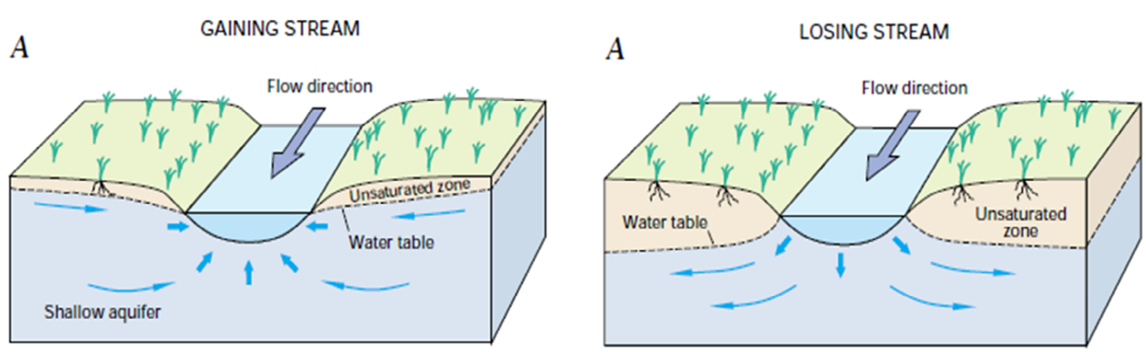

Figure 2: Gaining and losing stream conceptual diagrams showing groundwater flow direction from a stream (Winter, 1998).

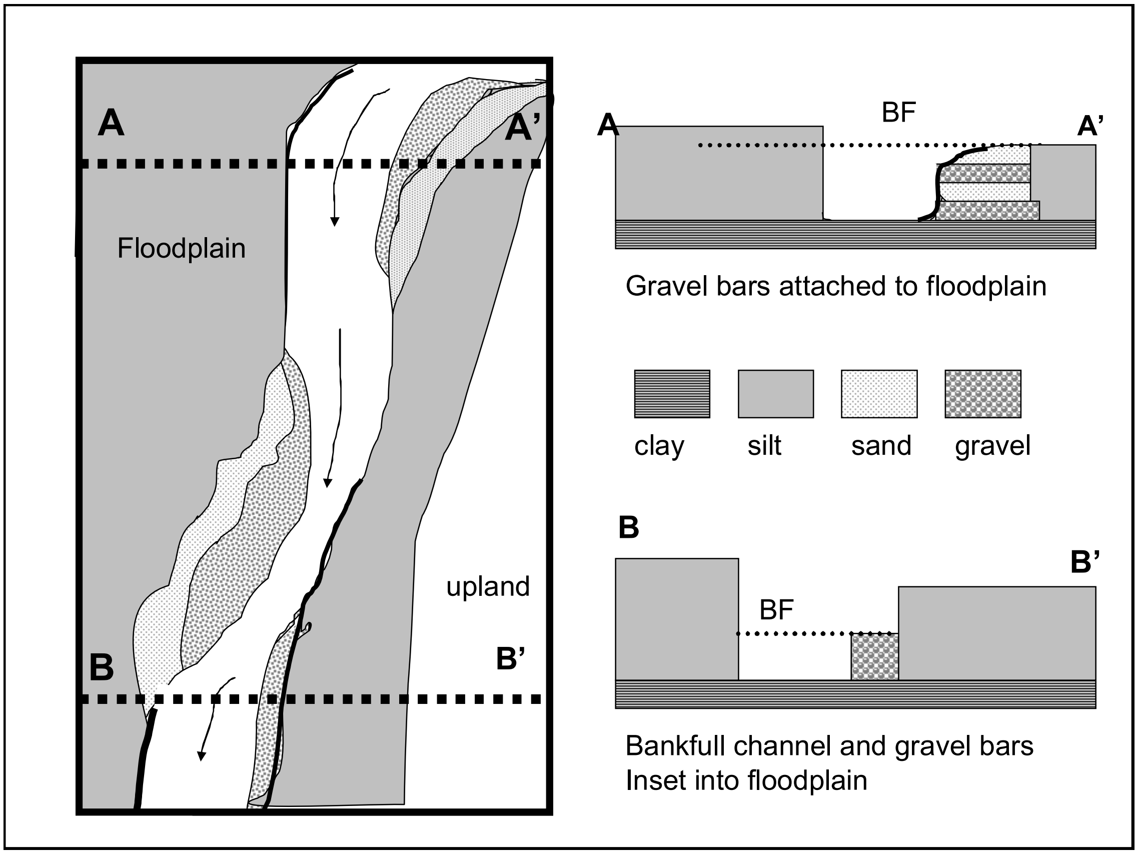

Figure 3: Conceptualization of differences between Little Paint Branch floodplains, A- an attached active floodplain with sediment bars; and B- incised stream with sediment bars incised into floodplain. BF represents baseflow.

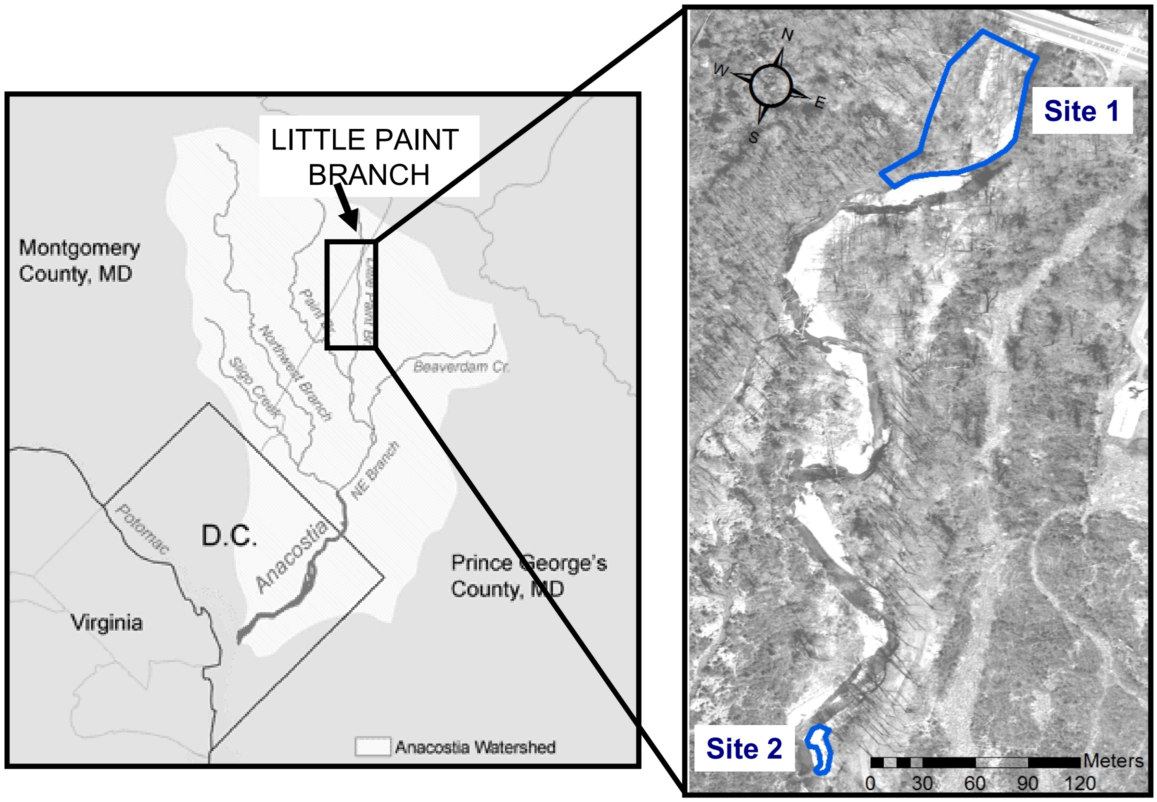

Figure 4: Study site of intact floodplain along Little Paint Branch, upstream of the junction with Paint Branch. Blue polygons indicate the sites within Little Paint Branch.

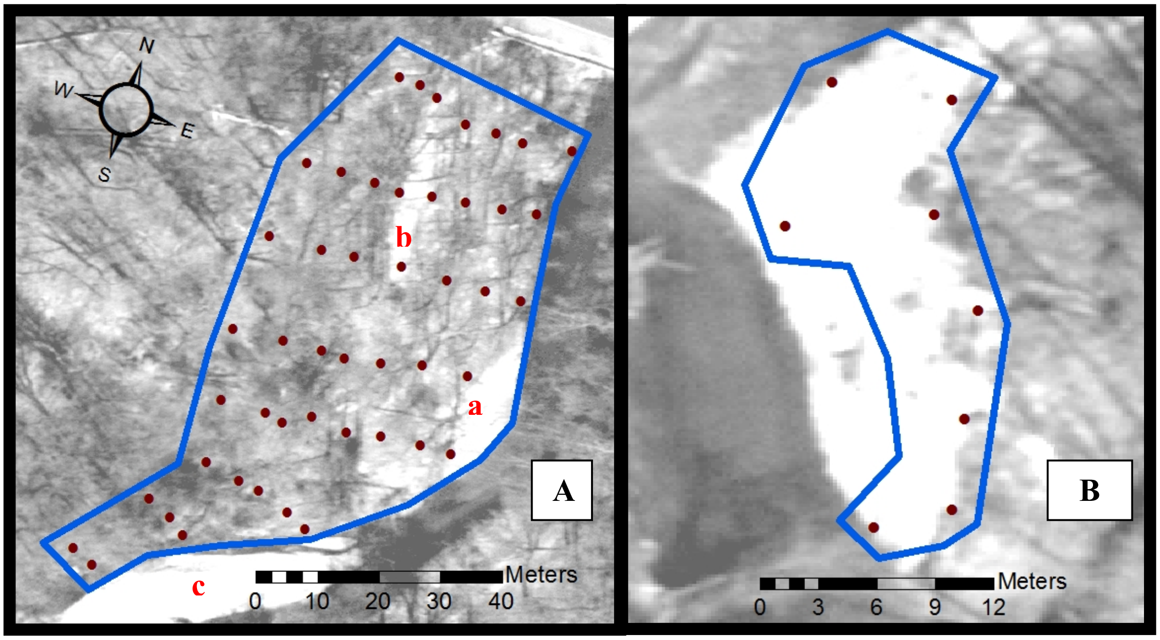

Figure 5: A. Upstream study site showing gravel bars accreting onto floodplain (a), chute channel (b), and a mid-channel gravel bar (c); B. Downstream site on sediment bar incised into floodplain.

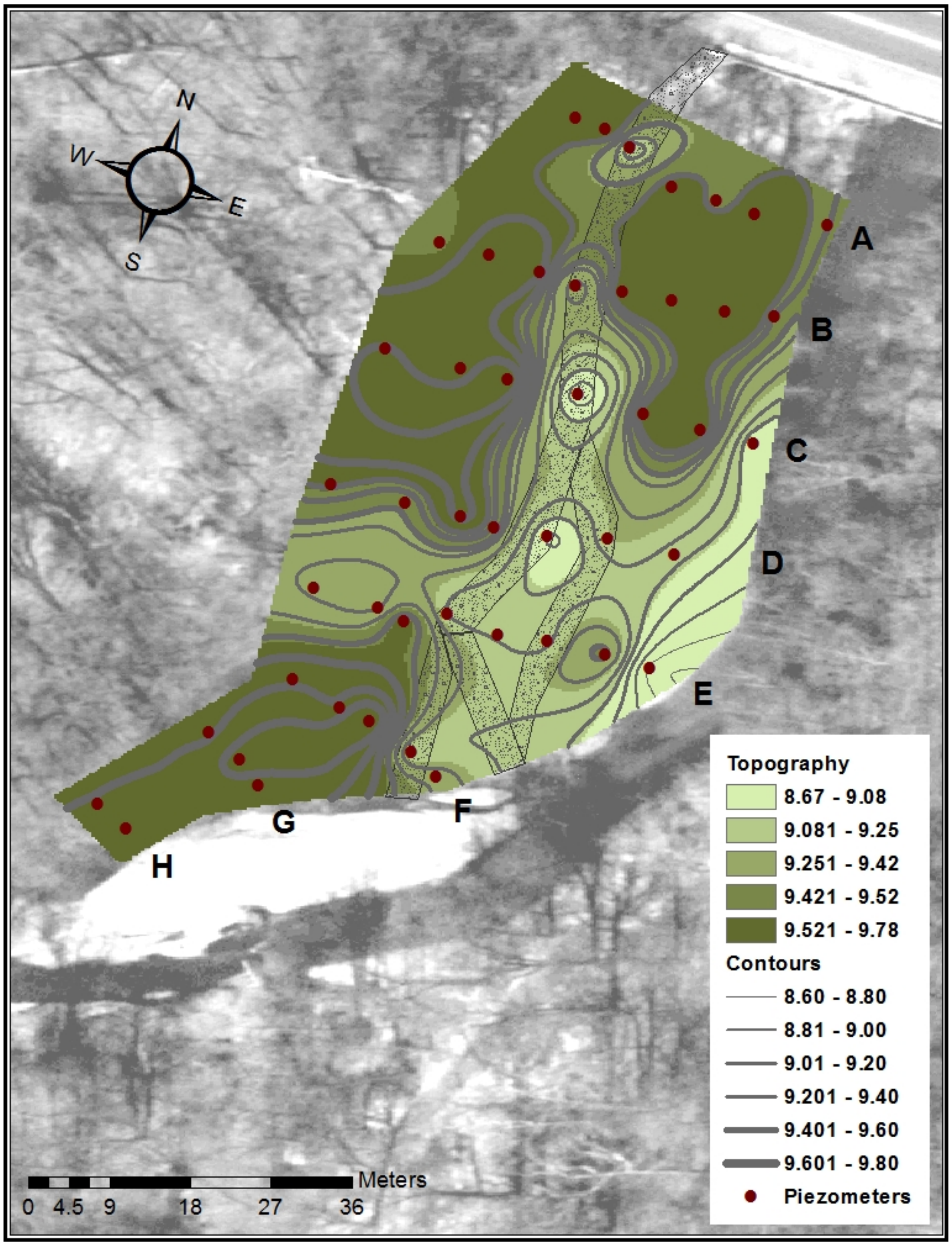

Figure 6: Topography of the floodplain adjacent to the stream channel at Site 1. The study site consists of a gravel bar that has accreted onto the floodplain (D1, E1) and a chute channel that runs parallel and splits off into 3 directions.

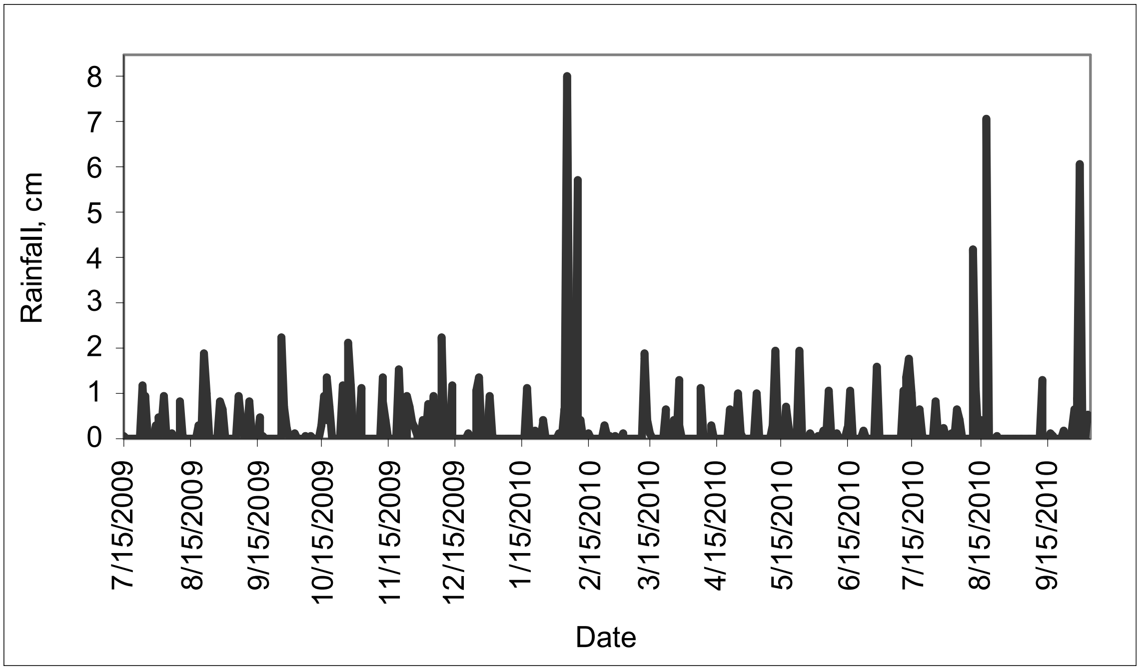

Figure 7: Daily precipitation from the Beltsville gauge for the study period. Average precipitation during July 1st to October 4th was 0.22±0.62 cm.

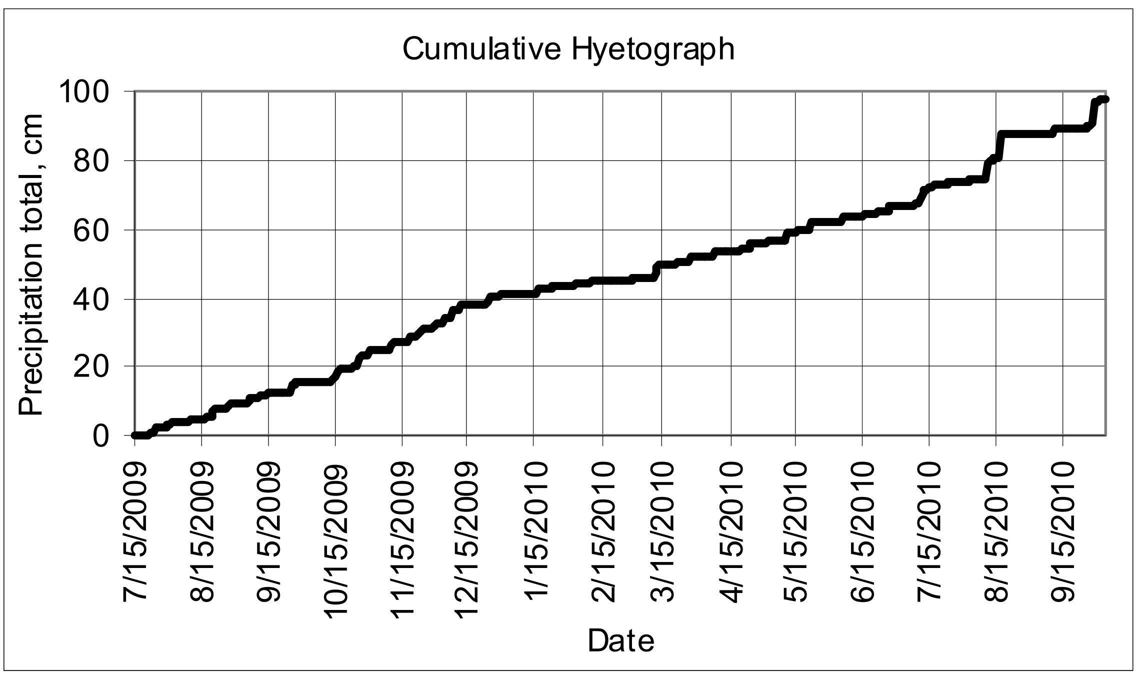

Figure 8: Cumulative precipitation for the Beltsville Gauge over the study period. Total precipitation during July 1st to October 4th was 98 cm.

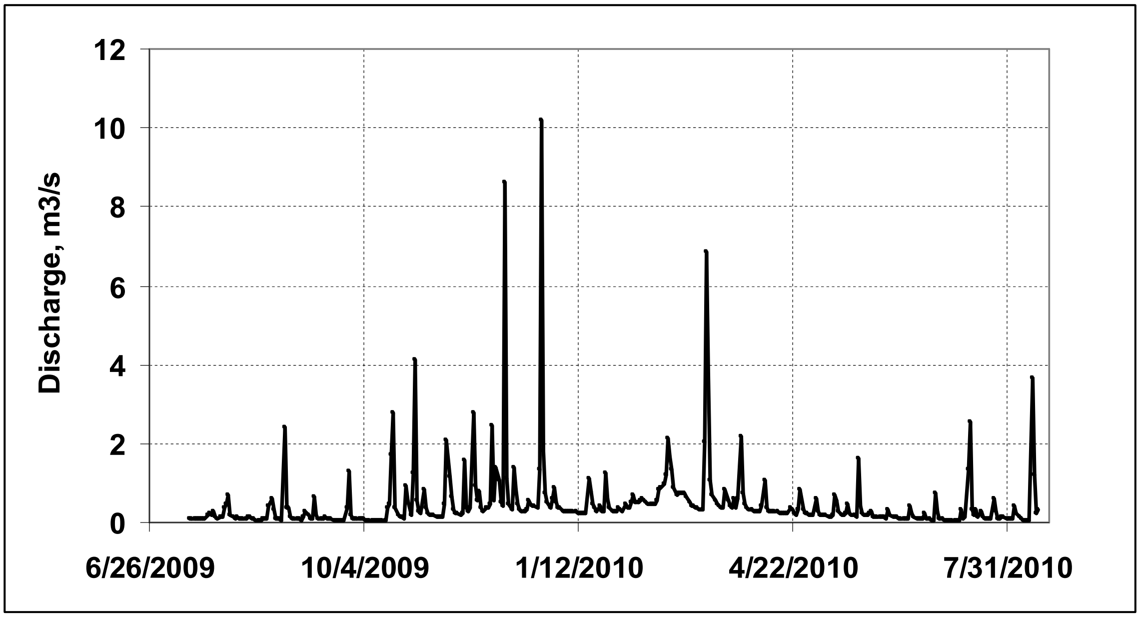

Figure 9: Daily average discharge in Little Paint Branch for the study period. Note seasonal increases in baseflow and the relative magnitudes of the winter and summer floods.

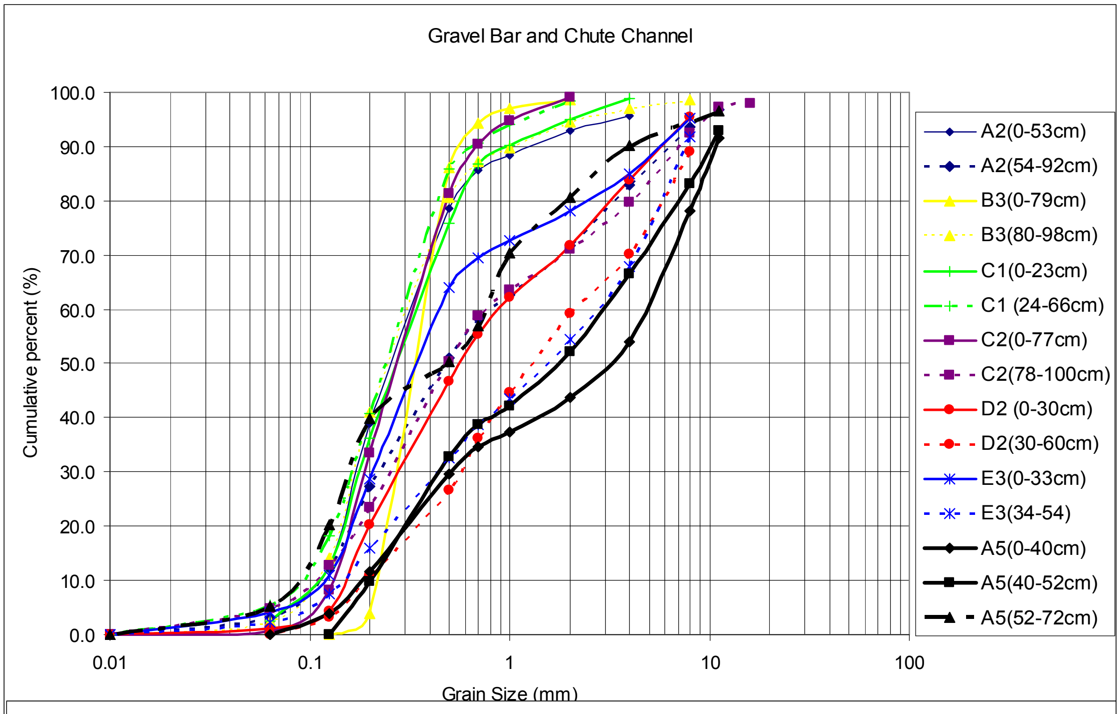

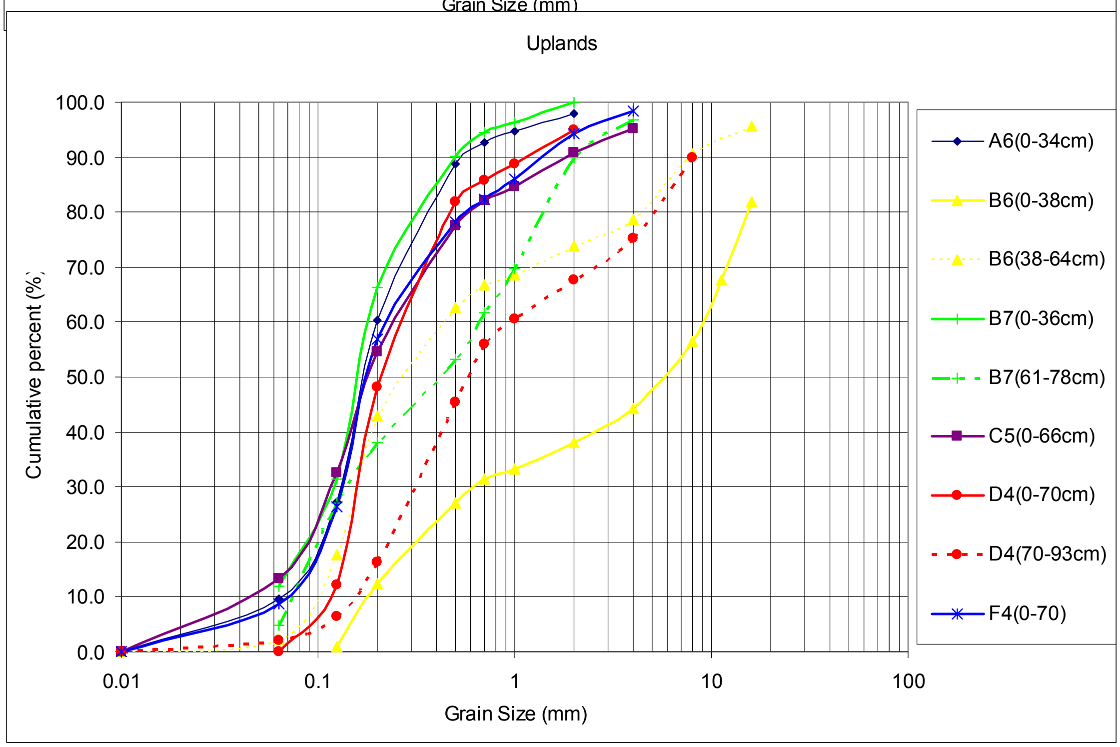

Figure 10: Soil profiles used to estimate D_{10} and D_{50} values. Top: Gravel Bar (Piezometers: A2, B3, C1, C2, D2, E3) and chute channel piezometers (A5). Bottom: Uplands (Piezometers: A6, B6, B7, C5, D4, F4). Samples sorted by colors. Solid line is for top core; dotted lines deeper in core samples for that piezometer. Legend displays piezometer and depth of soil core sample.

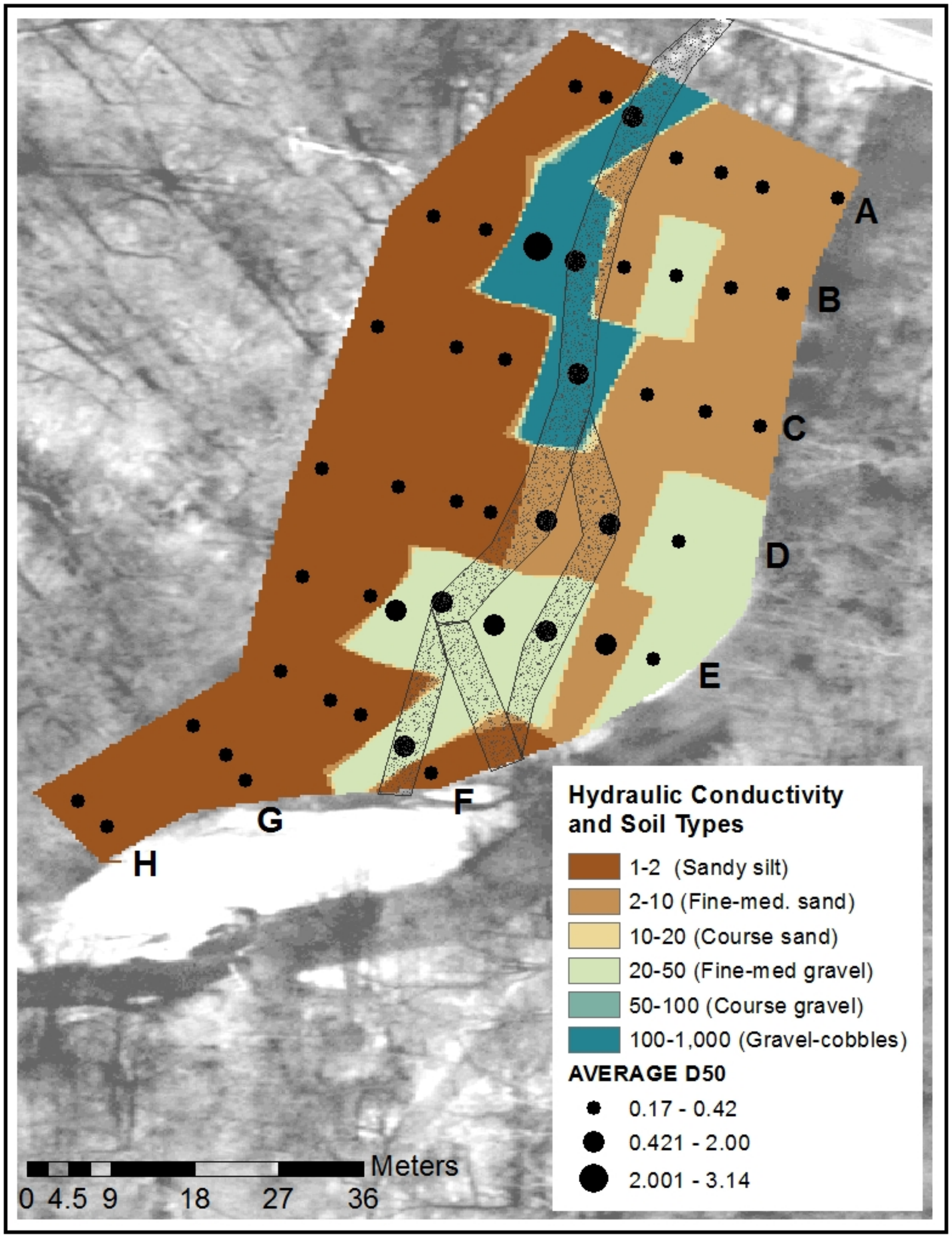

Figure 11: Hydraulic conductivity values and average D50 values for Site 1 piezometers.

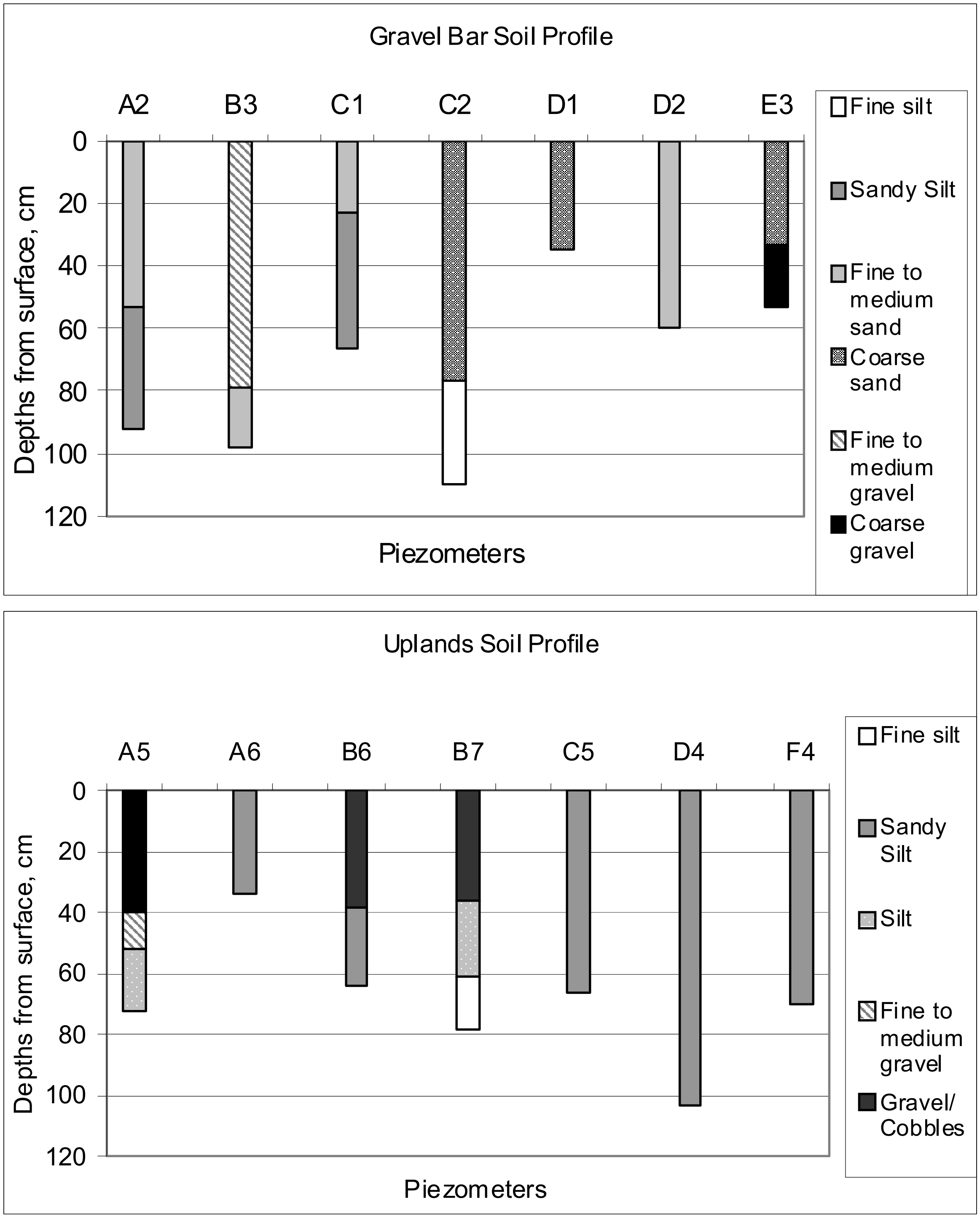

Figure 12: Soil profile for Site 1- (A) floodplain soil profiles; (B) upland soil profiles. Average surface elevation at (A): 9.602 meters. Average surface elevation at (B): 9.301 meters.

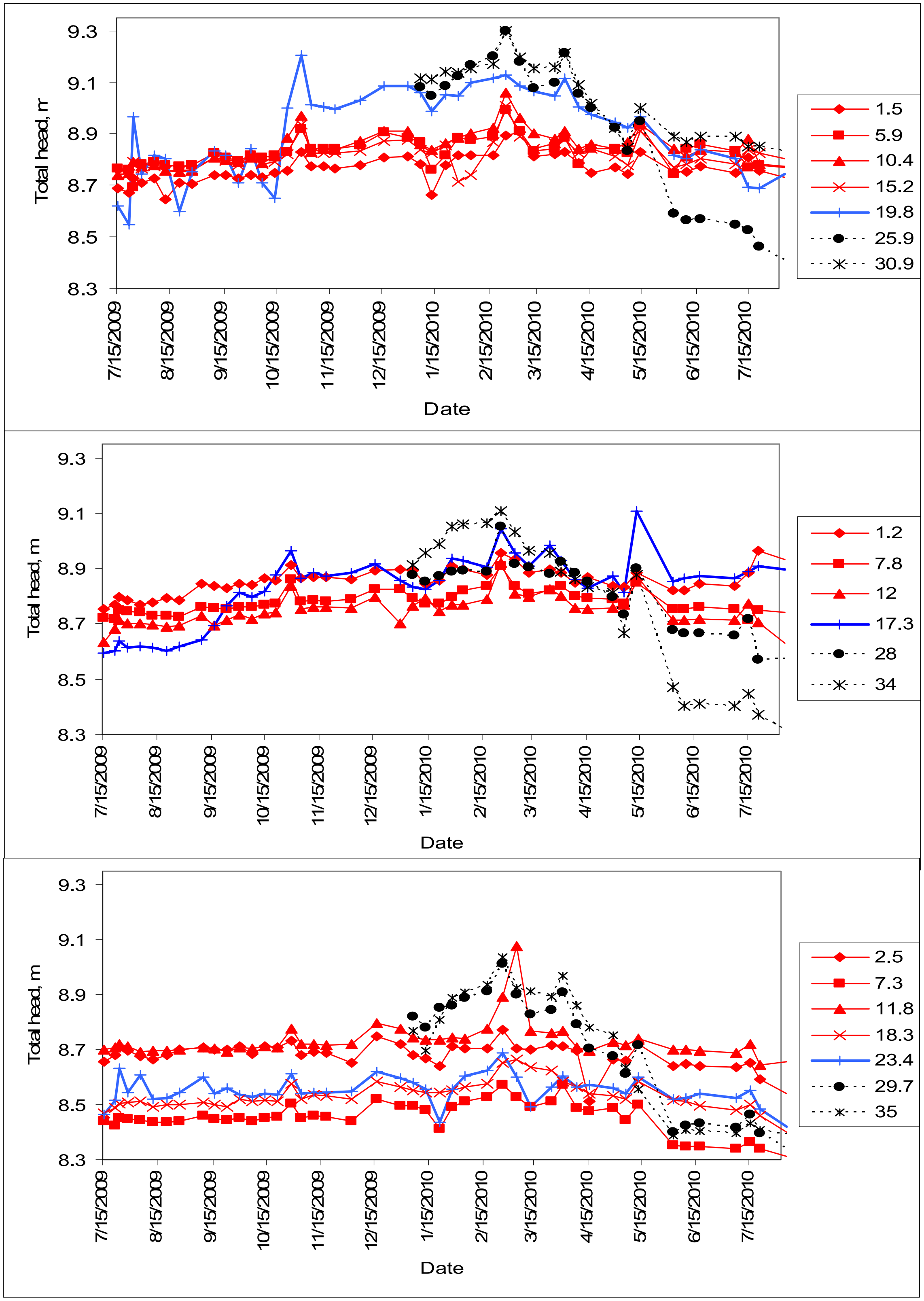

Figure 13: Transect time series (Top) Transect A; (Middle) Transect C; (Bottom) Transect E. Red lines represent accreting gravel bar piezometers; Blue lines represent chute channel piezometers; Black dotted lines represent uplands piezometers. Legend indicates distance from stream in meters for each piezometer. Major storm event were removed to show seasonality.

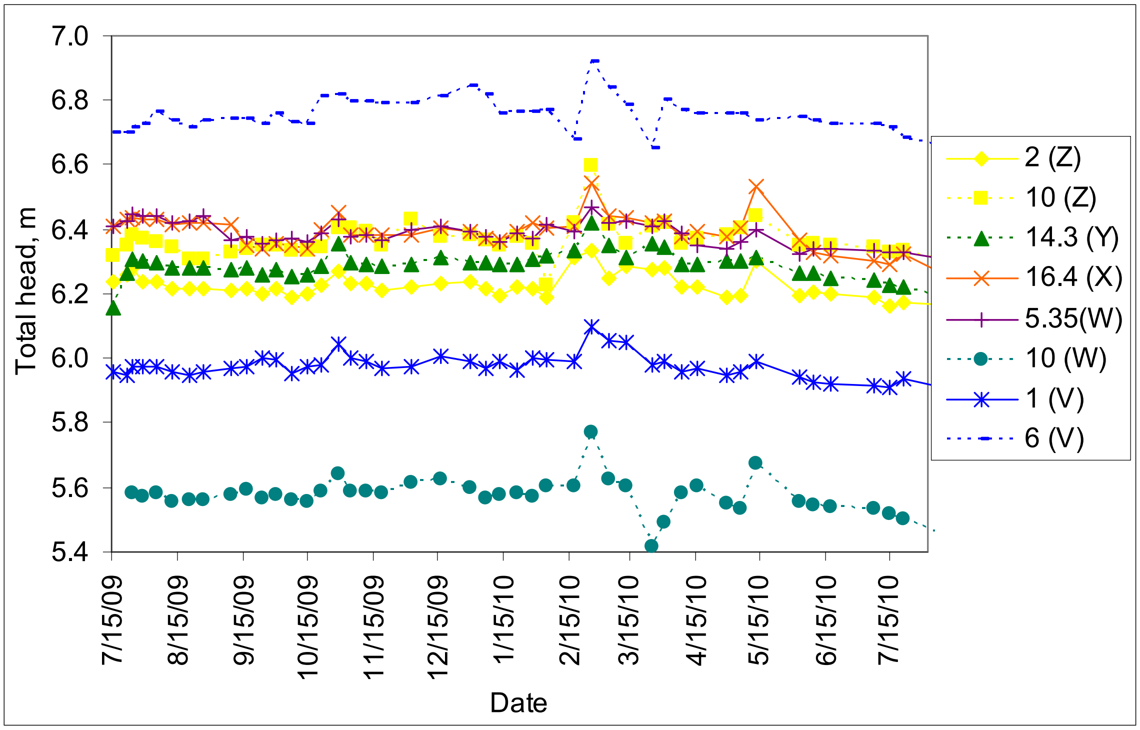

Figure 14: Site 2 time series of water level elevations showing transects and distance from the stream in legend (meters). Colors indicated transect; Dotted lines back transects farther in gravel bar; Solid lines are piezometers closest to stream.

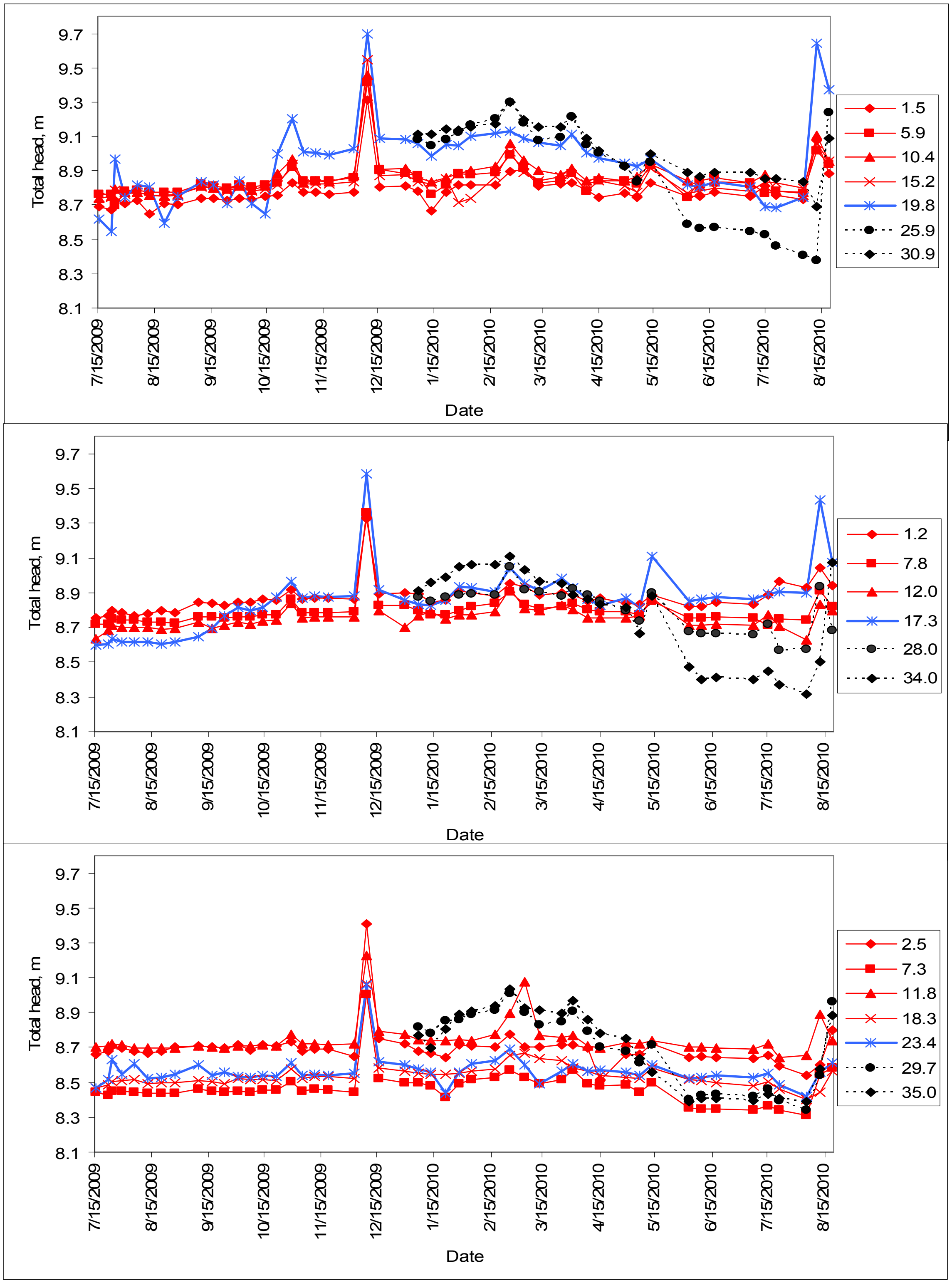

Figure 15: Complete time series (Top) Transect A; (Middle) Transect C; (Bottom) Transect E. Red lines inset gravel bar piezometers; Blue line chute channel piezometers; Black dotted lines are upland piezometers. Legend indicates distance from stream in meters for each piezometer. Peaks indicate major storm events.

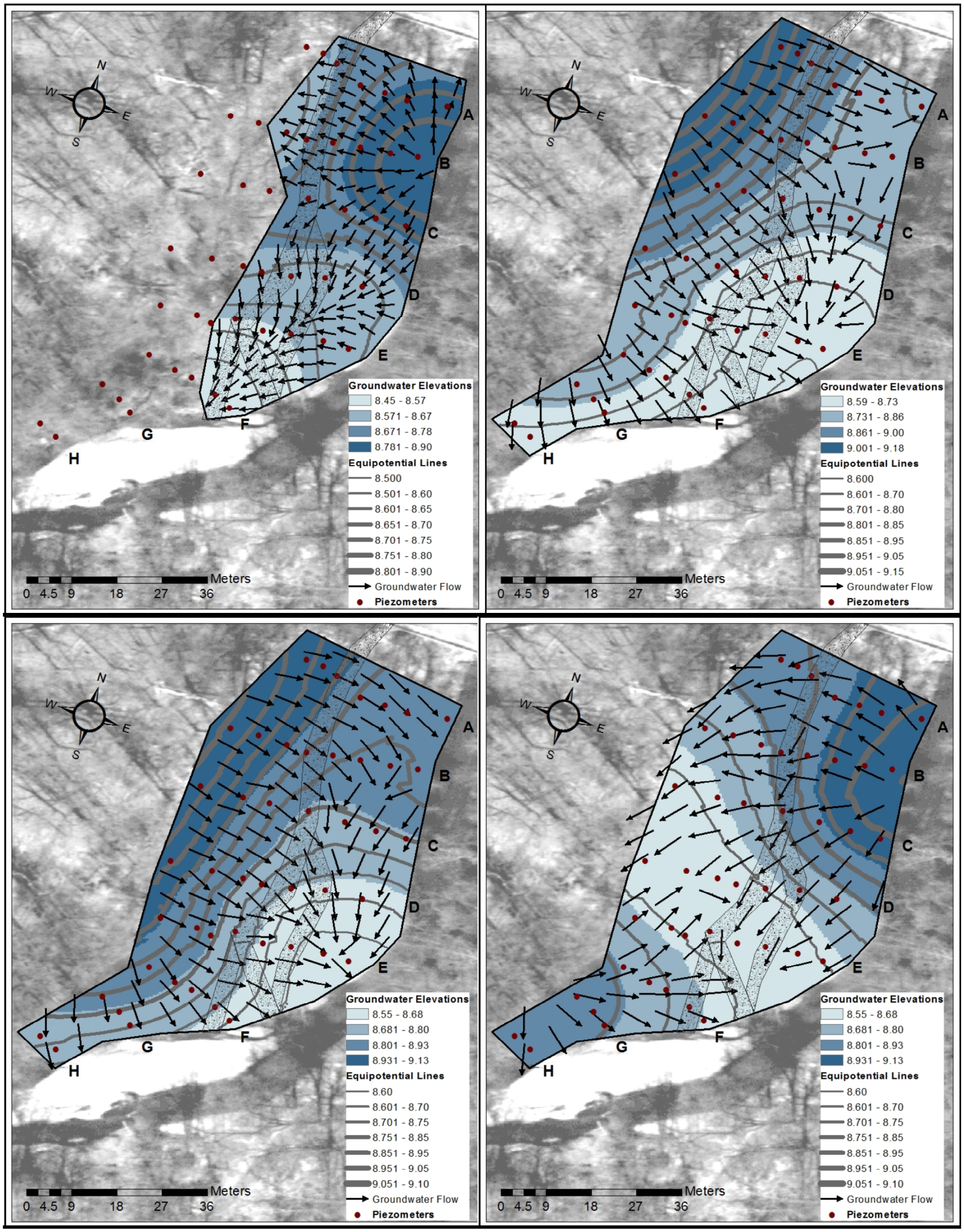

Figure 16: Site 1 equipotential maps for each season. Low to high elevations are represented by light to dark blue shading and thin to thick contours lines respectively. Top left, Fall; Top right, Winter; Bottom left, Spring; Bottom Right, summer.

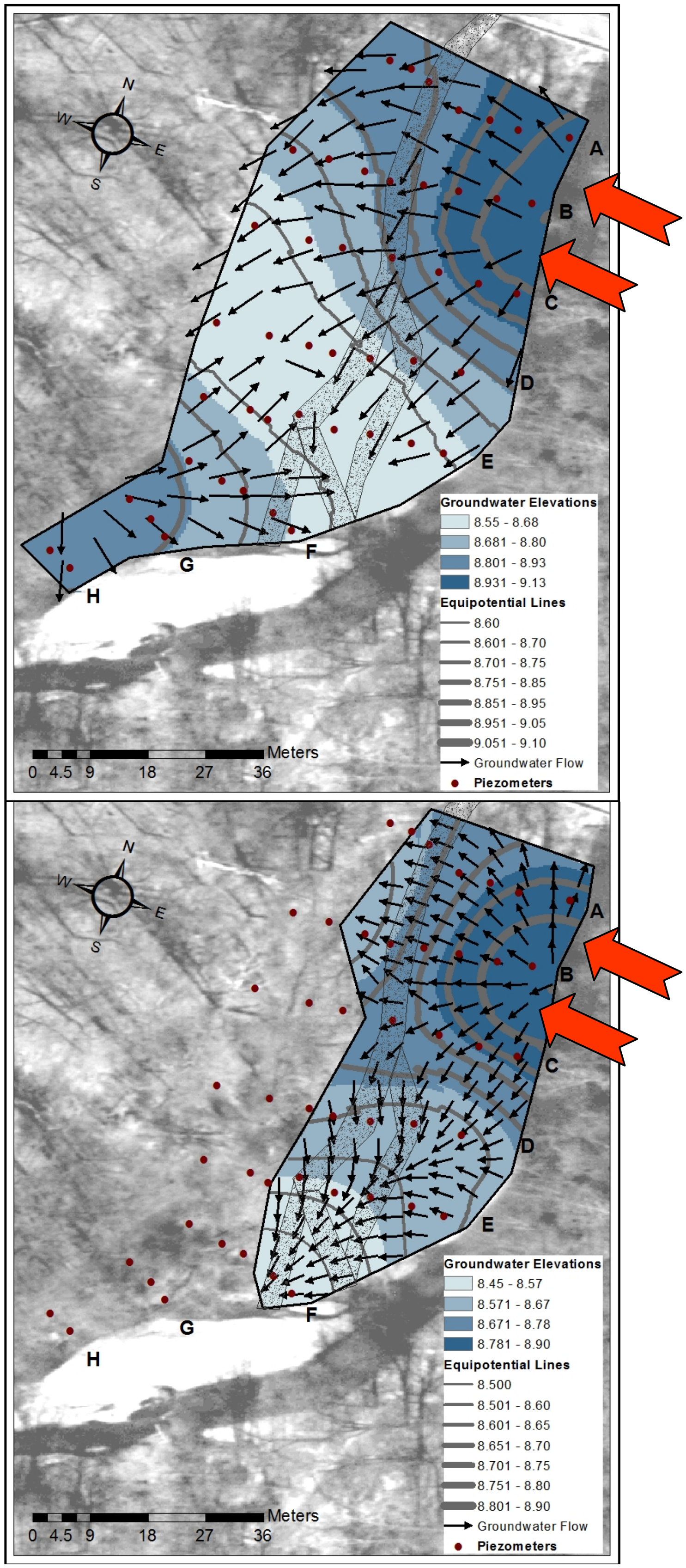

Figure 17: Enlarged equipotential maps of (Top) summer and (Bottom) fall. Low to high elevations are represented by light to dark blue shading and thin to thick contours lines respectively.

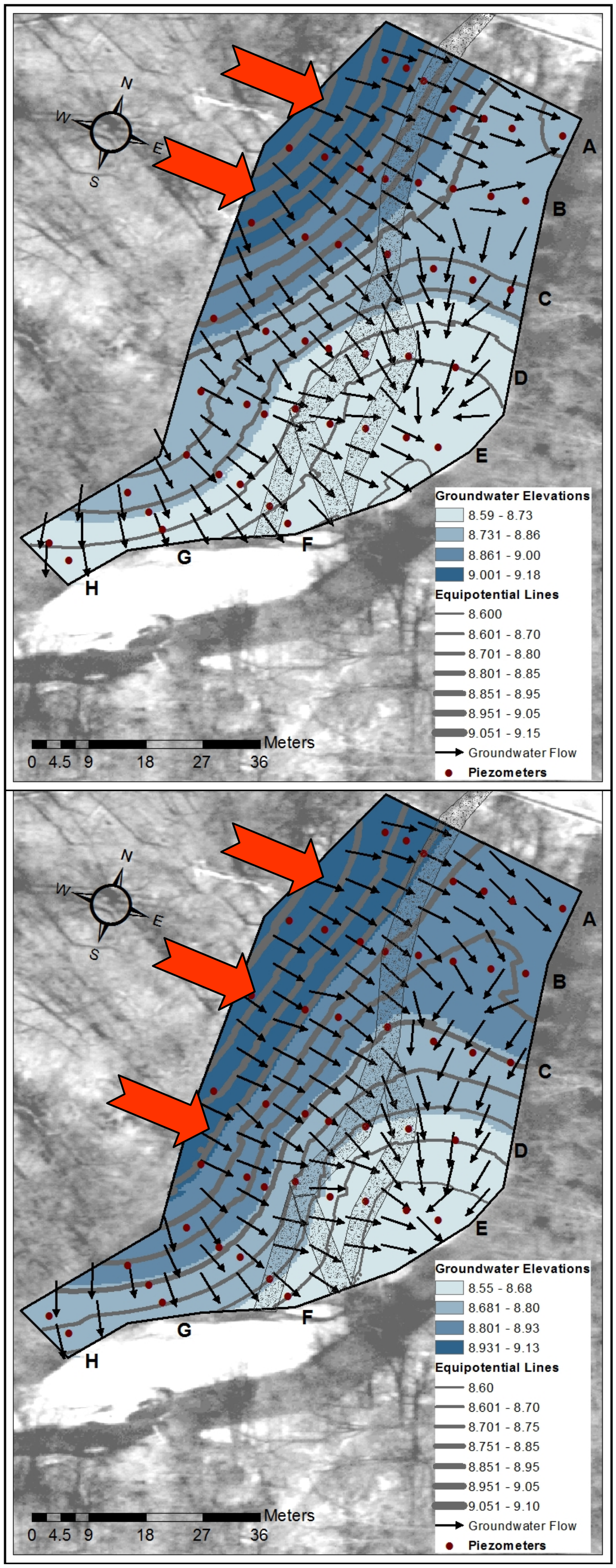

Figure 18: Enlarged equipotential maps of (Top) winter and (Bottom) spring. Low to high elevations are represented by light to dark blue shading and thin to thick contours lines respectively.

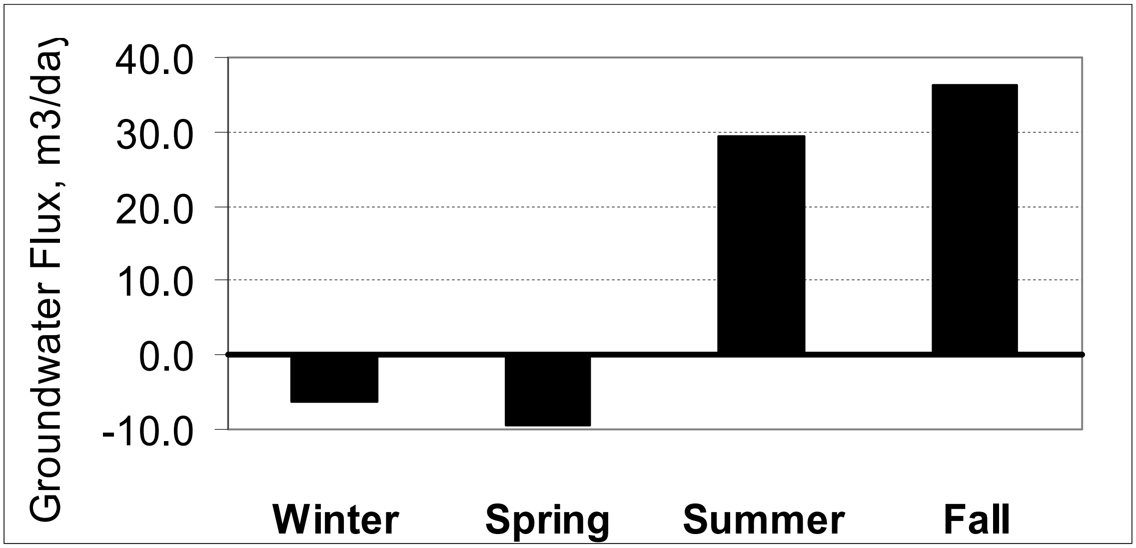

Figure 19: Seasonal groundwater flux graph. Shows Figure 17/18 dark blue area with orange arrows flux rates seasonally.

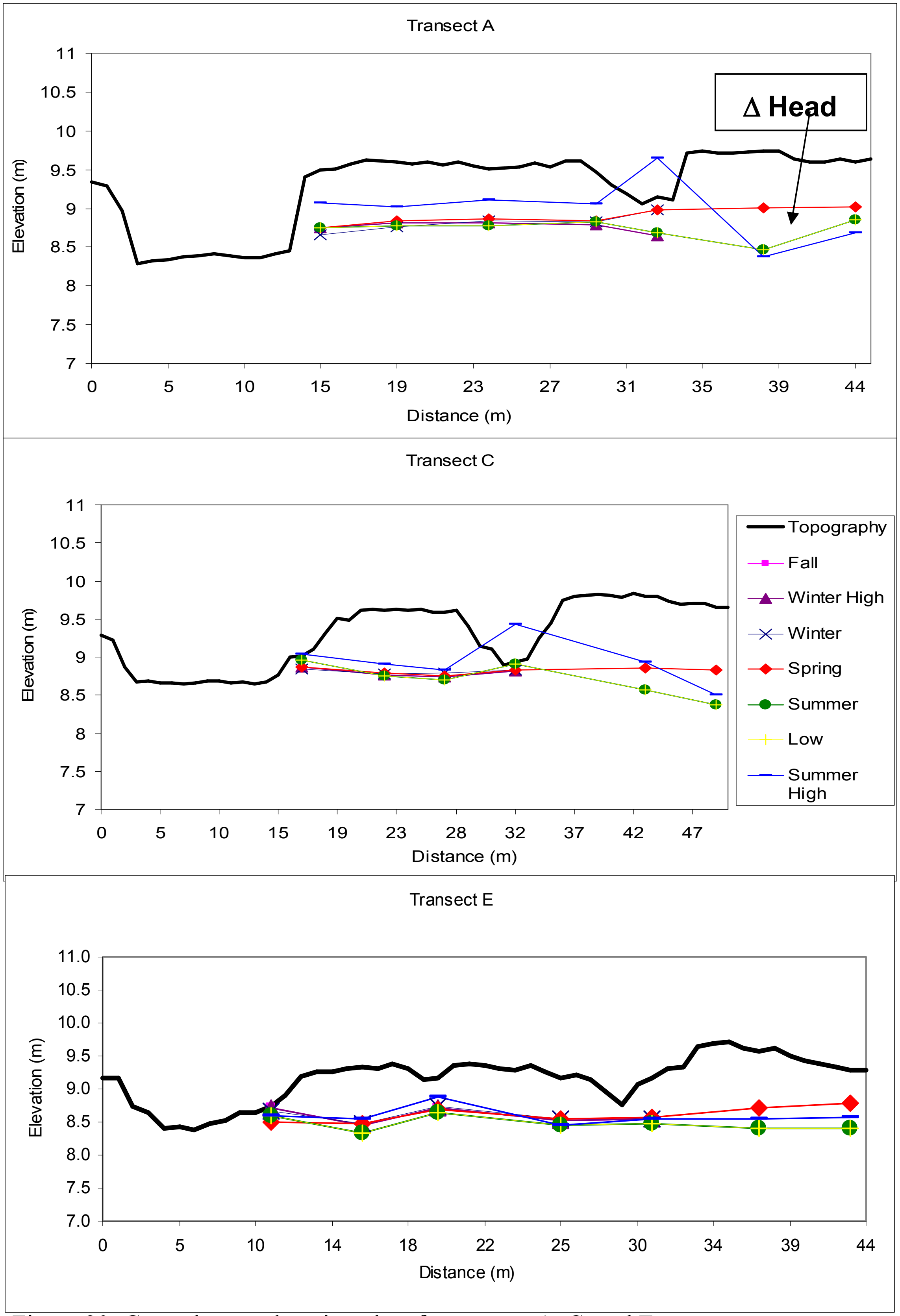

Figure 20: Groundwater elevation plots for transect A, C, and E.

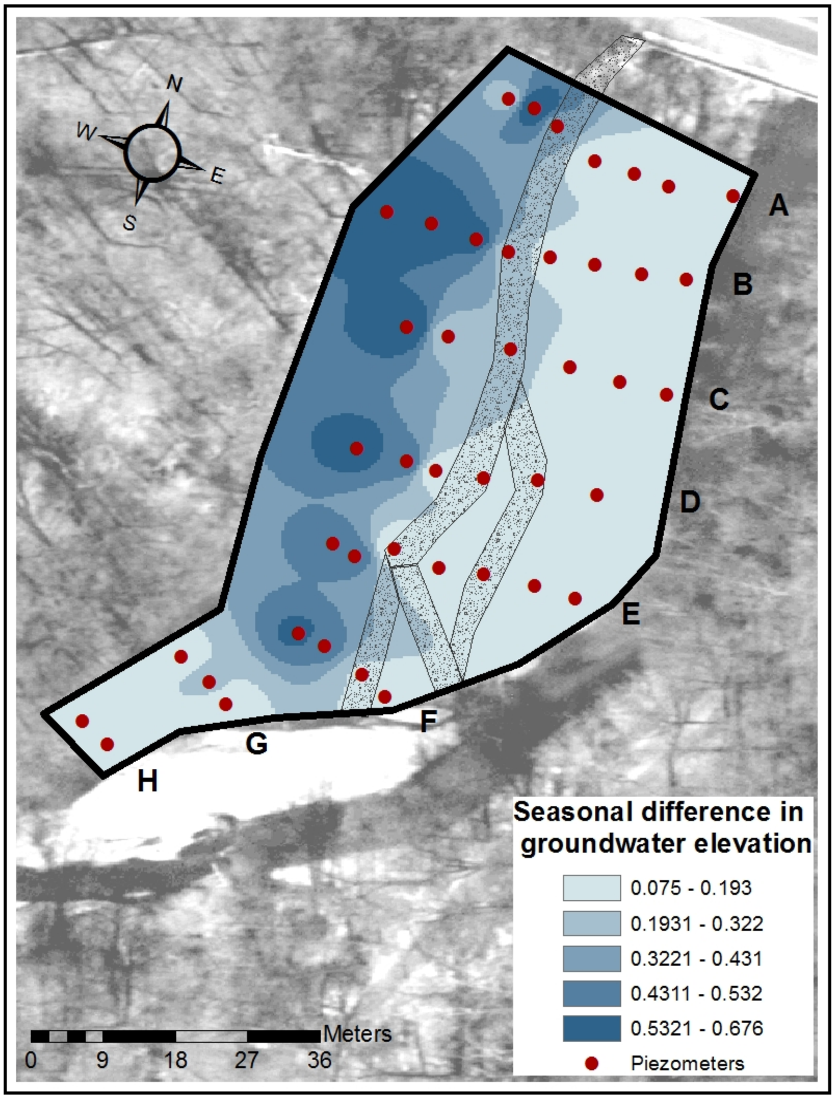

Figure 21: Seasonal difference in groundwater elevations. Dark blue indicates largest change; light blue shows smallest changes in elevation between seasons.

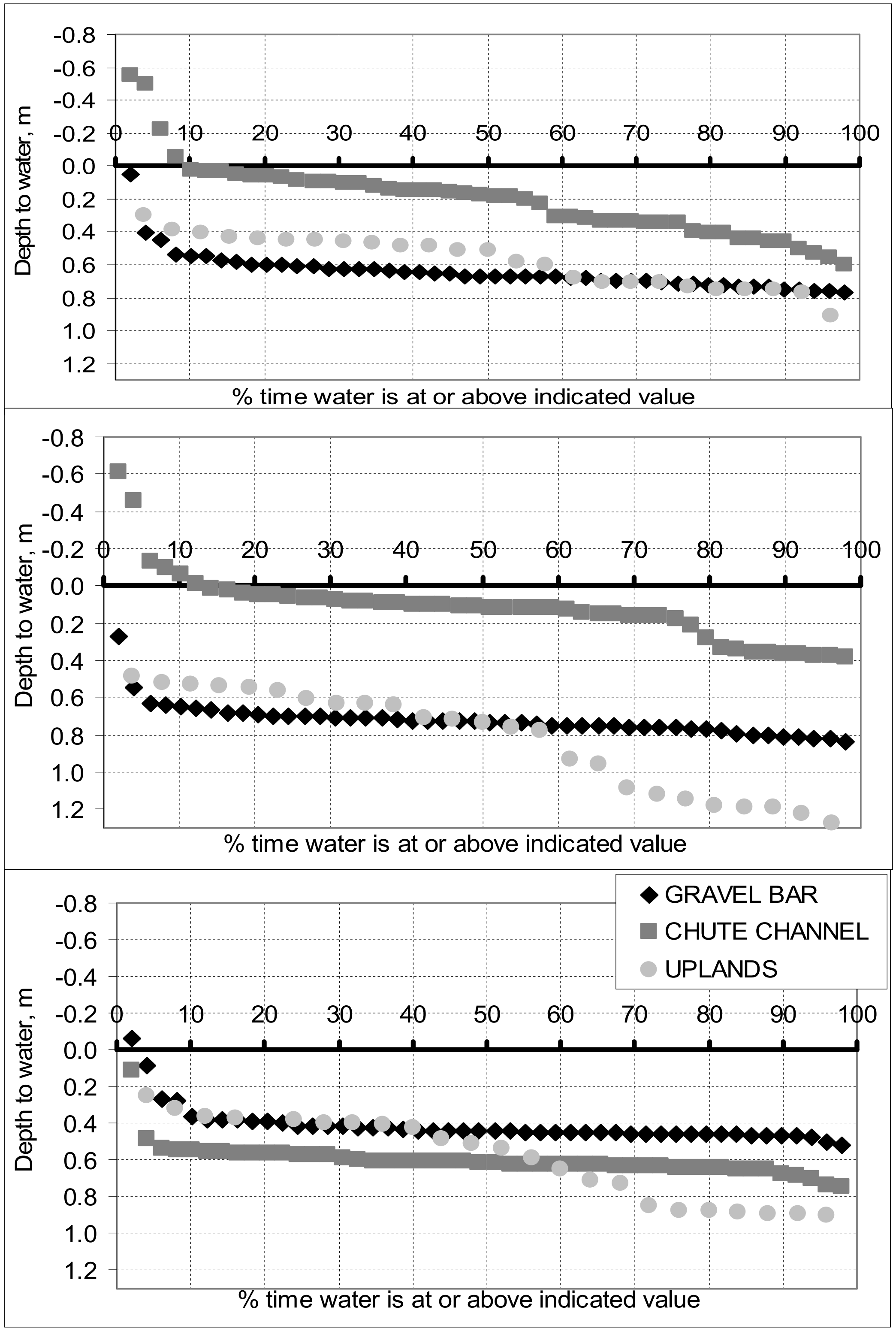

Figure 22: Annual flow duration curves (Top) A transect; (Middle) C transect; (Bottom) E transect. Solid black thick line indicates surface level.

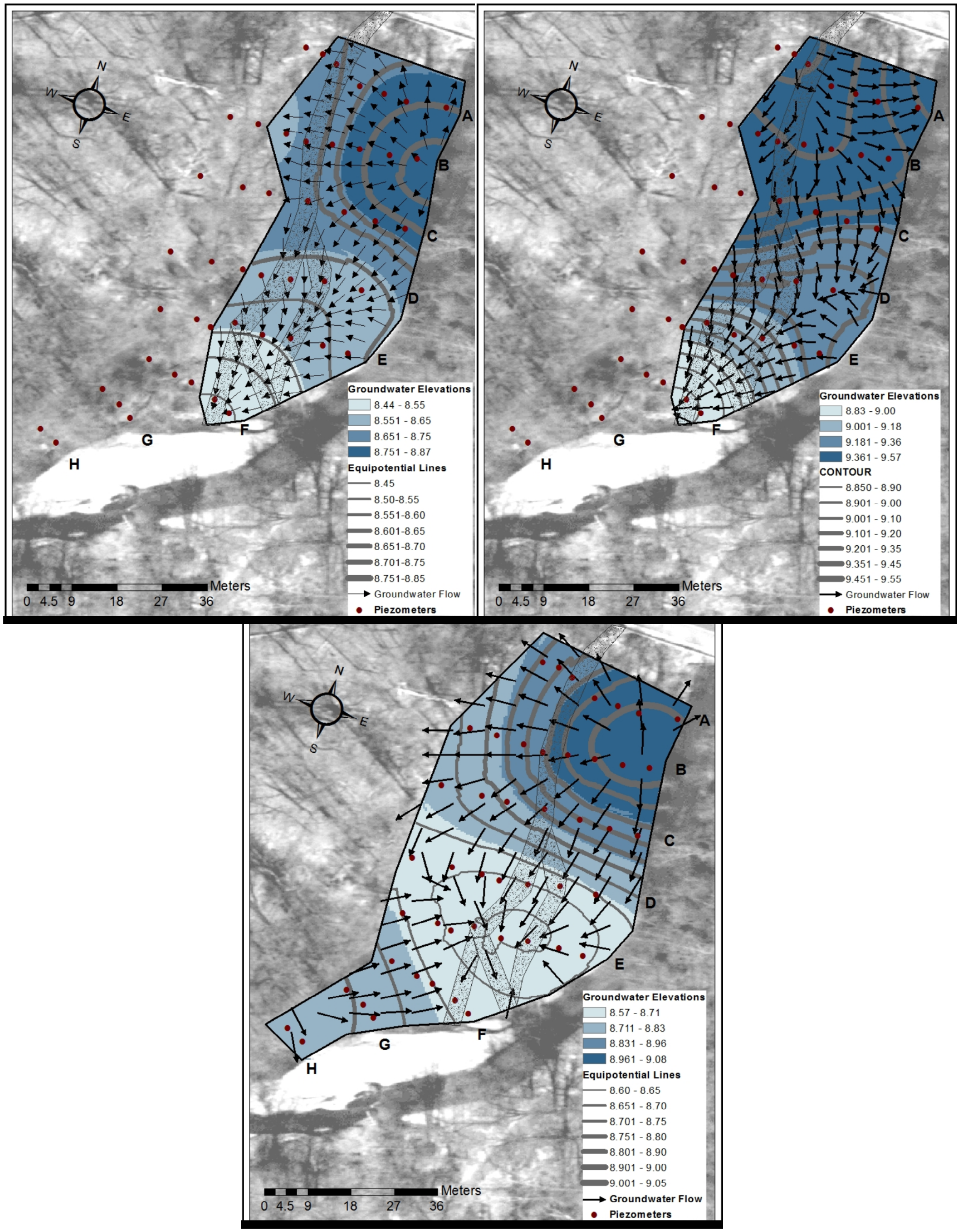

Figure 23: Site 1 equipotential maps of highs and lows conditions. Top left, Low; Top right, High snow; Bottom, High rain. Low to high elevations are represented by light to dark blue shading and thin to thick contours lines respectively.

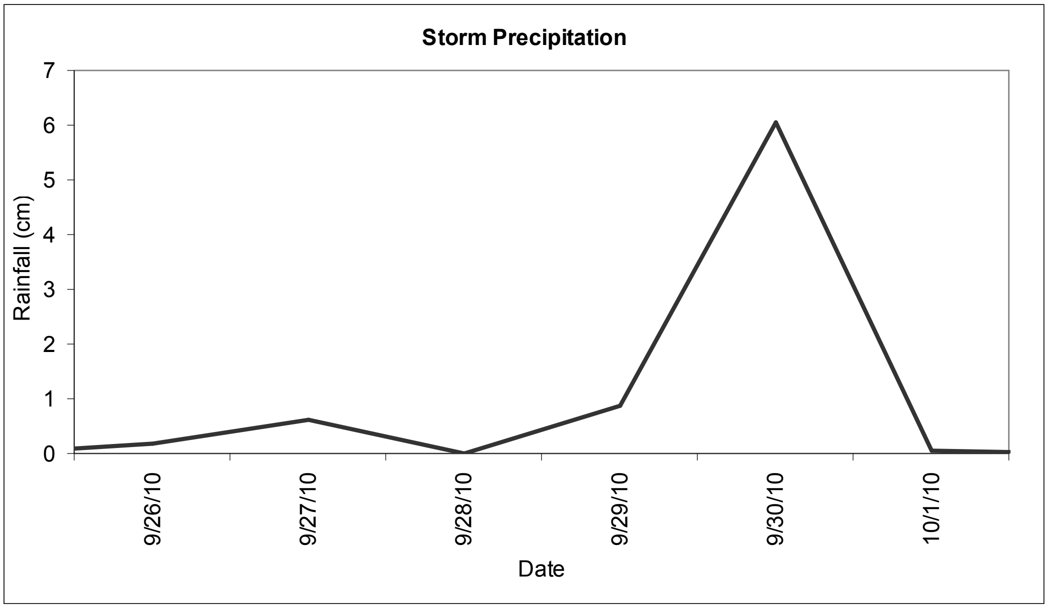

Figure 24: Time series of fall tropical storm from September 29th, 2010 to October 1st, 2010 taken from Beltsville gauge.

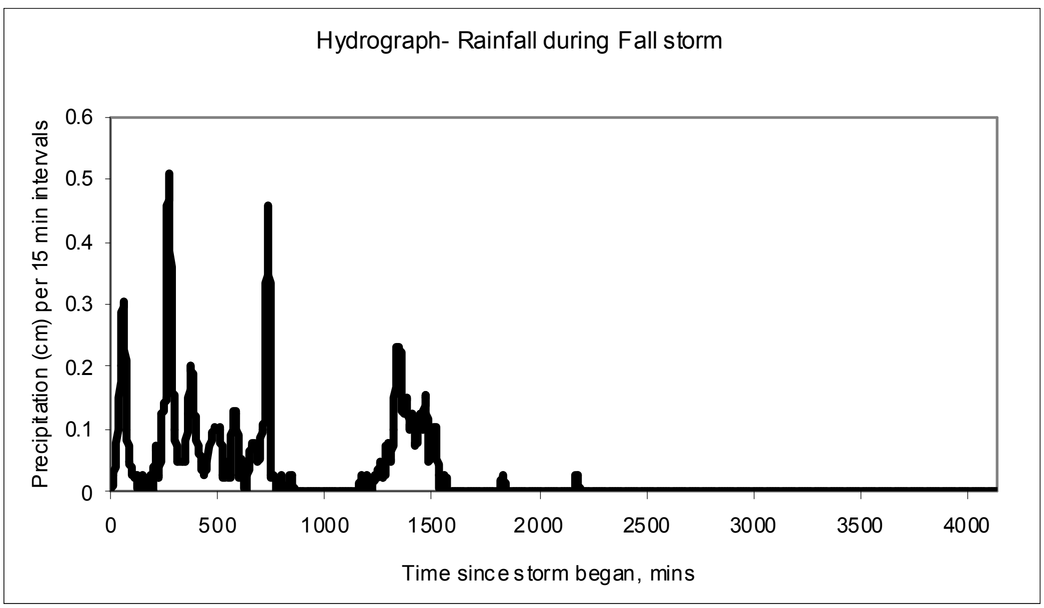

Figure 25: Detailed time plot of fall tropical storm from September 29th, 2010 to October 1st, 2010 in 15 minute intervals.

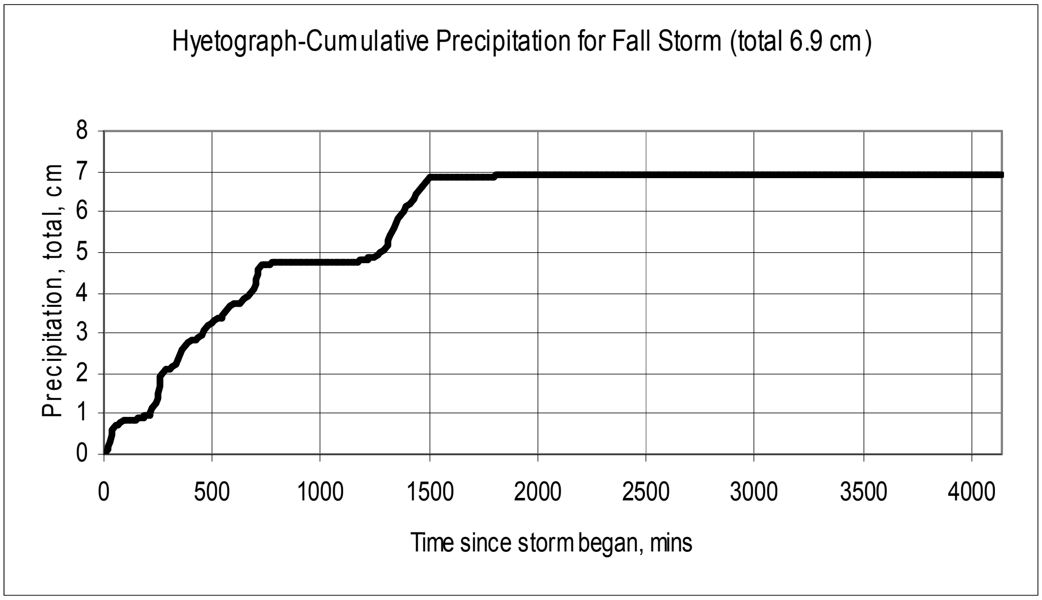

Figure 26: Hyetographs distribution of rainfall with time shows the largest peak occurring at the 270th minute containing 0.508 cm of precipitation.

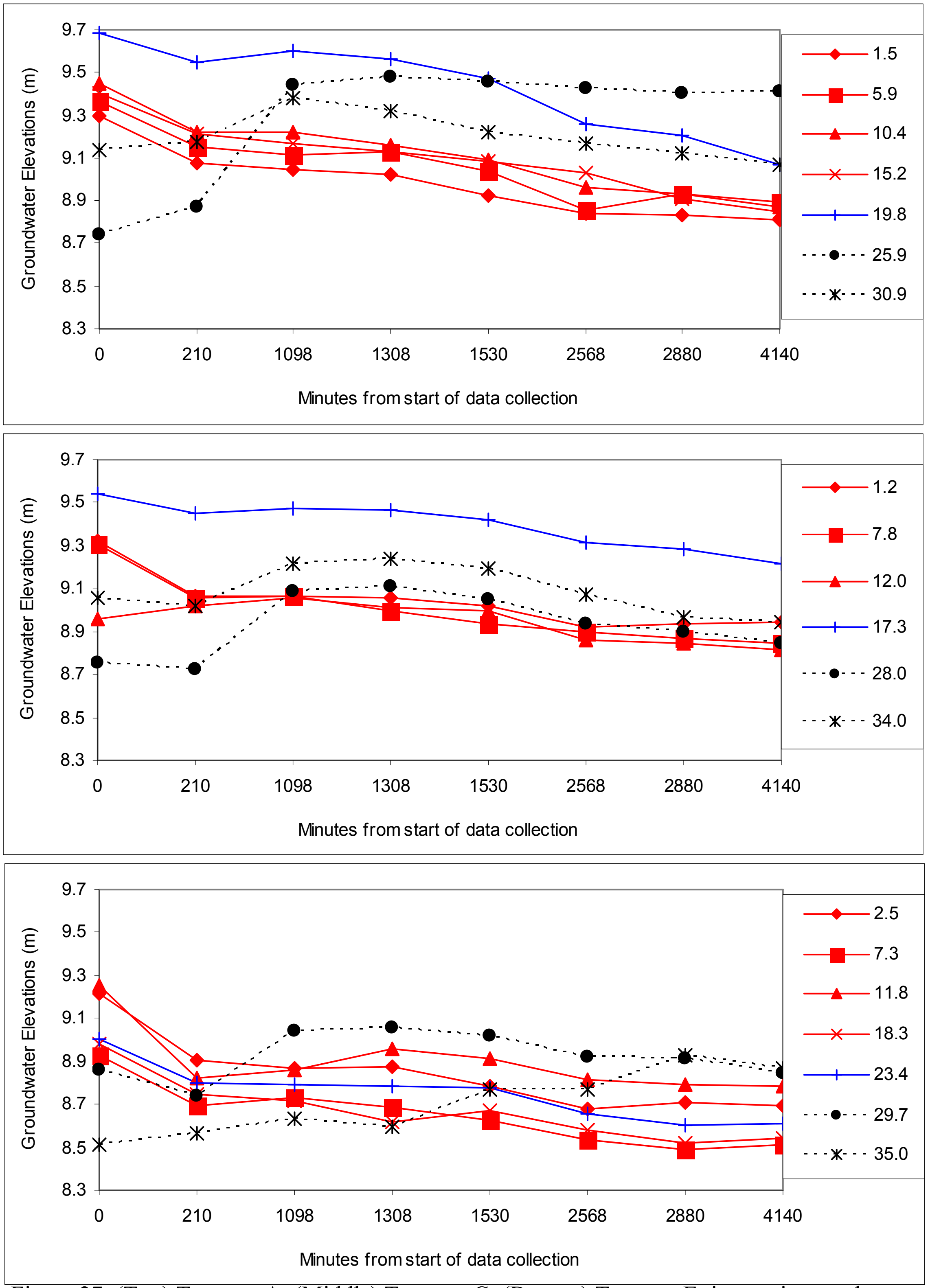

Figure 27: (Top) Transect A; (Middle) Transect C; (Bottom) Transect E time series graphs during the tropical storm on September 29th, 2010. Red lines are accreting gravel bar piezometers; Blue line are chute channel piezometers; Black dotted lines are uplands piezometers. Distance from stream labeled in legend.

Appendices B-Additional Figures not used in text.

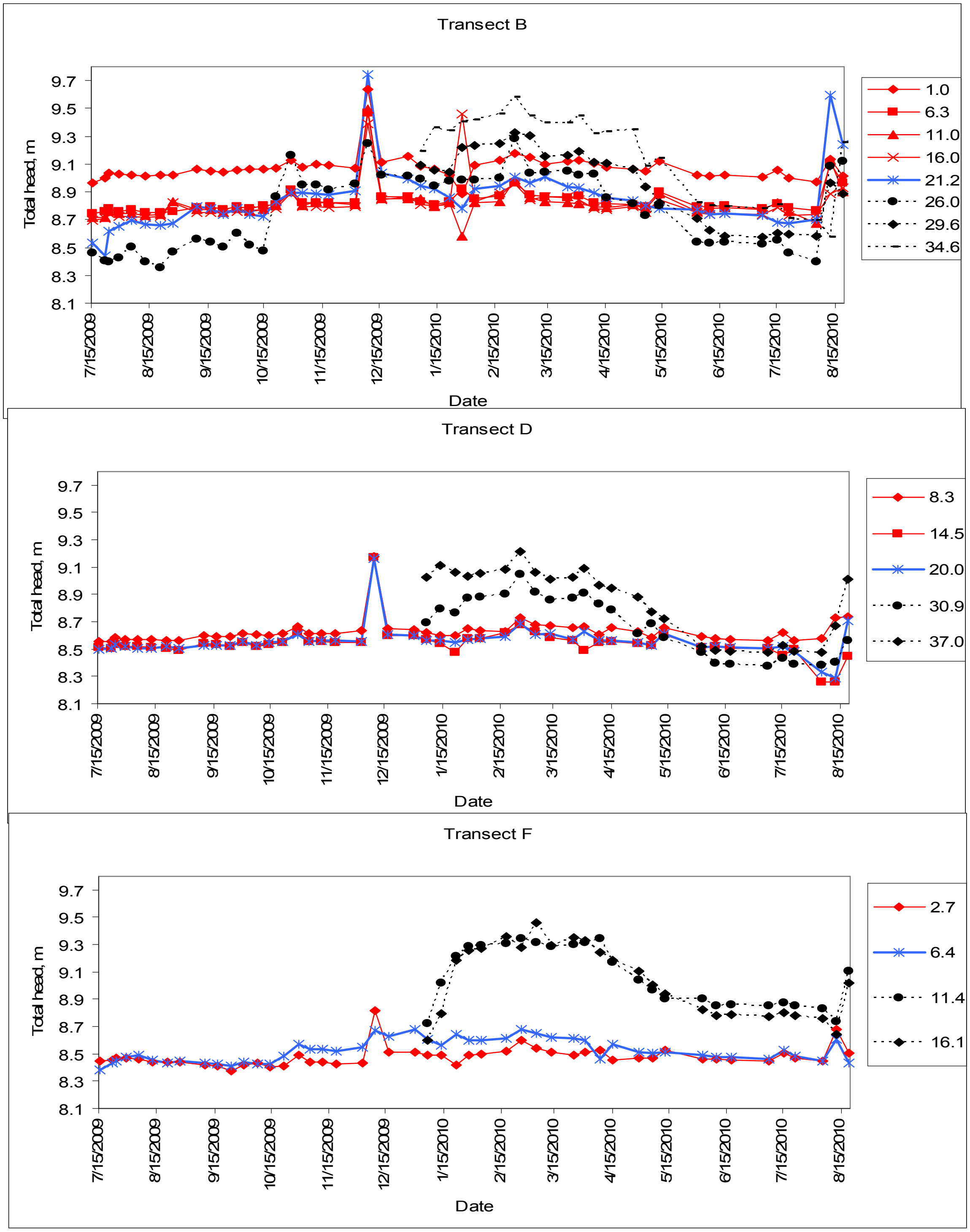

A1: Extra complete time series- (Red lines inset gravel bar piezometers; Blue line chute channel piezometers; Black dotted lines are upland piezometers.

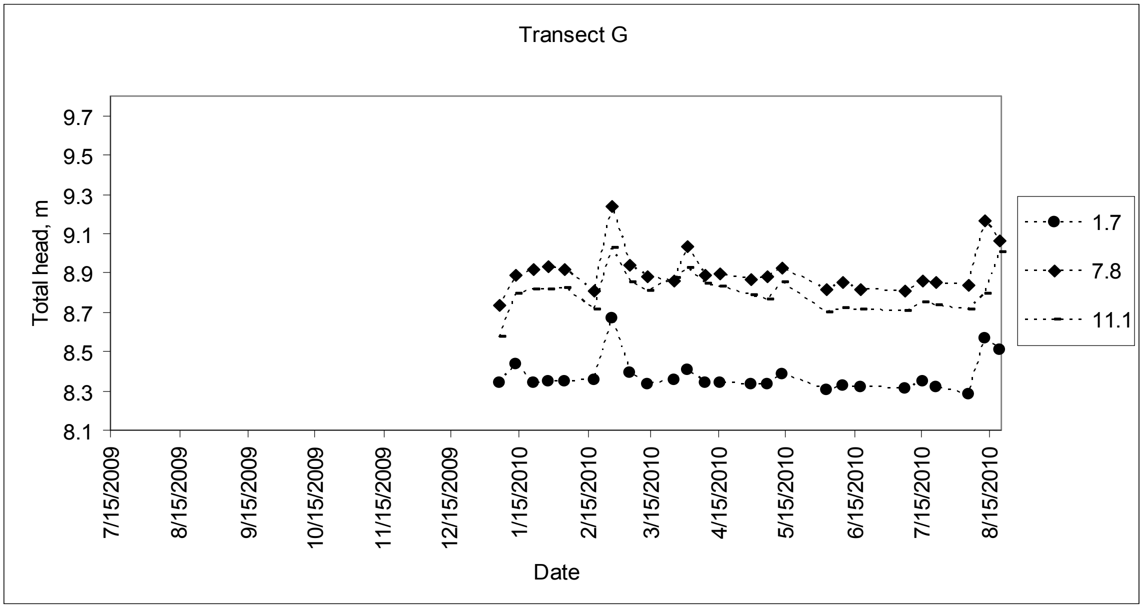

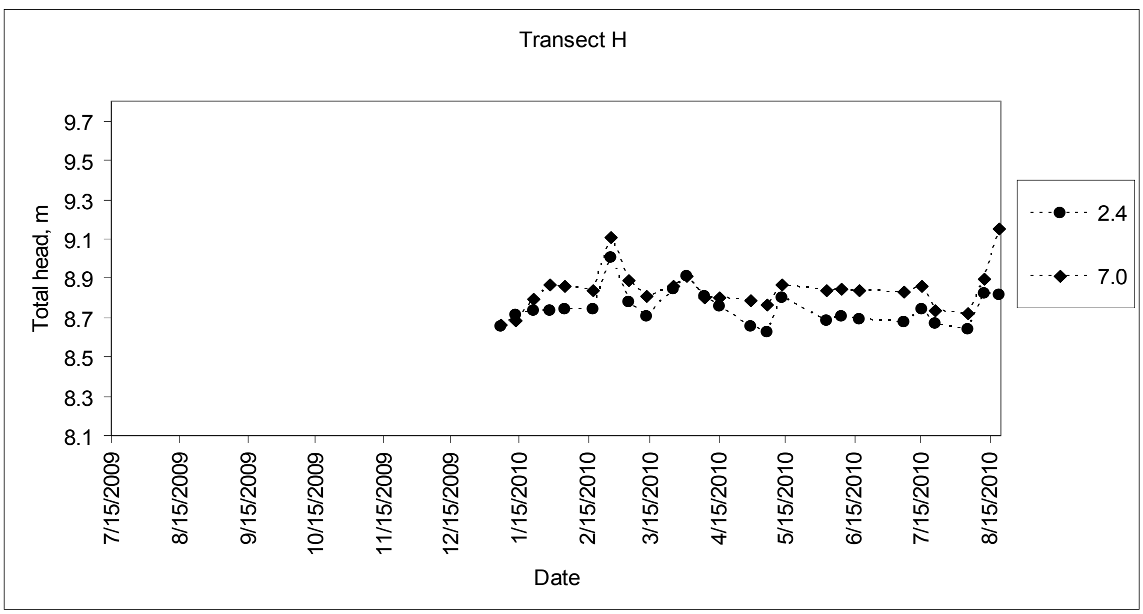

A2: Extra complete time series- (Red lines inset gravel bar piezometers; Blue line chute channel piezometers; Black dotted lines are upland piezometers.

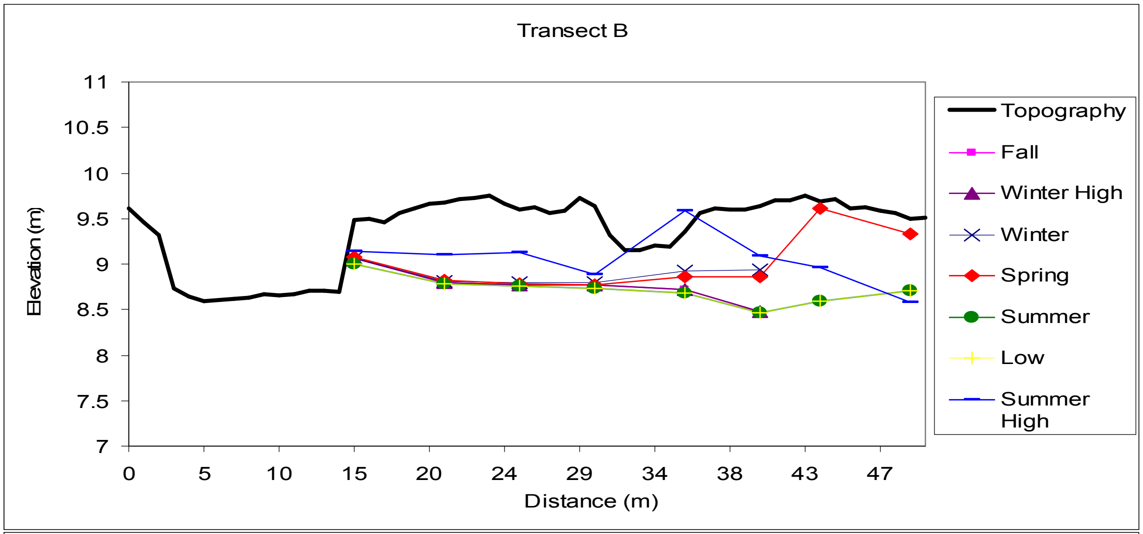

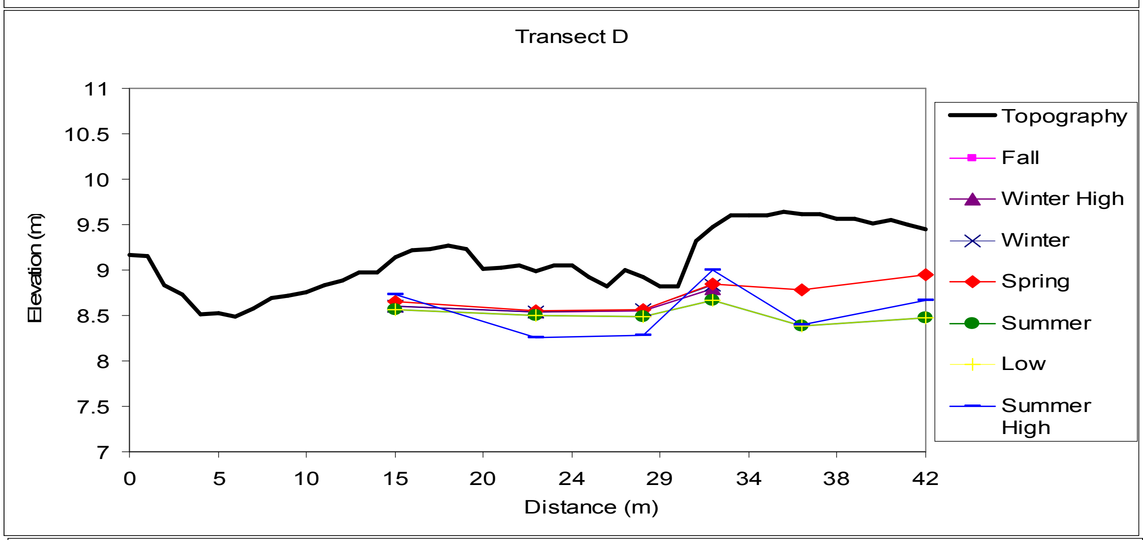

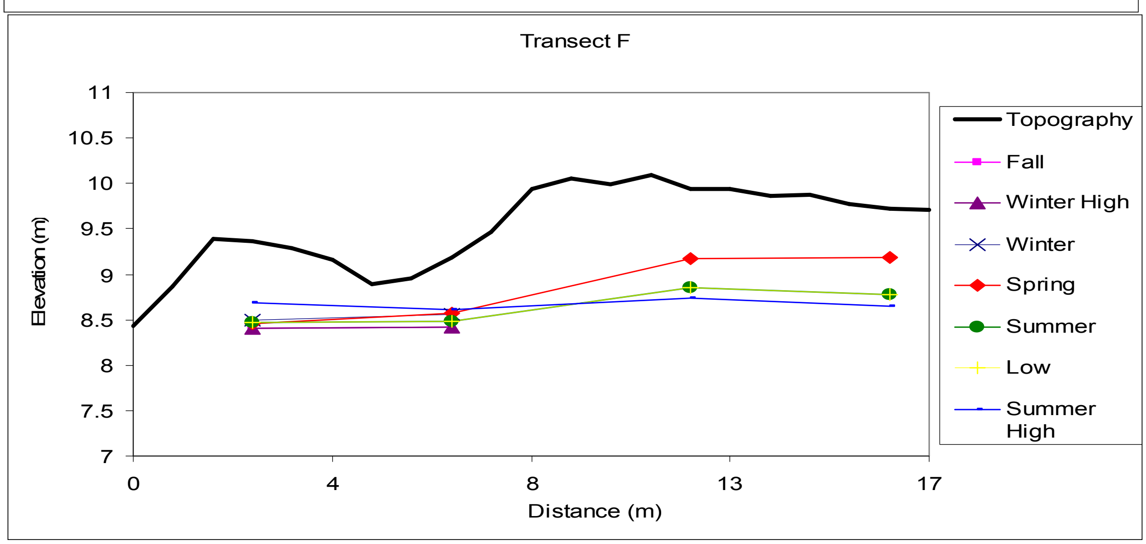

A3: Extra Groundwater elevation plots.

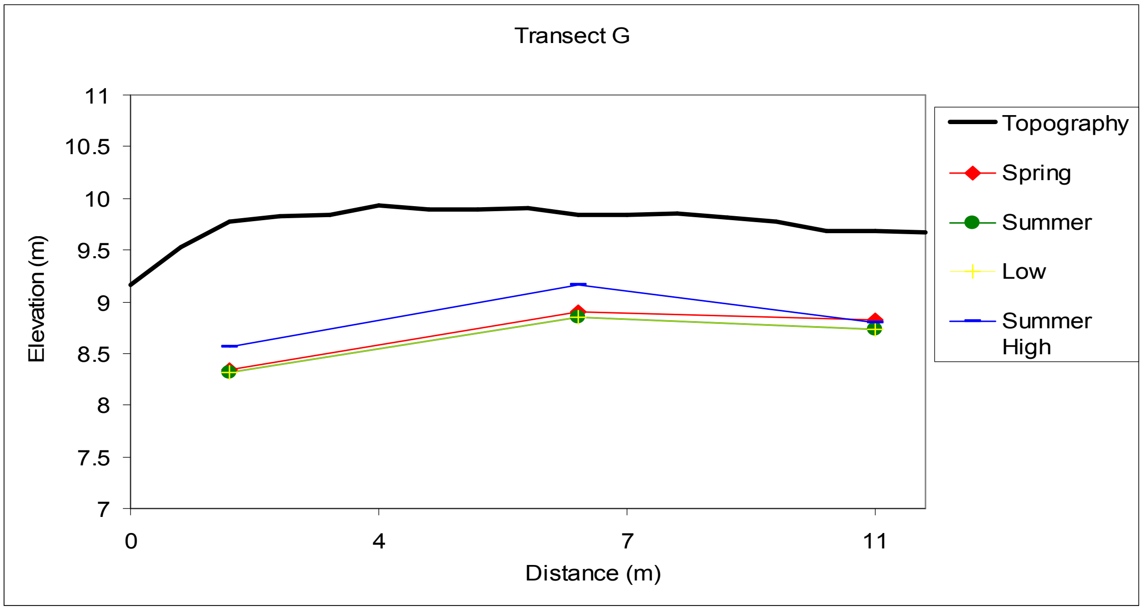

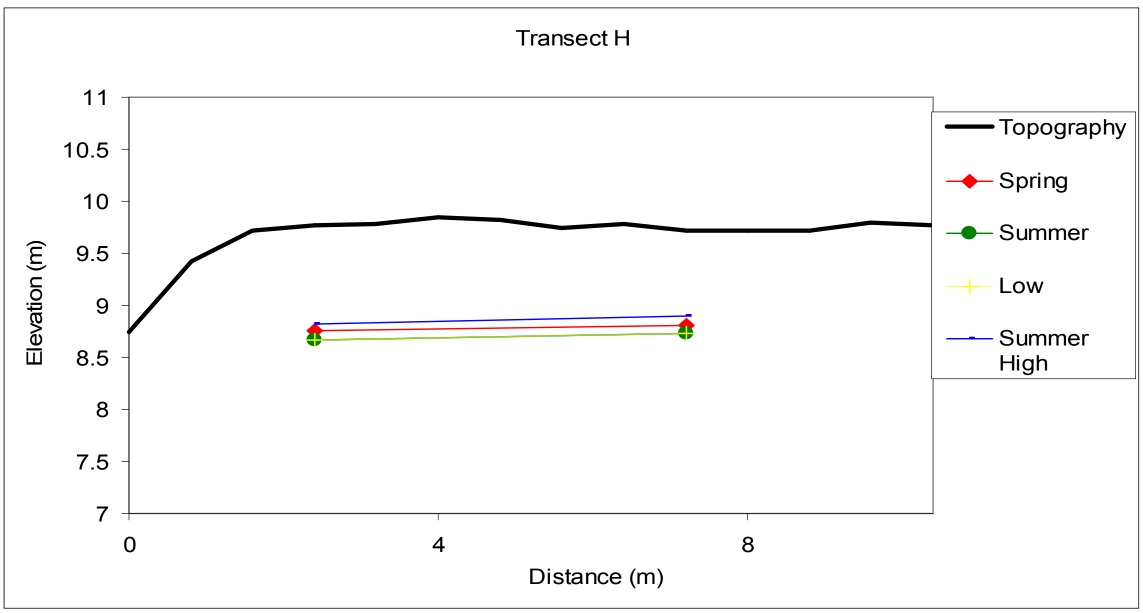

A4: Extra Groundwater elevation plots.

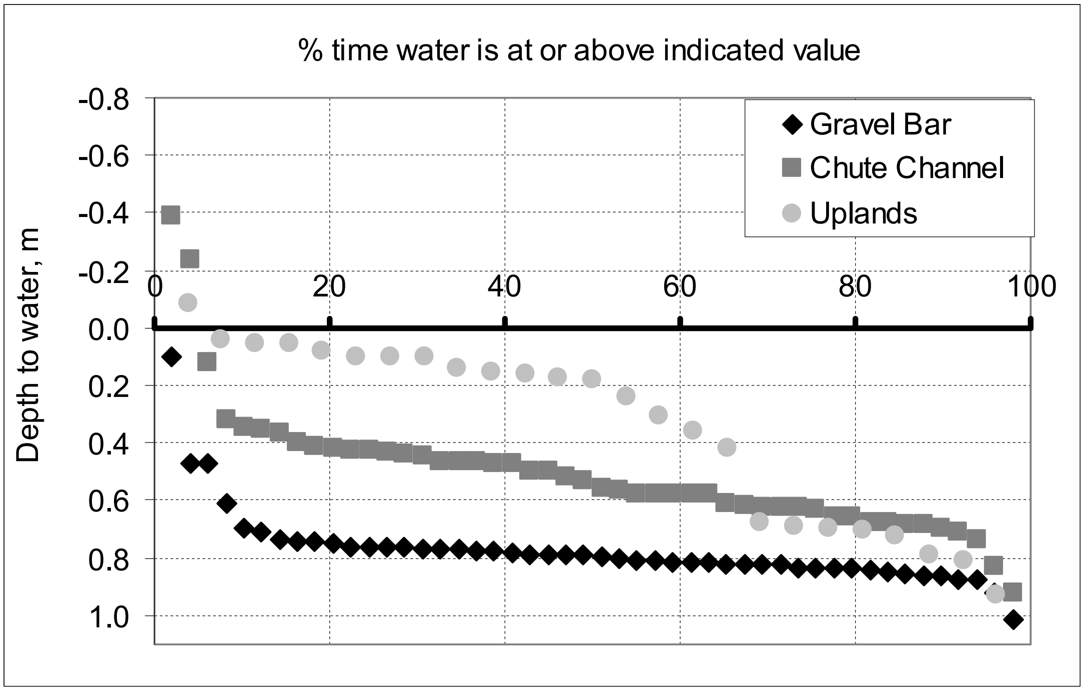

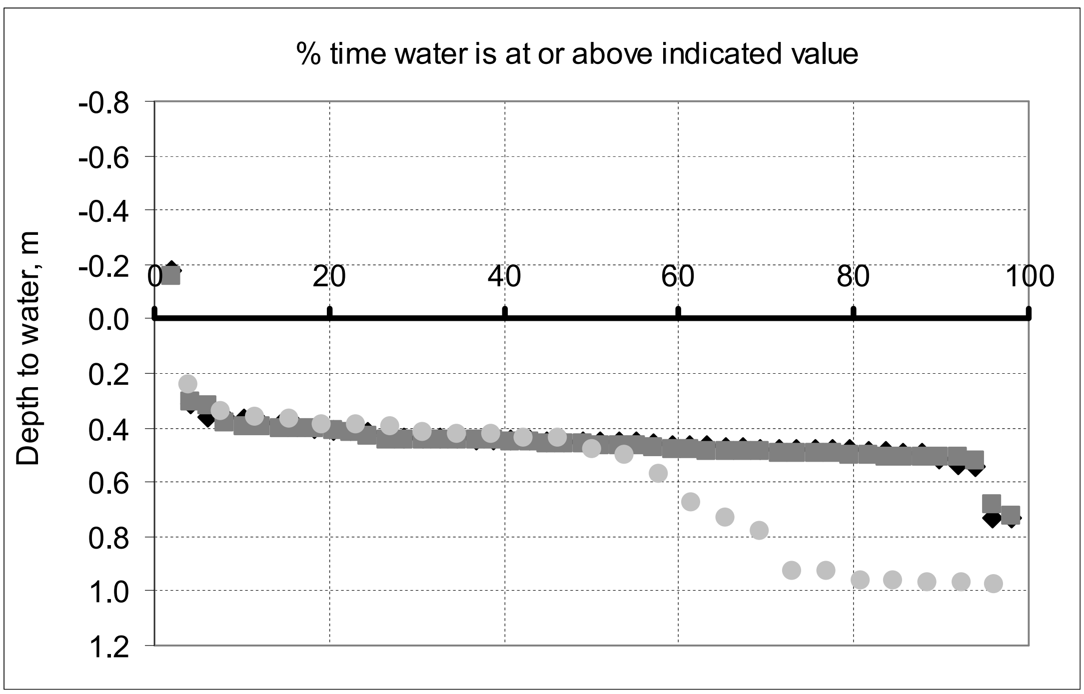

A5: Annual flow duration curves (Top) B transect; (Bottom) D transect. Solid black thick line indicates surface level.

Appendices C-Data

- Tables below shows data collected for groundwater heads for study period.
- Site benchmark was 10.

TRANSECT A						Bank Elevation= 9.34		
Piezometer	**A1**	**A2**	**A2a**	**A3**	**A4**	**A5**	**A6**	**A7**
Topography Elevation	9.499	9.601	9.601	9.509	9.606	9.149	9.735	9.604
7/15/2009	8.69	8.765	8.963	8.738	8.745	8.62		
7/22/2009	8.67	8.762	8.963	8.749	8.746	8.548		
7/24/2009	8.727	8.694	8.963	8.791	8.789	8.966		
7/29/2009	8.71	8.783	8.963	8.773	8.764	8.743		
8/5/2009	8.727	8.789	8.963	8.778	8.774	8.816		
8/12/2009	8.646	8.778	8.963	8.758	8.755	8.805		
8/20/2009	8.708	8.773	8.963	8.753	8.758	8.597		
8/27/2009	8.704	8.777	8.963	8.758	8.763	8.754		
9/9/2009	8.74	8.824	8.963	8.809	8.806	8.835		
9/16/2009	8.741	8.81	8.963	8.799	8.797	8.817		
9/23/2009	8.727	8.797	8.963	8.791	8.779	8.708		
9/30/2009	8.739	8.818	8.983	8.81	8.805	8.843		
10/7/2009	8.731	8.808	8.963	8.787	8.782	8.71		
10/14/2009	8.75	8.817	8.973	8.814	8.792	8.648		
10/21/2009	8.758	8.831	8.983	8.885	8.819	9.000		
10/29/2009	8.83	8.921	8.998	8.971	8.936	9.205		
11/4/2009	8.773	8.844	8.987	8.829	8.824	9.013		
11/11/2009	8.773	8.842	8.983	8.84	8.826	9.004		
11/18/2009	8.764	8.84	8.973	8.838	8.825	8.995		
12/2/2009	8.777	8.857	8.963	8.874	8.835	9.03		
12/9/2009	9.31	9.412	9.553	9.459	9.546	9.698		
12/16/2009	8.807	8.908	9.015	8.909	8.874	9.087		
12/30/2009	8.813	8.884	8.987	8.912	8.877	9.084		
1/6/2010	8.784	8.869	8.963	8.858	8.837	9.058	9.082	9.115
1/13/2010	8.664	8.762	8.963	8.837	8.824	8.986	9.046	9.112
1/21/2010	8.778	8.817	8.963	8.862	8.854	9.053	9.085	9.14
1/28/2010	8.815	8.885	8.963	8.884	8.713	9.049	9.124	9.136
2/4/2010	8.818	8.877	8.963	8.9	8.741	9.098	9.167	9.154
2/17/2010	8.815	8.887	8.996	8.924	8.868	9.116	9.202	9.171
2/25/2010	8.894	8.992	8.963	9.058	9.009	9.129	9.297	9.298
3/5/2010	8.908	8.911	8.978	8.961	8.89	9.087	9.179	9.197
3/13/2010	8.813	8.832	8.963	8.903	8.841	9.063	9.075	9.152
3/25/2010	8.821	8.84	8.963	8.879	8.863	9.045	9.097	9.156
3/31/2010	8.828	8.884	9.033	8.912	8.877	9.114	9.215	9.213
4/8/2010	8.787	8.782	8.963	8.841	8.823	9.004	9.055	9.089
4/15/2010	8.747	8.841	8.963	8.86	8.843	8.976	9.002	9.017
4/29/2010	8.771	8.843	9.026	8.841	8.811	8.945	8.923	8.924
5/6/2010	8.746	8.824	8.963	8.867	8.778	8.924	8.833	8.847
5/13/2010	8.831	8.931	9.015	8.938	8.911	8.967	8.948	9.000
6/2/2010	8.753	8.746	8.963	8.842	8.771	8.817	8.589	8.891
6/9/2010	8.751	8.84	8.963	8.814	8.784	8.803	8.565	8.867
6/17/2010	8.774	8.859	8.991	8.838	8.802	8.837	8.57	8.891
7/7/2010	8.749	8.832	8.963	8.831	8.781	8.805	8.548	8.891
7/15/2010	8.81	8.768	8.963	8.879	8.836	8.691	8.525	8.851
7/21/2010	8.755	8.779	8.963	8.781	8.827	8.687	8.464	8.851
8/5/2010	8.733	8.771	8.963	8.774	8.802	8.744	8.407	8.834
8/12/2010	9.077	9.018	9.242	9.104	9.061	9.644	8.378	8.691
8/19/2010	8.882	8.94	9.044	8.959	8.957	9.369	9.241	9.09

TRANSECT B Bank= 9.613

Piezometer	**B1**	**B2**	**B3**	**B3b**	**B4**	**B5**	**B6**	**B7**	**B8**
Topography Elevations	9.488	9.679	9.594	9.594	9.640	9.356	9.636	9.687	9.500
7/15/2009	8.965	8.747	8.716	9.018	8.696	8.529	8.461		
7/22/2009	9.002	8.761	8.717	9.018	8.708	8.438	8.408		
7/24/2009	9.037	8.777	8.756	9.021	8.742	8.617	8.394		
7/29/2009	9.028	8.758	8.742	9.024	8.724	8.649	8.427		
8/5/2009	9.018	8.771	8.746	9.018	8.721	8.698	8.501		
8/12/2009	9.014	8.754	8.731	9.018	8.718	8.67	8.394		
8/20/2009	9.022	8.753	8.735	9.018	8.722	8.663	8.358		
8/27/2009	9.019	8.757	8.833	9.018	8.821	8.676	8.465		
9/9/2009	9.062	8.787	8.771	9.018	8.755	8.792	8.562		
9/16/2009	9.05	8.794	8.773	9.018	8.752	8.781	8.539		
9/23/2009	9.04	8.77	8.751	9.018	8.75	8.735	8.503		
9/30/2009	9.059	8.795	8.781	9.018	8.76	8.777	8.602		
10/7/2009	9.062	8.782	8.762	9.018	8.765	8.734	8.517		
10/14/2009	9.062	8.801	8.771	9.018	8.774	8.724	8.478		
10/21/2009	9.067	8.808	8.802	9.028	8.783	8.828	8.868		
10/29/2009	9.124	8.913	8.897	9.053	8.895	8.891	9.162		
11/4/2009	9.075	8.82	8.802	9.028	8.791	8.89	8.947		
11/11/2009	9.097	8.822	8.829	9.028	8.792	8.886	8.95		
11/18/2009	9.091	8.821	8.822	9.018	8.786	8.882	8.916		
12/2/2009	9.072	8.825	8.805	9.018	8.797	8.909	8.956		
12/9/2009	9.638	9.47	9.493	9.539	9.392	9.745	9.251		
12/16/2009	9.115	8.862	8.848	9.043	8.846	9.036	9.018		
12/30/2009	9.156	8.865	8.851	9.046	8.868	8.989	9.016		
1/6/2010	9.084	8.828	8.853	9.039	8.811	8.94	8.993	9.093	9.193
1/13/2010	9.066	8.806	8.796	9.039	8.799	8.922	8.94	9.056	9.361
1/21/2010	9.018	8.832	8.82	9.018	8.81	8.857	8.975	9.039	9.342
1/28/2010	8.883	8.924	8.58	9.27	9.461	8.78	8.982	9.217	9.401
2/4/2010	9.094	8.848	8.826	9.038	8.828	8.92	8.987	9.231	9.418
2/17/2010	9.126	8.875	8.829	9.049	8.892	8.946	8.998	9.246	9.462
2/25/2010	9.177	8.961	8.986	9.041	8.957	9.01	9.284	9.324	9.582
3/5/2010	9.149	8.88	8.859	9.018	8.846	8.961	9.034	9.304	9.446
3/13/2010	9.102	8.865	8.832	9.079	8.862	9.007	9.041	9.153	9.397
3/25/2010	9.122	8.86	8.826	9.041	8.863	8.933	9.048	9.161	9.397
3/31/2010	9.128	8.872	8.814	9.029	8.843	8.931	9.018	9.188	9.449
4/8/2010	9.107	8.823	8.795	9.018	8.777	8.892	9.031	9.113	9.318
4/15/2010	9.074	8.816	8.786	9.018	8.77	8.858	8.858	9.107	9.329
4/29/2010	9.066	8.809	8.808	9.018	8.794	8.838	8.814	9.064	9.347
5/6/2010	9.046	8.796	8.781	9.018	8.755	8.798	8.732	8.933	9.084
5/13/2010	9.118	8.898	8.884	9.018	8.841	8.777	8.802	8.824	9.142
6/2/2010	9.018	8.796	8.762	9.018	8.751	8.776	8.54	8.708	8.824
6/9/2010	9.014	8.791	8.781	9.018	8.741	8.737	8.531	8.623	8.804
6/17/2010	9.019	8.803	8.787	9.018	8.744	8.744	8.539	8.582	8.794
7/7/2010	9.007	8.782	8.772	9.018	8.737	8.733	8.525	8.574	8.778
7/15/2010	9.053	8.818	8.819	9.018	8.79	8.679	8.55	8.605	8.81
7/21/2010	9.003	8.785	8.76	9.018	8.73	8.677	8.462	8.597	8.709
8/5/2010	8.968	8.765	8.672	9.018	8.739	8.699	8.398	8.581	8.693
8/12/2010	9.134	9.107	9.125	9.383	8.888	9.592	9.084	8.963	8.575
8/19/2010	9.012	8.964	8.9	9.13	8.929	9.238	9.121	8.888	9.258

TRANSECT C						Bank= 9.283	
Piezometer	**C1**	**C2**	**C2c**	**C3**	**C4**	**C5**	**C6**
Topography Elevations	9.009	9.62	9.62	9.593	8.929	9.8	9.651
7/15/2009	8.752	8.72	8.901	8.634	8.596		
7/22/2009	8.769	8.716	8.901	8.682	8.604		
7/24/2009	8.796	8.751	8.92	8.715	8.637		
7/29/2009	8.787	8.745	8.901	8.702	8.615		
8/5/2009	8.769	8.741	8.902	8.701	8.617		
8/12/2009	8.778	8.731	8.927	8.699	8.615		
8/20/2009	8.794	8.731	8.926	8.691	8.604		
8/27/2009	8.784	8.726	8.916	8.694	8.619		
9/9/2009	8.844	8.76	8.926	8.729	8.644		
9/16/2009	8.836	8.759	8.924	8.694	8.695		
9/23/2009	8.828	8.754	8.921	8.713	8.767		
9/30/2009	8.845	8.763	8.921	8.732	8.814		
10/7/2009	8.842	8.761	8.901	8.718	8.798		
10/14/2009	8.865	8.771	8.921	8.736	8.817		
10/21/2009	8.858	8.774	8.921	8.743	8.877		
10/29/2009	8.914	8.861	8.941	8.836	8.963		
11/4/2009	8.863	8.783	8.901	8.754	8.866		
11/11/2009	8.869	8.784	8.901	8.762	8.883		
11/18/2009	8.868	8.782	8.901	8.76	8.873		
12/2/2009	8.862	8.789	8.901	8.758	8.883		
12/9/2009	9.324	9.359	9.464	9.355	9.585		
12/16/2009	8.893	8.825	8.927	8.799	8.918		
12/30/2009	8.898	8.825	8.94	8.702	8.856		
1/6/2010	8.892	8.794	8.924	8.766	8.832	8.877	8.911
1/13/2010	8.845	8.772	8.913	8.792	8.825	8.852	8.958
1/21/2010	8.855	8.774	8.901	8.747	8.856	8.873	8.988
1/28/2010	8.908	8.796	8.901	8.771	8.937	8.888	9.051
2/4/2010	8.896	8.823	8.901	8.77	8.927	8.891	9.059
2/17/2010	8.878	8.837	8.901	8.789	8.906	8.887	9.063
2/25/2010	8.956	8.907	9.031	8.92	9.043	9.05	9.107
3/5/2010	8.934	8.835	8.901	8.81	8.955	8.915	9.033
3/13/2010	8.884	8.809	8.901	8.796	8.909	8.903	8.965
3/25/2010	8.896	8.821	8.901	8.824	8.985	8.881	8.955
3/31/2010	8.885	8.836	8.901	8.802	8.93	8.923	8.888
4/8/2010	8.848	8.801	8.901	8.757	8.862	8.885	8.861
4/15/2010	8.868	8.793	8.901	8.755	8.828	8.851	8.834
4/29/2010	8.836	8.79	8.901	8.756	8.871	8.796	8.812
5/6/2010	8.832	8.772	8.901	8.768	8.813	8.735	8.664
5/13/2010	8.886	8.848	8.901	8.871	9.109	8.899	8.878
6/2/2010	8.82	8.752	8.901	8.712	8.853	8.678	8.47
6/9/2010	8.823	8.754	8.901	8.713	8.863	8.665	8.403
6/17/2010	8.844	8.76	8.901	8.718	8.874	8.667	8.412
7/7/2010	8.835	8.754	8.901	8.715	8.864	8.656	8.402
7/15/2010	8.886	8.715	8.901	8.773	8.89	8.718	8.446
7/21/2010	8.965	8.749	8.901	8.704	8.907	8.569	8.371
8/5/2010	8.931	8.743	8.901	8.63	8.897	8.575	8.316
8/12/2010	9.044	8.909	8.946	8.831	9.434	8.932	8.504
8/19/2010	8.942	8.822	9.431	8.799	9.076	8.683	9.072

TRANSECT D							Bank=9.165	
Piezometer	**D1**	**D2**	**D2d**	**D3**	**D4**	**D4d**	**D5**	**D6**
Topography Elevations	9.138	8.986	9.001	9.479	9.613	9.452	9.551	
7/15/2009	8.555	8.511	8.568	8.501	8.352			
7/22/2009	8.553	8.502	8.568	8.504	8.758			
7/24/2009	8.583	8.535	8.568	8.535	8.782			
7/29/2009	8.572	8.52	8.634	8.519	8.769			
8/5/2009	8.573	8.523	8.613	8.505	8.773	8.735		
8/12/2009	8.573	8.513	8.63	8.505	8.755	8.727		
8/20/2009	8.564	8.507	8.588	8.516	8.77	8.702		
8/27/2009	8.565	8.494	8.603	8.508	8.777	8.732		
9/9/2009	8.6	8.538	8.602	8.53	8.787	8.761		
9/16/2009	8.595	8.537	8.608	8.529	8.79	8.774		
9/23/2009	8.595	8.521	8.588	8.527	8.772	8.772		
9/30/2009	8.617	8.546	8.628	8.554	8.787	8.752		
10/7/2009	8.604	8.523	8.626	8.525	8.784	8.797		
10/14/2009	8.6	8.536	8.578	8.547	8.789	8.772		
10/21/2009	8.611	8.546	8.588	8.553	8.807	8.842		
10/29/2009	8.665	8.629	8.613	8.605	8.899	9.034		
11/4/2009	8.614	8.554	8.605	8.558	8.808	8.846		
11/11/2009	8.616	8.553	8.602	8.565	8.806	8.859		
11/18/2009	8.615	8.547	8.588	8.563	8.804	8.855		
12/2/2009	8.633	8.547	8.603	8.554	8.807	8.85		
12/9/2009	9.175	9.169	9.151	9.167	9.437	9.447		
12/16/2009	8.652	8.602	8.631	8.606	8.84	8.924		
12/30/2009	8.64	8.597	8.602	8.6	8.874	8.907		
1/6/2010	8.623	8.571	8.61	8.566	8.835	8.856	8.696	9.029
1/13/2010	8.597	8.538	8.602	8.563	8.83	8.803	8.794	9.113
1/21/2010	8.6	8.476	8.568	8.546	8.746	8.853	8.764	9.063
1/28/2010	8.647	8.579	8.586	8.569	8.857	8.863	8.871	9.034
2/4/2010	8.633	8.579	8.588	8.58	8.866	8.87	8.883	9.054
2/17/2010	8.63	8.623	8.599	8.595	8.877	8.877	8.905	9.085
2/25/2010	8.731	8.677	8.66	8.689	8.944	9.078	9.05	9.211
3/5/2010	8.679	8.63	8.599	8.608	8.874	8.901	8.914	9.064
3/13/2010	8.673	8.585	8.568	8.615	8.896	8.852	8.863	9.014
3/25/2010	8.655	8.562	8.568	8.569	8.857	8.856	8.874	9.025
3/31/2010	8.663	8.494	8.568	8.629	8.858	8.901	8.91	9.088
4/8/2010	8.608	8.552	8.568	8.561	8.818	8.816	8.833	8.971
4/15/2010	8.657	8.555	8.568	8.563	8.842	8.807	8.784	8.947
4/29/2010	8.626	8.538	8.568	8.547	8.821	8.787	8.613	8.879
5/6/2010	8.586	8.528	8.568	8.526	8.792	8.748	8.684	8.776
5/13/2010	8.658	8.609	8.568	8.614	8.89	8.893	8.588	8.722
6/2/2010	8.591	8.509	8.568	8.509	8.772	8.832	8.474	8.521
6/9/2010	8.576	8.516	8.568	8.522	8.783	8.782	8.393	8.488
6/17/2010	8.57	8.508	8.568	8.514	8.775	8.776	8.386	8.485
7/7/2010	8.566	8.508	8.568	8.505	8.768	8.761	8.378	8.479
7/15/2010	8.621	8.456	8.568	8.517	8.749	8.769	8.433	8.526
7/21/2010	8.566	8.501	8.568	8.486	8.67	8.764	8.389	8.48
8/5/2010	8.581	8.256	8.568	8.331	8.617	8.76	8.379	8.473
8/12/2010	8.731	8.256	8.568	8.287	9.002	8.844	8.403	8.669
8/19/2010	8.737	8.448	8.67	8.706	8.971	9.443	8.564	9.013

TRANSECT E							Bank= 8.535	
Piezometer	**E1**	**E2**	**E2e**	**E3**	**E4**	**E5**	**E6**	**E7**
Topography Elevations	8.737	9.445	9.445	9.16	9.176	9.168	9.567	9.287
7/15/2009	8.658	8.442	8.652	8.7	8.469	8.465		
7/22/2009	8.679	8.425	8.652	8.71	8.487	8.516		
7/24/2009	8.707	8.452	8.652	8.721	8.505	8.631		
7/29/2009	8.696	8.449	8.652	8.713	8.51	8.545		
8/5/2009	8.678	8.444	8.652	8.694	8.513	8.609		
8/12/2009	8.665	8.436	8.652	8.698	8.491	8.521		
8/20/2009	8.679	8.437	8.652	8.698	8.5	8.525		
8/27/2009	8.701	8.439	8.667	8.699	8.499	8.545		
9/9/2009	8.71	8.461	8.683	8.71	8.508	8.6		
9/16/2009	8.701	8.448	8.713	8.703	8.501	8.541		
9/23/2009	8.699	8.445	8.652	8.694	8.494	8.559		
9/30/2009	8.712	8.451	8.652	8.707	8.522	8.535		
10/7/2009	8.686	8.441	8.652	8.706	8.514	8.53		
10/14/2009	8.712	8.453	8.652	8.714	8.515	8.542		
10/21/2009	8.708	8.458	8.652	8.709	8.511	8.536		
10/29/2009	8.733	8.506	8.672	8.777	8.577	8.614		
11/4/2009	8.68	8.451	8.652	8.719	8.521	8.542		
11/11/2009	8.692	8.462	8.652	8.72	8.536	8.546		
11/18/2009	8.688	8.458	8.652	8.716	8.534	8.543		
12/2/2009	8.651	8.441	8.652	8.721	8.521	8.55		
12/9/2009	9.408	9.005	9.067	9.226	9.062	9.059		
12/16/2009	8.75	8.519	8.669	8.796	8.583	8.62		
12/30/2009	8.722	8.496	8.669	8.776	8.563	8.598		
1/6/2010	8.68	8.497	8.672	8.745	8.551	8.579	8.82	8.77
1/13/2010	8.669	8.48	8.652	8.736	8.545	8.558	8.781	8.696
1/21/2010	8.642	8.412	8.652	8.736	8.545	8.436	8.854	8.807
1/28/2010	8.714	8.492	8.652	8.745	8.554	8.558	8.861	8.891
2/4/2010	8.706	8.513	8.652	8.742	8.563	8.606	8.888	8.909
2/17/2010	8.703	8.527	9.02	8.777	8.575	8.625	8.913	8.938
2/25/2010	8.773	8.573	8.766	8.895	8.653	8.688	9.012	9.037
3/5/2010	8.703	8.53	9.024	9.076	8.665	8.602	8.901	8.925
3/13/2010	8.7	8.493	8.742	8.769	8.638	8.494	8.831	8.912
3/25/2010	8.717	8.514	8.672	8.76	8.625	8.565	8.845	8.893
3/31/2010	8.712	8.571	8.652	8.77	8.584	8.606	8.909	8.968
4/8/2010	8.697	8.49	8.652	8.707	8.566	8.566	8.792	8.862
4/15/2010	8.511	8.478	8.652	8.695	8.54	8.571	8.704	8.781
4/29/2010	8.663	8.487	8.652	8.728	8.531	8.56	8.678	8.753
5/6/2010	8.66	8.446	8.652	8.718	8.52	8.539	8.614	8.635
5/13/2010	8.722	8.499	8.652	8.742	8.584	8.601	8.717	8.557
6/2/2010	8.642	8.351	8.652	8.702	8.516	8.52	8.4	8.388
6/9/2010	8.649	8.35	8.652	8.702	8.512	8.526	8.425	8.409
6/17/2010	8.641	8.347	8.652	8.695	8.498	8.54	8.431	8.405
7/7/2010	8.636	8.341	8.652	8.688	8.481	8.525	8.418	8.398
7/15/2010	8.654	8.364	8.652	8.721	8.502	8.553	8.463	8.434
7/21/2010	8.593	8.34	8.652	8.644	8.461	8.485	8.396	8.409
8/5/2010	8.541	8.313	8.652	8.655	8.402	8.422	8.342	8.392
8/12/2010	8.599	8.548	8.675	8.888	8.442	8.558	8.542	8.579
8/19/2010	8.799	8.582	8.652	8.738	8.562	8.615	8.96	8.881

TRANSECT F, G, H		Bank F= 8.427				Bank G= 8.412			Bank H= 8.411	
Piezometer	**F1**	**F2**	**F2f**	**F3**	**F4**	**G1**	**G2**	**G3**	**H1**	**H2**
Topography Elevations	9.36	9.188	9.94	9.728	9.687	9.769	9.841	9.687	9.765	9.719
7/15/2009	8.448	8.38	8.391							
7/22/2009	8.451	8.433	8.391							
7/24/2009	8.467	8.445	8.555							
7/29/2009	8.471	8.477	8.59							
8/5/2009	8.463	8.492	8.582							
8/12/2009	8.438	8.454	8.556							
8/20/2009	8.442	8.433	8.567							
8/27/2009	8.437	8.445	8.567							
9/9/2009	8.42	8.433	8.533							
9/16/2009	8.41	8.427	8.545							
9/23/2009	8.377	8.412	8.531							
9/30/2009	8.42	8.437	8.568							
10/7/2009	8.43	8.427	8.55							
10/14/2009	8.407	8.424	8.552							
10/21/2009	8.411	8.487	8.553							
10/29/2009	8.489	8.573	8.693							
11/4/2009	8.443	8.535	8.544							
11/11/2009	8.439	8.536	8.546							
11/18/2009	8.427	8.523	8.544							
12/2/2009	8.431	8.551	8.567							
12/9/2009	8.816	8.67	9.155							
12/16/2009	8.512	8.625	8.663							
12/30/2009	8.512	8.68	8.656							
1/6/2010	8.491	8.604	8.628	8.72	8.601	8.34	8.734	8.571	8.654	8.664
1/13/2010	8.489	8.565	8.626	9.018	8.798	8.436	8.891	8.796	8.713	8.684
1/21/2010	8.419	8.641	8.562	9.211	9.183	8.338	8.918	8.817	8.732	8.795
1/28/2010	8.493	8.599	8.63	9.283	9.261	8.348	8.929	8.813	8.734	8.869
2/4/2010	8.497	8.602	8.637	9.292	9.273	8.35	8.919	8.823	8.739	8.862
2/17/2010	8.516	8.613	8.643	9.31	9.356	8.353	8.811	8.716	8.742	8.835
2/25/2010	8.596	8.68	8.823	9.342	9.276	8.666	9.24	9.023	9.008	9.108
3/5/2010	8.542	8.647	8.664	9.317	9.463	8.395	8.937	8.849	8.778	8.886
3/13/2010	8.511	8.621	8.642	9.283	9.295	8.332	8.878	8.81	8.709	8.81
3/25/2010	8.491	8.617	8.624	9.302	9.352	8.354	8.86	8.872	8.845	8.86
3/31/2010	8.513	8.599	8.672	9.313	9.333	8.41	9.031	8.922	8.911	8.912
4/8/2010	8.529	8.461	8.616	9.346	9.243	8.339	8.887	8.847	8.805	8.802
4/15/2010	8.456	8.567	8.612	9.17	9.188	8.34	8.898	8.828	8.754	8.802
4/29/2010	8.468	8.515	8.601	9.044	9.104	8.336	8.868	8.789	8.651	8.786
5/6/2010	8.466	8.504	8.603	8.965	9.003	8.334	8.881	8.762	8.626	8.762
5/13/2010	8.525	8.511	8.683	8.905	8.942	8.388	8.925	8.849	8.8	8.869
6/2/2010	8.464	8.488	8.589	8.905	8.821	8.304	8.812	8.701	8.682	8.836
6/9/2010	8.461	8.475	8.586	8.853	8.777	8.329	8.848	8.721	8.705	8.847
6/17/2010	8.457	8.476	8.58	8.86	8.785	8.32	8.816	8.716	8.688	8.835
7/7/2010	8.448	8.462	8.569	8.85	8.774	8.311	8.808	8.709	8.68	8.827
7/15/2010	8.507	8.528	8.654	8.873	8.799	8.351	8.86	8.749	8.742	8.856
7/21/2010	8.467	8.483	8.606	8.85	8.779	8.318	8.855	8.734	8.67	8.736
8/5/2010	8.449	8.446	8.563	8.832	8.757	8.282	8.839	8.71	8.638	8.72
8/12/2010	8.682	8.605	8.746	8.733	8.643	8.566	9.166	8.793	8.819	8.897
8/19/2010	8.502	8.434	9.083	9.108	9.017	8.505	9.061	9.003	8.812	9.149

Citations

Alyamani, M.S., Sen, Z., 1993. Determination of hydraulic conductivity from complete grain-size distribution curves. Ground Water 31 (4), 551–555.

Anderson, J.K., Wondzell, S.M., Gooseff, M.N., Haggerty, R., 2005. Patterns in stream longitudinal profiles and implications for hyporheic exchange flow at the H.J. Andrews experimental forest, Oregon, USA. Hydrological Processes 19, 2931–2949.

Arnold, C.L.J., Gibbons, C.J., 1996. Impervious surface coverage—the emergence of a key environmental indicator. Journal of the American Planning Association 62, 243–256.

Bates, P.D., Stewart, M.D., Desitter, A., Anderson, M.G., Renaud, J.-P., Smith, J.A., 2000. Numerical simulation of floodplain hydrology. Water Resources Research 36, 2517–2530.

Bencala, K.E., 2000. Hyporheic zone hydrological processes. Hydrol. Process. 14, 2797-2798.

Benke, A.C., Chaubey, I., Ward, M., & Dunn, E.L., 2000. Flood pulse dynamics of an unregulated river floodplain in the Southeastern U.S. coastal plain. Ecology 81, 2730–2741.

Blanchet, Z.D., 2009. Effect on bar formation on channel stability and sediment loads in an urban watershed. Unpublished master thesis. University of Maryland.

Blench, T., 1957. Regime behaviour of canals and rivers. Butterworths Scientific Publications, London, U.K.

Bohlen, C. C., and Friday. R., 1994. Riparian and terrestrial issues in the Chesapeake. 28pp in Human Activities and Ecosystem Function: Reconciling Economics and Ecology, Solomons, Maryland.

Booth, D. B., 1990. Stream-channel incision following drainage basin urbanization. Water Resources Bulletin 26, 407-417.

Booth, D.B., Karr, J.R., Schauman S., et al. 2001. Urban stream rehabilitation in the Pacific Northwest. Wash Water Resources 12, 1-11.

Boulton, A. J., Findlay, S., Marmonier, P., Stanley, E. H., and Valett, H. M., 1998. The functional significance of the hyporheic zone in streams and rivers. Annual Review of Ecology and Systematics 29, 59-81.

Braune, M. J., and Wood, A., 1999. Best management practices applied to urban runoff quantity and quality control. Water Science and Technology 39, 117-121.

Brunke, M., and Gonser, T., 1997. The ecological significance of exchange processes between rivers and groundwater. Freshwater Biology 37 (1), 1–33.

Burt, T.P., 1997. The hydrological role of buffer zones within the drainage basin system. In: Haycock, N.E., Burt, T.P., Goulding, K.W.T., Pinay, G. (Eds.), Buffer Zones: Their Processes and Potential in Water Protection, Quest Environmental, Harpenden, UK, pp. 21–32.

Burt, T.P., and Haycock, N.E., 1996. Linking floodplains to rivers. In: Anderson, M.G., Walling, D.E., Bates, P. (Eds.), Floodplain Processes, Wiley, New York, pp. 461–492.

Burt, T.P., Matchett, L.S., Goulding, K.W.T., Webster, C.P. and Haycock, N.E. 1999. Denitrification in riparian buffer zones: the role of floodplain sediments. Hydrological Processes 13, 1451–63.

Burt, T.P., Pinay, G., Matheson, F.E., Haycock, N.E., Butturini, A., Clement, J.C., Danielescu, S., Dowrick, D.J., Hefting, M.M., Hillbricht- Ilkowska, A. and Maitre, V. 2002. Water table fluctuations in the riparian zone: comparative results from a pan-European experiment. Journal of Hydrology 265, 129–48.

Burt, T.P., Stewart, M.D., Bates, P.D., Claxton, A.J., Anderson, M.G., Price, D.A., 2002. Water table fluctuations within the floodplain of the River Severn, England. Journal of Hydrology 262, 1–20.

Butturini, A., Bernal, S., Sabater, S., Sabater, F., 2002. The influence of riparian-hyporheic zone on the hydrological responses in an intermittent stream. Hydrol. Earth Syst. Sci. 6 (3), 515–525.

Castleberry, D. T., Cech J. J., Erman, D. C., Hankin, D., Healey, M., Kondolf, G. M., Mangel, M., Mohr, M., Moyle, P. B., Nielsen, J., Speed, T. P., Williams, J.G., 1996. Uncertainty and instream flow standards. Fisheries 21, 20- 21.

Cey, E.E., Rudolph, D.L, Aravena, R. and Parkin, G., 1999. Role of the riparian zone in controlling the distribution and fate of agricultural nitrogen near a small stream in southern Ontario. Journal of Contaminant Hydrology. 37, 45-67.

Church, M., 1992. Channel morphology and typology. In: Colow, P., Pettes, G.E. (Eds.), The River Handbook. Blackwell Scientific Publications, Oxford, UK, pp. 26–143.

Cirmo, C.P., and McDonnell, J.J., 1997. Linking the hydrologic and biogeochemical controls of nitrogen transport in near-stream zones of temperate-forested catchments: a review. Journal of Hydrology 199, 88–120.

Clement, J.C., Aquilina, L., Bour, O., Plaine, K., Burt, T.P., Pinay, G., 2003. Hydrological flowpaths and nitrate removal rates within a riparian floodplain along a fourth-order stream in Brittany (France). Hydrol. Process. 17, 1177–1195.

Dahm, C. N., Grimm, N. B., Marmonier, P., Valett, H. M., and Vervier, P., 1998. Nutrient dynamics at the interface between surface waters and groundwaters. Freshwater Biology 40, 427-451.

Darby, S.E. and Thornes, C.R., 1992. Impact of channelisation on the Mimmshall Brook, Hertfordshire, UK. Regulated Rivers 7, 193-204.

Duff, J.H., Triska, F.J., 1990. Denitrification in sediments from the hyporheic zone adjacent to a small forested stream. Can. J. of Fish. Aquat. Sci. 47, 1140–1147.

Dunne, T., and Leopold L.B., 1978. Water in Environmental Planning. San Francisco: W. H. Freeman and Co.

Eggleston, J., and Rojstacze, S. 2001. The Value of grain-size hydraulic conductivity estimates: Comparison with high resolution in-situ field hydraulic conductivity. Geophysical research letters. 28(22), 4255-4258.

Fetter, C.W., 2001 Applied Hydrology, Fourth Edition, Merril Publishing Company, Columbus Ohio.

Gibert, J., Danielopol, D.L., and Stanford, J.A.,(editors). 1994. Groundwater ecology. Academic Press, San Diego, California.

Gillham, R.W., 1984. The capillary fringe and its effect on watertable response. Journal of Hydrology 67, 307–324.

Gilliam, J. W., 1994. Riparian wetlands and water quality. J.Environ. Qual. 23(5), 896-900.

Gleick, P. H., 1998. The world's waters: The biennial report on fresh water resources. Island Press, Washington, D.C.

Gooseff, M.N., Anderson, J.K,, Wondzell, S., LaNier, J., Haggerty, R., 2006a. Retraction notice. Retracted: A modelling study of hyporheic exchange pattern and the sequence, size, and spacing of stream bedforms in mountain stream networks, Oregon, USA. Hydrological Processes 20, 2441 (retraction of Hydrological Processes (2005) 19: 2915).

Gooseff, M.N., Anderson, J.K., Wondzell, S., LaNier, J., Haggerty, R., 2006b. A modelling study of hyporheic exchange pattern and the sequence, size, and spacing of stream bedforms in mountain stream networks, Oregon, USA. Hydrological Processes 20, 2443–2457.

Grimm N., Grove J.M., Pickett S.T.A., and Redman C.L., 2000. Integrated approaches to long-term studies of urban ecological systems. BioSci. 50, 571–584.

Groffman, P. M., Crawford, M.K., 2003. Denitrification potential in urban riparian zones. Journal of Environmental Quality 32, 1144.

Groffman, P.M., Boulware, N.J., Zipperer, W. C., Pouyat, R.V., Band, L.E., and Colosimo, M.F. 2002. Soil nitrogen cycle processes in urban riparian zones. Environmental Science and Technology 36:4547–4552.

Groffman, P. M., Bain, D. J., Band, L. E., Belt, K. T., Brush, G. S., Grove, J. M., Pouyat, R. V., Yesilonis, I. C., and Zipperer, W. C., 2003. Down by the riverside: Urban riparian ecology. Frontiers in Ecology and the Environment*,* Vol. 1, 315–321.

Hack, J. T., 1960. Interpretation of erosional topography in humid temperate regions. American Journal of Science 258A, 80–97.

Hammer, T.R., 1972. Stream channel enlargement due to urbanization. Water Resources Research 8, 1530-1540.

Harvey, J.W., and K. E. Bencala. 1993. The effect of streambed topography on surface-subsurface water exchange in mountain catchments, Water Resour. Res., 29, 89-98.

Haycock, N.E., Burt, T.P., 1993. Role of floodplain sediments in reducing the nitrate concentration of subsurface run-off: a case study in the Cotswolds, UK. Hydrological Processes 7, 287–295.

Haycock, N.E., Burt, T.P., Goulding, K.W.T., Pinay, G., 1997. Buffer zones: their processes and potential in water protection, Quest Environmental, Harpenden, UK. pp. 115–127.

Hazen, A., 1892. Some physical properties of sands and gravels. Mass. State Board of Health, 24th Annual Report, 539–556.

Hendricks, S.P. & White D.S., 1988. Hummocking by lotic Chara: observations on alterations of hyporheic temperature patterns. Aquatic Botany, 31, 13–22.

Henry, K. S., Valett, H. M., Morrice, J. A., Dahm, C. N., Wroblicky, G. J., Santistevan, M. A. and Campana, M. E., 1994. Ground water-surface water exchange in two headwater streams. In Stanford, J. A. and Valett, H. M.

(Eds), in Proceedings of the Second International Conference on Ground Water Ecology. American Water Resource Association Technical Publication Series, Bethesda, MD. pp. 319±328.

Herzog, B.L., Stohl, C.J. Follmer, L.R., Morse, W.J., and Su, W.J. 1989. Investigation of failure mechanisms and migration of organic chemicals at Wilsonville, Illinois. Ground Water 9(2), 82-89.

Hill, A.R., 1990. Ground water flow paths in relation to nitrogen chemistry in the near-stream zone. Hydrobiologia, 206: 39-52.

Hill, A.R., 1996. Nitrate removal in stream riparian zones. J. Environ. Qual. 25, 743–755.

Hill, A.R., 1997. The potential role of in-stream and hyporheic environments as buffer zones. In: Haycock, N.E., Burt, T.P., Goulding, K.W.T., Pinay, G. (Eds.),

Hill, M.T., Platts, W.S., Beschta, R.L., 1991. Ecological and geomorphological concepts for instream and out-of-channel flow requirements. Rivers 2, 198-210.

Howard, A. D., 1992, Modelling channel migration and floodplain sedimentation in meandering streams, *in* Carling, C. A., and Petts, G. E., eds., Lowland floodplain rivers: New York, John Wiley, p. 1–41.

Hupp, C.R., 1992. Riparian vegetation recovery patterns following stream channelization: a geomorphic perspective. Ecology 73, 1209–1226.

Hupp, C. R., Demas, C. R., Kroes, D. E., Day, R. H., and Doyle, T. W., 2008. Recent sedimentation patterns with the central Atchafalaya Basin, Louisiana. Wetlands 28, 125–40.

Johnson, W.C., Burgess, R.L., Keammerer, W.R., 1976. Forest overstory vegetation and environment on the Missouri River floodplain in North Dakota. Ecological Monographs 46, 59-84.

Jones, J.B., and P. J. Mulholland (Editors). 2000. Streams and ground waters. Academic Press, San Diego, California.

Junk, W.J., Bayley, P.B., Sparks, R.E., 1989. The flood pulse concept in river-floodplain system. Canadian Special Publication of Fisheries and Aquatic Sciences 106, 110–127.

Kaplan, D., Muñoz-Capena, R., Wan, Y., Hedgepeth, M., Zheng, F., Roberts, R., Rossmanith, R., 2010. Linking river, floodplain, and vadose zone hydrology to improve restoration of a coastal river affected by saltwater intrusion. Journ. Enviornmental Qual. 39(5), 1570-1584

Kasahara, T, Wondzell S.M., 2003. Geomorphic controls on hyporheic exchange flow in mountain streams. Water Resources Research 39, 1005.

King, S.L. and. Grant, W.E., 1996. A Simulation Model of the Impacts of Green-Tree Reservoir Management on Bottomland Hardwood Seedling Growth and Survival. Ecological Modelling 87, 69-82.

Knighton, D. 1998. Fluvial forms and processes: a new perspective. Arnold, London, United Kingdom.

Krause, S., and Bronstert, A., 2004. Approximation of groundwater–surface water-interactions in a mesoscale lowland river catchment, Hydrology: Science & Practice for the 21st Century, 2004, vol. 2. British Hydrological Society, 408–415.

Krause, S., and Bronstert, A., 2007. Water balance simulations and groundwater–surface water-interactions in a mesoscale lowland river catchment. Hydrol. Process. doi:10.1002/hyp.6182.

Kroes, D. E., Hupp, C. R., and Noe, G. B., 2007. Sediment, nutrient, and vegetation trends along the tidal forested Pocomoke River, Maryland, p. 113–37. In W. H. Conner, T. W. Doyle, and K. W. Krauss (eds.) Ecology of Tidal Freshwater Forested Wetlands of the Southeastern United States. Springer, Netherlands.

Kwak, T.J., 1988. Lateral Movement and Use of Floodplain Habitat by Fishes of the Kankakee River, Illinois. American Midland Naturalist 120, 241-249.

Lane, E.W., 1955. The importance of fluvial morphology in hydraulic engineering. Proc. Am. Soc. Civil Eng. 81(745), 1–17.

Larkin, R. G., and J. M. Sharp Jr., 1992. On the relationship between river basin geomorphology aquifer hydraulics and ground-water flow direction in alluvial aquifers, Geol. Soc. Am. Bull., 104, 1608-1620.

Lautz, L. K. (2008), Estimating groundwater evapotranspiration rates using diurnal water-table fluctuations in a semi-arid riparian zone, Hydrogeol. J., 16(3), 483-497.

Lazaro, T. M., 1990. Urban hydrology: a multidisciplinary perspective, revised edition. Lancaster, PA: Technomic Publishing Company.

Lee, K..H., Isenhart, T.M., Schultz, R.C., Mickelson, S.K., 2000. Multispecies riparian buffers trap sediment and nutrients during rainfall simulations. J. Environ. Qual. 29, 1200–1205.

Leopold, L. B., and Maddock, T., 1953. The hydraulic geometry of stream channels and some physiographic implications. U.S. Geological Survey Professional Paper No. 252. US Government Printing Office, Washington, DC.

Leopold, L. B., M. G. Wolman, and J. P. Miller. 1964. Fluvial Processes in Geomorphology. Freeman Press, San Francisco

Loheide, S.P., Booth, E.G., 2010. Effects of changing channel morphology on vegetation, groundwater, and soil moisture regimes in groundwater-dependent ecosystems, Geomorphology doi:10.1016/j.geomorph.2010.04.016

Lowrance, R., Todd, R., Fail, J., Hendrickson, O., Leonard, R., Asmussen, L., 1984. Riparian forests as nutrient filters in agricultural watersheds. Bioscience 34 (6), 374–377.

Lowrance, R., Vellidis, G., Hubbard, R.K., 1995. Denitrification in a restored coastal plain forest. J. Environ. Qual. 21, 401–405.

Malard, F., K. Tockner, Ward, J.V., 1999. Shifting dominance of subcatchment water sources and flow paths in a glacial flood plain (Val Roseg, Switzerland). Arct. Antarct. Alp. Res. 31, 135–150.

Mertes, L.A.K., 1997. Documentation and significance of the perirheic zone on inundated floodplains. Water Resources Research 33, 1749–1762.

Miall, A.D., 1996. The Geology of Fluvial Deposits. Springer, Berlin, 582 pp.

Micheli, E.R., Kirchner, J.W., 2002. Effects of wet meadow riparian vegetation on streambank erosion. 1. Remote sensing measurements of streambank migration and erodibility. Earth Surf. Process. Landforms 27, 627–639.

Miller, A.J., 1990. Flood hydrology and geomorphic effectiveness in the central Appalachians. Earth Surface Processes and Landforms 15, 119-134.

Naiman, R.J., Magnuson, J.J., McKnight, D.M., and Stanford J. A., 1995. The Freshwater Imperative: A Research Agenda. Island Press, Washington, D.C.

Naiman, R.J., Décamps, H., McClain, M.E., 2005. Riparian: Ecology, Conservation, and Management of Streamside Communities. Elsevier Academic Press, Burlington, MA.

Noe, G. B. and Hupp. C. R., 2005. Carbon, nitrogen, and phosphorus accumulation in floodplains of Atlantic Coastal Plain rivers, USA. Ecological Applications 15, 1178–90.

Nortcliff, S., Thornes, J.B., 1984. Floodplain response of a small tropical stream. In: Walling, D.E., Burt, T.P. (Eds.), Catchment Experiments in Fluvial Geomorphology', Geo Books, pp. 73–86.

Osterkamp, W. R. and. Hedman, E. R., 1977. Variation of width and discharge for natural high-gradient stream channels. Water Resources Research 13, 256–58.

Palmer, M. A., Bernhardt,E.D. , Allan, J.D., Lake P.S.,, Alexander, G., Brooks, S., Carr, J., Clayton S.,, Dahm, C.N., Follstad Shah, J., Galat, D.L., Loss, S.G.., Goodwin, P., Hart, D.D., Hassestt, B., Jenkinson, R., Kondolf, R., Lave, R. Meyer, J.L., O'Donnell, T.K.., Pagano, L. and Sudduth, E., 2005. Standards for ecologically successful river restoration. Journal of Applied Ecology 47, 208–217.

Palone, R.S., Todd, A.H., (Eds.), 1997. Chesapeake Bay Riparian Handbook: A Guide for Establishing and Maintaining Riparian Forest Buffers. USDA For. Serv. NA-TP-2-97 USDA-FS, Radnor, PA.

Park, E., and Parker, J.C. 2008. A Simple Model for Water Table Fluctuations in Response to Precipitation, Journal of Hydrology. 356, 344-349.

Paul, M.J., and Meyer, J.L., 2001. Streams in the urban landscape. Annu Rev Ecol Syst 32, 333-65.

Pickett, S.T.A., Cadenasso M.L., Grove J.M., et al. 2001. Urban ecological systems: linking terrestrial ecological, physical, and socio-economic components of metropolitan areas. Annu Rev Ecol Syst 32, 127-57**.**

Pizzuto, J.E., Hession, W.C., McBride, M., 2000. Comparing gravel-bed rivers in paired urban and rural catchments of southeastern Pennsylvania. Geology 28, 79-82.

Poff, N. L., Allan J. D., Bain, M. B., Karr, J. R., Prestegaard, K. L., Richter, B. D., Sparks R. E., Stromberg J. C., 1997. The natural flow regime. Bioscience 47, 769–784.

Poole, G.C., Stanford, J.A., Running, S.W., 2006. Multiscale geomorphic drivers of groundwater flow paths: subsurface hydrologic dynamics and hyporheic habitat diversity. Journal of the North American Benthological Society 25 (2), 288–303.

Prestegaard K.L., 1988. Morphological controls on sediment delivery pathways. Pages 533- 540 in Walling DE, ed. Sediment budgets. Wallingford (UK): IAHS Press. International Association of Hydrological Sciences Publication nr 174.

Richter, B.D., Baumgartner, J.V, Wigington R, Braun, D.P., 1997. How much water does a river need? Freshwater Biology 37, 231- 249.

Rosenberry D.O., Winter T.C., 1997. Dynamics of water-table fluctuations in an upland between two prairie-pothole wetlands in North Dakota. J Hydrol 191, 266-289

Rosgen, D.L., 1994. A classification of natural rivers. Catena 22, 169–199.

Rouch R. (1992) Caracte´ristiques et conditions hydrodynamiques des e´coulements dans les se´diments d'un ruisseau des Pyre´ne´es. Implications e´cologiques. Stygologia, 7, 13–25.

Rovey, C.W. II., 1990. Stratigraphy and sedimentology of Silurian and Devonian carbonates, eastern Wisconsin, with implications for ground-water flow into Lake Michigan. Unpublished Ph.D. dissertation, Univ. of Wisconsin-Milwaukee. 427.

Rovey, C.W. II. and Cherkauer, D.S., 1994a. Relation between hydraulic conductivity and texture in a carbonate aquifer: Observations. Ground Water. 32 (1), 53-62.

Rovey, C.W. II. and Cherkauer, D.S., 1994b. Relation between hydraulic conductivity and texture in a carbonate aquifer: Regional continuity. Ground Water. 32 (2), 227-238.

Rovey, C. W. and Cherkauer, D. S.,1995. Scale dependency of hydraulic conductivity measurements, Ground Water, 33(5), 769-780.

Schilling, K.E., Zhang, Y.K., Drobney, P., 2004. Water table fluctuations near an incised stream, Walnut Creek, Iowa. J. Hydrol. 286, 236–248.

Schultz, R.C., Colletti, J.P., Isenhart, T.M., Marquez, C.O., Simpkins, W.W., Ball, C.J., 2000. Riparian forest buffer practices. In: Garrett, H.E., (Ed.), North American Agroforestry: An Integrated Science and Practice, American Society of Agronomy, Madison, WI.

Schumm, S.A., 1971. Fluvial geomorphology: channel adjustment and river metamorphosis. In: River Mechanics. H.W. Shen (editor). H.W. Shen, Fort Collins, Colo., pp. 5-1–5-22.

Shankman, D. and L.J. Smith, 2004. Stream Channelization and Swamp Formation in the U.S. Coastal Plain. Physical Geography 25, 22-38

Shumm, S.A., 1963. A tentative classification of alluvial river channels. Circular, vol. 477. U.S. Geological Survey, Washington, DC. 10 pp.

Sophocleous, M., 2002. Interactions between groundwater and surface water: the state of science. Hydrogeol. J. 10, 52–67.

Squillace, P.J., 1996. Observed and simulated movement of bank storage water. Ground Water 34, 121–134.

Stanford, J.A., Ward, J.V., Liss, W.J., Frissell, C.A., Williams, R.N., Lichatowich, J.A., Coutant, C.C., 1996. A general protocol for restoration of regulated rivers. Regulated Rivers: Research & Management 12, 391-414.

Steiger, J., Tabacchi, E., Dufour, S., Corenblit, D., Peiry, J.L., 2005. Hydrogeomorphic processes affecting riparian habitat within alluvial channel–floodplain river systems: a review for the temperate zone. River Research and Applications 21 (7), 719–737.

Storey, R.G., Howard, K.W.F., Williams, D.D., 2003. Factors controlling riffle-scale hyporheic exchange flows and their seasonal changes in a gaining stream: a three-dimensional groundwater flow model. Water Resources Research 39 (2), 1034.

Strahler, A.N., 1957. Quantitative analysis of watershed geomorphology. Am. Geophys. Union Trans. 38, 913-920.

Taylor, S.R., Moltyaner, G.I., Howard, K.W.F., and Killey, R.W.D., 1987. A comparison of field and laboratory methods for determining contaminant flow parameters. Ground Water. 25(3), 312-330.

Tockner, K., Malard, F. & Ward, J.V. 2000. An extension of the flood pulse concept. Hydrological Processes 14, 2861–2883.

Trimble, S.W., 1997. Contribution of stream channel erosion to sediment yield from an urbanizing watershed., Science 278, 1442-44.

Triska, F.J., Kennedy, V.C., Avanzino, R.J., Zellweger, G.W., Bencala, K.E., 1989. Retention and transport of nutrients in a third-order stream in northwestern California: hyporheic processes. Ecology 70 (6), 1893–1905.

Triska, F.J., Duff, J.H., Avanzino, R.J., 1993. The role of water exchange between a stream channel and its hyporheic zone in nitrogen cycling at the terrestrial–aquatic interface. Hydrobiologia 251, 167–184.

Tucci, P. and Hileman, G. E., 1992. Potential effects of dredging the South Fork Obion River on ground-water levels near Sidonia, Weakley County, Tennessee. U.S. Geological Survey, Water-Resources Investigations Report 90, 4041.

Tyus, H.M., 1990. Effects of altered stream flows on fishery resources. Fisheries 15, 18-20.

Valett, H. M., Morrice, J. A., Dahm, C. N., and Campana, M. E., 1996. Parent lithology, surface-groundwater exchange, and nitrate retention in headwater streams. Limnology and Oceanography 41, 333-345.

Waddington, J.M., Roulet, N., Hill, A.R., 1993. Runoff mechanisms in a forested groundwater discharge wetland. Journal of Hydrology 147, 37–60.

Walsh, C. J., Fletcher, T.D., and Ladson, A.R., 2005. Stream restoration in urban catchments through redesigning stormwater systems: looking to the catchment to save the stream. Journal of the North American Benthological Society 24, 690–705.

White, D.S., 1990. Biological relationships to convective flow patterns within stream beds. Hydrobiologia, 196, 149–158.

Winter, T.C., Harvey, J.W., Franke, O.L., Alley, W.M., 1998. Groundwater and surface water – a single resource. US Geol. Surv. Circ., 1139.

Woessner, W.W., 2000. Streams and fluvial plain ground water interactions: rescaling hydrogeologic thought. Ground Water 38 (3), 423–429.

Wolman, M.G., Miller, J.P., 1960. Magnitude and frequency of forces in geomorphic processes. Journal of Geology 68, 54–74.

Wondzell, S.M., and F.J. Swanson., 1996. Seasonal and storm dynamics of the hyporheic zone of a 4th-order mountain stream. I: Hydrologic processes. Journal of North American Benthological Society 15 (1), 3-19

Wondzell, S.M., Swanson, F.J., 1999. Floods, channel change, and the hyporheic zone. Water Resources Research 35, 555-567.

Wroblicky, G.J., Campana, M.E, Dahm, C.N., Valett, H.M, Morrice, J.A., Henry, K.S., Baker, M.A., 1994. Simulation of stream-groundwater exchange and near-stream flow paths of two first-order mountain streams using MODFLOW. The Second International Conference on Ground Water Ecology, 187-198.

Wroblicky, G.J., Campana, M.E., Vallet, H.M., Dahm, C.N., 1998. Seasonal variations in surface-subsurface water exchanges and lateral hyporheic area of two stream-aquifer systems. Water Resources. Research 34 (3), 317–328.

Zhang, Y.K., Schilling, K.E., 2006. Effects of land cover on water table, soil moisture, evapotranspiration, and groundwater recharge: A field observation and analysis. Journal of Hydrology 319, 328–338